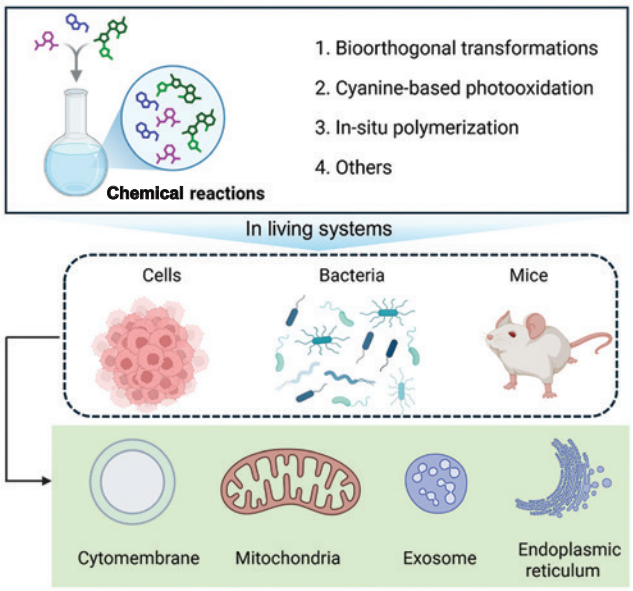
https://doi.org/10.59761/RCR5244

Precision-engineered chemical reactions in living systems for advanced biomedical applications

Shaojun Shi,[a] Kaiyang Tao,[a] Weijie Xu,[a] Ziheng Tong,[a] Zhaoran Hu,[a] Shuguo Zheng,[a,b]* Chunfei Wang[a,b,c]*

[a] *School of Pharmacy, Wannan Medical University, Wuhu 241002, People's Republic of China*
[b] *Grade III Laboratory of Pharmacology of TCM, National Administration of Traditional Chinese Medicine, Wannan Medical University, Wuhu 241002, People's Republic of China*
[c] *Department of Biomedical Sciences, Faculty of Medicine, University of Macau, Macao Special Administrative Region 999078, People's Republic of China*

The study of abiotic chemical reactions within living systems represents a transformative frontier in biomedical research, driven by the multidisciplinary integration, including synthetic biology, chemical biology, pharmacy and chemistry. The employment of bioorthogonal chemistry, and analogous methodologies facilitates the precise modulation of biological processes with high specificity, high fidelity and minimal off-target effects. This review systematically summarizes recent advances in the design and application of such *in situ* chemical reactions in living systems. A range of reaction types are introduced in the current review that have found significant application, including bioorthogonal transformations, cyanine-based photooxidation, *in situ* polymerization, and the like. A discussion of the mechanisms underlying these reactions and their key advantages are also comprehensively included. Subsequently, a generalization and summarization of representative biomedical applications is conducted, encompassing the domains of cellular behavior regulation, fluorescence imaging and antitumor therapy. Finally, we delineate the prevailing challenges and future directions for the development and translation of *in situ* chemical tools. The precise orchestration of chemistry in living environments holds great promise for unlocking novel diagnostic and therapeutic platforms, paving the way toward more effective and personalized treatments for complex diseases.
The bibliography includes 134 references.



Keywords: abiotic chemical reactions, living systems, bioorthogonal transformations, photooxidation, photopolymerization.

Contents

1. Introduction 2
2. Commonly used chemical reactions *in situ* 3
2.1. Bioorthogonal reaction: precision tools for probing and manipulating living systems 3
2.2. Cyanine photooxidation: cornerstone for optical imaging and drug delivery 5
2.3. Polymerization: simulation of biomacromolecules to fabricate functional supramolecular 6
2.4. Other reactions in living systems 7
3. Biomedical applications of chemical reactions *in situ* 8
3.1. Regulation of cellular behavior 8
3.1.1. Protein — mediated cell surface engineering 8
3.1.2. Functionalization of biomimetic catalytic surfaces 8
3.1.3. Intracellular polymerization regulates the cytoskeleton 10
3.2. Fluorescence imaging 12
3.2.1. Intracellular synthesis of luminescent substrates 12
3.2.2. Reductive activation polymerization imaging 13
3.2.3. Bioorthogonal polymerization for artificial organelle imaging 13
3.2.4. Metal-catalyzed fluorogenic reactions 15
3.3. Antitumor research 17
3.3.1. Endogenous microenvironment-triggered polymerization 17
3.3.2. Light-triggered *in situ* antitumor reactions 24
3.3.3. Metal-catalyzed prodrug activation 28
3.3.4. Bioorthogonal polymerization therapy 34
4. Conclusion 36
5. List of abbreviations 38
6. References 39

Received 12 May 2026
© 2026 Uspekhi Khimii, ZIOC RAS, Russian Academy of Sciences

1. Introduction

Cells operate as sophisticated chemical factories, sustaining life through thousands of meticulously regulated metabolic reactions.[1–3] These reactions seem simple, but they play a crucial role in human life, which are broadly categorized into catabolic processes that break down molecules to release energy. Meanwhile, anabolic processes utilize this energy to synthesize complex biomolecules. Within this native network, specificity and efficiency are primarily governed by natural catalysts such as enzymes and nucleic acids.[4] However, the inherent complexity and tightly controlled nature of these endogenous pathways present a fundamental challenge for directly introducing exogenous diagnostic or therapeutic agents without interfering with vital physiological processes. Fortunately, the rapid development of bioorthogonal chemistry has overcome this limitation, providing a powerful suite of abiotic reaction tools. These reactions are designed to proceed with high specificity and biocompatibility within living systems, operating independently of native biochemical processes.[5–7] The successful performance of *in situ* synthesis, activation, or release of functional molecules, which not only minimizes off-target toxicity by concentrating therapeutic action at target sites, but also enables real-time monitoring of treatment efficacy, representing a transformative step toward intelligent and personalized medical interventions.

Cancer remains a leading cause of mortality worldwide, posing persistent challenges in diagnosis and treatment.[8,9] Despite the success of contemporary clinical treatments including surgery, chemotherapy, radiotherapy, targeted therapy, and immunotherapy, these modalities still suffer from several intrinsic limitations, including poor selectivity, severe systemic toxicity, multidrug resistance, variable therapeutic efficacy, and tumor heterogeneity. In particular, conventional chemotherapeutic agents indiscriminately damage rapidly proliferating normal tissues, whereas targeted delivery systems based on nanocarriers have emerged as an effective strategy to improve drug accumulation within tumors, prolong circulation time, reduce systemic toxicity, and enhance therapeutic efficacy.[10] These limitations have stimulated the development of precision medicine strategies, including abiotic chemical reactions that enable site-specific activation of therapeutic agents.[11–13] These limitations underscore the urgent need for innovative strategies with enhanced precision, efficacy, and real-time monitoring capabilities, driving the rise of precision medicine paradigms. As a pioneering theranostic approach, abiotic chemical reactions within living cells leverage the unique characteristics of the tumor microenvironment (TME) and bioorthogonal chemistry to enable targeted drug activation and real-time imaging. By delivering precursor substances or prodrugs to tumor cells and triggering specific chemical reactions *via* TME features[14–16] such as acidity, high reductive potential, and abnormal enzyme expression, this strategy achieves selective *in situ* activation of therapeutic agents, markedly improving treatment selectivity and efficacy.

The complexity of the intracellular chemical environment, coupled with the extreme sensitivity of cells to external stimuli, has posed significant challenges to the realization of molecular structure transformation, particularly within the context of chemical reactions within living cells. The exploration of these problems is currently in its nascent stage, due to the technological limitations that are currently in place. Abiotic chemical reactions are defined as a process that utilizes the intracellular environment to carry out chemical reactions in living systems to obtain biocompatible products. These processes primarily comprise chemical bond binding reactions and chemical bond cleavage releasing reactions. In light of these observations, it is evident that these reactions are predominantly initiated by the distinctive characteristics of the tumor microenvironment, encompassing factors[17–21] such as acidic pH, elevated levels of reactive oxygen species (ROS), and overexpressed enzymes, among others. By leveraging these endogenous stimuli, chemical reactions *in situ* can be selectively triggered within tumor tissues or cells, enabling localized therapeutic effects and precise diagnostic readouts.

Chemical reactions that occur *in situ* at their precise site of function within a living cell or organism are fundamental to life. In comparison with conventional drug therapy, their spatial and temporal specificity is not merely convenient but biologically essential for several key advantages:

(1) Unparalleled spatial precision or targeted activation: this constitutes the fundamental benefit. Rather than administering a potent (and potentially toxic) active drug that circulates throughout the body, one administers inert or masked

S.**Shi**. Bachelor's degree in pharmaceutics from Wannan Medical University (2025). Master Student in pharmacology at the same University under the supervision of Prof. Chunfei Wang.
E-mail: 2179433829@qq.com
Current research interests: synthesis of polymers for the treatment of breast cancer and development of environment sensitive probes for bioimaging.
K.**Tao**. Bachelor Student in clinical pharmacy at Wannan Medical University.
E-mail: 13855300668@163.com
Current research interests: development of photosensitizers for antitumor agents and development of fluorescence probes for bioimaging.
W.**Xu**. Bachelor's degree in pharmacy from Wannan Medical University (2024). Master Student in pharmacology at the same University under the supervision of Prof. Chunfei Wang.
E-mail: 980630990@qq.com
Current research interests: development of photosensitizers for the treatment of brain glioma and development of fluorescence probes for imaging viscosity/polarity in microenvironment.
Z.**Tong**. Bachelor student in clinical pharmacy at Wannan Medical University.
E-mail: 17201711787@163.com
Current research interests: development of photosensitizers for antitumor agents and development of fluorescence probes for bioimaging.
Z.**Hu**. Bachelor Student in clinical pharmacy at Wannan Medical University. E-mail: 15155632642@163.com
Current research interests: development of photosensitizers for antitumor agents and development of fluorescence probes for bioimaging.
S.**Zheng**. Master's degree from Anhui University of Chinese Medicine (2003). PhD in pharmacology from China Pharmaceutical University (2006). Professor at Wannan Medical University.
E-mail: zhengsg2000@163.com
Current research interests: development of components from traditional Chinese medicines for the treatment of cardiovascular and cerebrovascular diseases.
C.**Wang**. Master's degree of pharmaceutics from Anhui University of Chinese Medicine (2016). PhD in biomedical sciences from University of Macau (2020) under the supervision of Prof. Xuanjun Zhang. Postdoctoral fellow (2025) (Faculty of Health Sciences, University of Macau). Associate Professor at Wannan Medical University. E-mail: yb67596@um.edu.mo
Current research interests: chemical sensors, biosensors, photopharmacology.

components (precursors) that only react to form the active agent at the desired sites.

(2) Overcoming delivery or stability challenges: a considerable number of potent therapeutic agents are challenging to administer due to their poor solubility in blood, rapid clearance by the kidneys or liver, instability in circulation (degradation by enzymes or low pH), or excessive toxicity for systemic administration. Consequently, inert or masked precursors can be engineered to be stable, soluble, and non-toxic. The active form is only generated *in situ*, circumventing these systemic delivery hurdles. For diagnostic probes, such an *in situ* reaction strategy can further realize programmable pharmacokinetic conversion, which ensures targeted lesion enrichment while enabling rapid clearance of reaction products to reduce their toxicity associated with their retention *in vivo*.[22]

(3) Amplification or signal generation for diagnostics: *in situ* reactions have been demonstrated to be a potent tool for diagnostics and imaging. A single disease biomarker has been demonstrated to specifically trigger the activation of multiple precursors, thereby amplifying the signal for ultra-sensitive detection.

(4) On-demand temporal control: the initiation of the reactions can be triggered externally and with a high degree of temporal precision.

(5) Construction of materials inside the body: this is a pioneering application for the construction of therapeutic agents directly at the disease site. In the presence of a disease-specific enzyme or biomolecule or initiator, certain reactants are known to form a scaffold for regenerative medicine or local drug retention.

(6) Enabling new therapeutic modalities: the implementation of certain efficacious therapeutic strategies is contingent upon the occurrence of *in situ* reactions. Examples of such technologies include sustained and controlled release drugs, antibody-drug conjugates (ADCs) and bioluminescence resonance energy transfer (BRET).

The significance of *in situ* reactions lies in their ability to confer specificity, efficiency and regulation upon the chemistry of life. These processes transform an otherwise chaotic mixture of biological molecules into a highly organized, spatially directed, and exquisitely controlled network of processes. This network enables complexity, adaptability, and very existence of living systems. Life is not merely a series of chemical reactions; rather, it is a meticulously orchestrated sequence of reactions the transpire in a specific temporal and spatial context. The advent of nanotechnology, molecular engineering, and biomaterials science has led to the development of a plethora of smart chemical platforms.[23–25] which have in turn enabled *in situ* chemical reactions within living systems. These include enzyme-activated nanoreactors.[26–28] light-responsive polymers.[29,30] pH-sensitive self-assembling molecules[31–33] and so forth. The implementation of such systems has been demonstrated to enhance therapeutic efficacy while concurrently providing powerful tools for early diagnosis and real-time monitoring of treatment responses.

Herein, this review provides a systematic summary of the recent advancements in precision-engineered chemical reactions in living systems. In the current review, we first introduce the commonly used chemical reactions *in situ*, mainly including bioorthogonal reactions, cyanine photooxidation, and polymerization. Subsequently, we proceed to explore the mechanisms of these reactions and discuss their respective advantages and disadvantages in biomedical applications. Subsequently, a systematic summary of representative applications, including the regulation of cellular behavior, fluorescence imaging, and anti-tumor research, is elaborately presented. Finally, the potential for clinical translation, the current challenges and future perspectives of chemical reactions *in situ* are strongly highlighted. Synthesizing the findings from recent research, this review aims to provide researchers with valuable insights into chemical reactions *in situ* and to promote the utilization of these emerging reactions in precision medicine.

2. Commonly used chemical reactions *in situ*

2.1. Bioorthogonal reaction: precision tools for probing and manipulating living systems

Click chemistry, first articulated by Sharpless and co-workers[34,35] in 2001, represents a transformative approach in synthetic chemistry, which emphasizes the use of modular, high-yielding, and biocompatible reactions that can rapidly assemble complex molecules from simple building blocks. This strategy has had a profound impact on various fields, including drug discovery and materials science, by facilitating the efficient and selective formation of covalent bonds under mild conditions. Among the most impactful developments in this field is copper-free click chemistry.[36–38] As delineated in Fig. 1, a notable illustration of copper-free click chemistry is the inverse electron-demand Diels–Alder (IEDDA) reaction between tetrazines and *trans*-cyclooctenes (TCOs).[39–41] This reaction is characterized by remarkable rapidity, selectivity, and ability to occur under physiological conditions without the necessity of metal catalysts. Due to its speed and specificity, tetrazine–TCO ligation has emerged as a potent instrument for *in vivo* applications, including prodrug activation, and imaging agent activation, among others.[42] In essence, click chemistry, particularly in its copper-free formulation, facilitates chemical transformations within living systems without disrupting native biochemical processes (Table 1). This development has ushered in a new era of precision medicine, enabling researchers to manipulate and monitor biological systems with unparalleled precision and specificity. This consideration assumes particular importance in the context of biomedical applications, wherein the preservation of cellular functionality is of paramount significance.

Bioorthogonal chemistry, an important extension of click chemistry, represents a rapidly evolving frontier in chemical biology. This field is devoted to the ingenious design and implementation of chemical reactions that operate seamlessly within the complex environment of living organisms.[5,45] The fundamental principle underlying this approach is the facilitation of reactions that exhibit exceptional biocompatibility. These reactions are characterized by their efficiency and selectively, with a notable absence of perturbation with the extensive network of endogenous biochemical pathways and processes that are fundamental to life.[7] This distinctive property enables researchers to introduce chemical probes or modifications directly into living cells, tissues, or even entire organisms (*in vivo* and *ex vivo*), facilitating the precise labeling, tracking, imaging, isolation, or manipulation of specific biomolecules.

The ideal bioorthogonal reaction as precision-engineered chemical reactions in living systems is characterized by several crucial attributes:[43,46,47]

(1) Rapid kinetics: reactions must occur swiftly to capture dynamic biological events and minimize exposure times of potentially reactive components.

(2) High selectivity: reactants must react only with each other, ignoring the multitude of other functional groups present

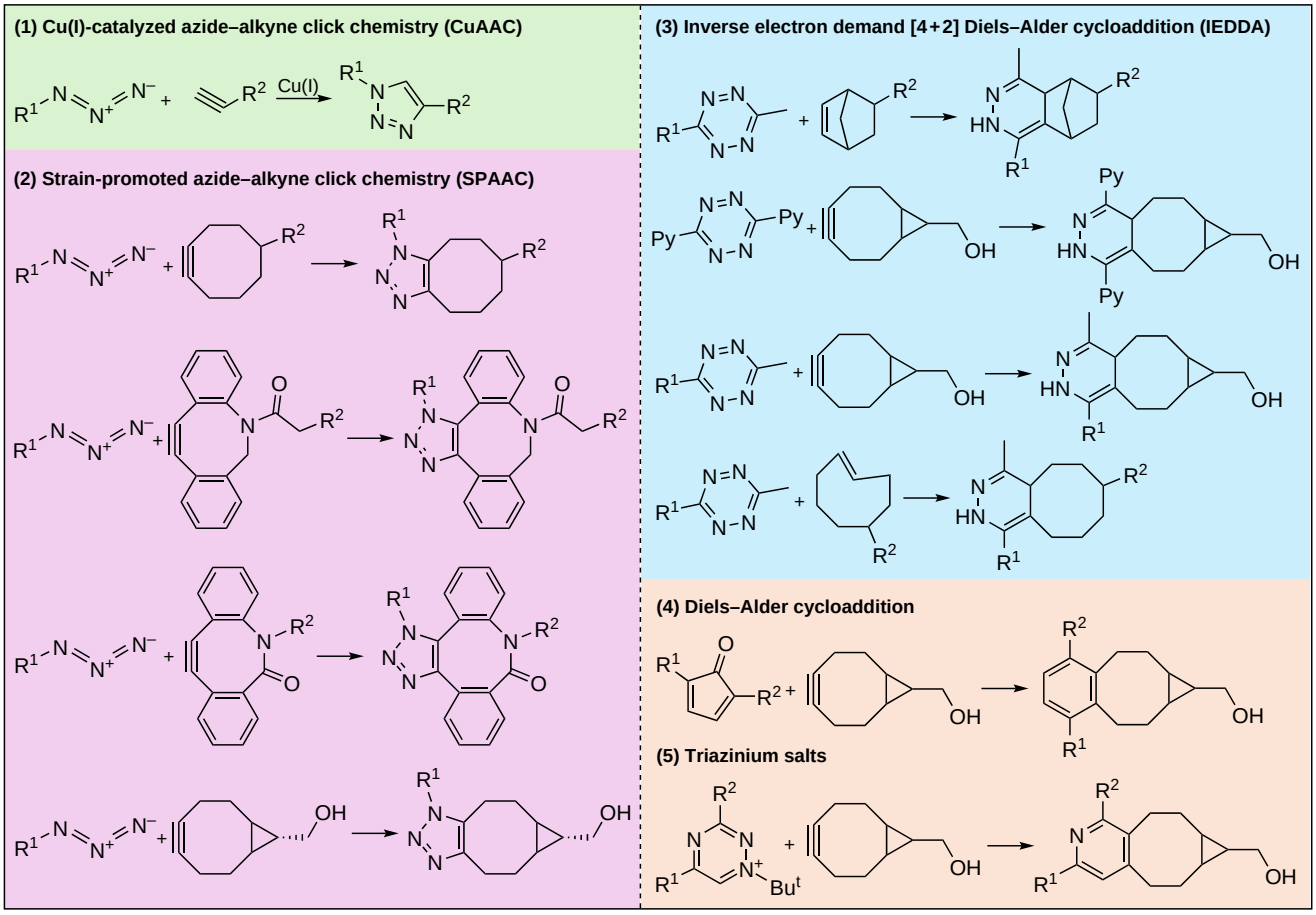


Figure 1. Well-established click reactions.

Table 1. Comparison of typical click reactions.

Reaction type	Representative reactive pair	Reaction rate constant, M^{-1} s	Metal catalyst requirement	Biocompatibility level	*In vivo* application maturity	Reagent cost	Core limitations	Main applicable scenarios	Refs
CuAAC	Azide + Alkyne	$1–10^2$	(Cu(I))	Moderate (copper cytotoxicity)	High	Low	Copper ion cytotoxicity, poor *in vivo* safety	*In vitro* biomolecule labeling, material modification	35
SPAAC	Azide + cyclooctyne	$10^{-2}–1$	None	Good	High	High	Slow reaction rate, large molecular weight, complex synthesis	*In vivo* metabolic labeling, long-term imaging	43
IEDDA	Tetrazine + TCO	$10–10^6$	None	Excellent	High	High	Limited TCO stability, high synthesis cost	Rapid *in vivo* prodrug activation, pre-targeted imaging	42
Nitrone–cyclo-alkene cyclo-addition	Nitrone + Cyclopropene	$10^{-3}–10^{-1}$	None	Good	Moderate	Moderate	Relatively slow kinetics, limited substrate types	Intracellular biomolecule tracking	44

in biological systems (like amines, thiols, alcohols, carboxylic acids, native carbonyls).

(3) Exceptional efficiency: It is imperative that reactions proceed to high conversion under physiological conditions (such as an aqueous buffer, neutral pH, ambient temperature) to ensure sufficient signal or modification.

(4) Biocompatibility: reactants and reaction products must exhibit low cytotoxicity and minimal perturbation of cellular functions and viability. Ideally, they should also be non-immune system.

(5) Mutually reactive pairs: typically, the approach relies on introducing two complementary components: a bioorthogonal functional group (‘chemical handle’) metabolically incorporated into the target biomolecule, and a cognate probe or reagent carrying the complementary reactive group.

This powerful toolkit has fundamentally transformed the study of biomolecules in their natural environment.

(1) Site-specific labeling with fluorophores enables real-time, super-resolution imaging of protein localization, trafficking, interactions, and conformational dynamics in living cells.[48,49] Bioorthogonal tags have also been demonstrated to facilitate protein purification or the installation of post-translational modifications for functional studies.

(2) The tracking of DNA replication, RNA transcription, localization, and turnover dynamics with high spatial and temporal resolution becomes possible through the use of nucleotide analogs bearing bioorthogonal handles.[50]

(3) The most transformative impact of this phenomenon has been, perhaps, in the field of glycobiology. Metabolic oligosaccharide engineering (MOE) facilitates the incorporation of unnatural sugar analogs bearing bioorthogonal tags into cell-surface or secreted glycans.[51,52] Subsequent labeling reveals glycan dynamics, composition, and roles in development, immunity, and disease.

(4) Tracking the synthesis, trafficking, and membrane dynamics of specific lipid classes offer insights into signaling, organelle identity, and membrane biogenesis.[53,54]

(5) Monitoring the uptake, distribution, and metabolism of bioactive compounds or nutrients within cells and organisms. The potential of bioorthogonal chemistry extends far beyond fundamental discovery into tangible medical applications,[6,55,56] such as targeted drug delivery and activation, advanced diagnostic imaging, immunotherapy, tissue engineering and biomaterials, personalized medicine, and the like.

Bioorthogonal chemistry has emerged as an indispensable and transformative discipline, providing chemists and biologists with unprecedented precision tools to interrogate and manipulate the molecular machinery of life in real-time and within living systems. The foundational principles of biocompatibility, speed, and selectivity underpin a vast array of applications, from illuminating fundamental biological mechanisms to drive the development of next-generation diagnostics and targeted therapeutics. As the field undergoes continuous innovation, characterized by novel reactions, improved delivery strategies, and profound biological integration, its influence on our understanding of health and disease, and the advancement of advancing medicine, is projected to escalate exponentially.

Notwithstanding the remarkable progress achieved in proof-of-concept studies, the clinical translation of bioorthogonal reactions remains constrained by several critical bottlenecks.[7,57] At the forefront are pharmacokinetic limitations; most bioorthogonal reagents suffer from short circulatory half-lives and rapid renal excretion, which drastically reduce their accumulation at target sites and necessitate the use of high administered doses to achieve therapeutic efficacy. Closely related to this is the issue of biological instability, which highly strained motifs such as TCO and cyclooctynes are particularly susceptible to nonspecific degradation and off-target side reactions in complex physiological environments,[58,59] thereby undermining reaction selectivity and reliability. A further practical hurdle lies in manufacturing, which the current multi-step synthetic routes, often characterized by low overall yields, render these reagents prohibitively expensive and difficult to produce at scale, which seriously hampers large-scale preclinical development. Finally, and equally important, there remains a conspicuous lack of systematic, long-term assessments regarding the immunogenic potential of the reaction products and their overall metabolic fate *in vivo*, a gap that must be addressed before further clinical advancement can be considered.

2.2. Cyanine photooxidation: cornerstone for optical imaging and drug delivery

The origins of cyanine fluorophores can be traced back to 1856, when the first compound was synthesized.[60,61] In the decades that followed, numerous variants were developed primarily as photosensitized molecules. Among these, the indocyanines, characterized by a polyene linker bridging two 3,3-dialkyl-indolenine heterocycles,[62–64] have now gained extensive usage in biological applications. Of particular significance are the heptamethine cyanines, which feature a seven-carbon chain connecting the two indolenine moieties.[65,66] Cyanines are known to typically exhibit absorption and emission maxima around 800 nm, placing them in the near-infrared (NIR) region. This is advantageous because it allows for deeper tissue penetration and reduced background autofluorescence is minimal, making them especially suitable for *in vivo* imaging systems.

As with many fluorophores, cyanines are susceptible to light-dependent degradation, which is commonly termed photobleaching. However, it is noteworthy that cyanine photobleaching occurs *via* a well-defined photooxidative cleavage reaction, a departure from the typical photobleaching mechanism. Despite the identification of carbonyl-containing products resulting from this cleavage in multiple studies, key mechanistic aspects remain scattered across the literature. It is noteworthy that ROS responsible for this process have been inconsistently assigned, with proposals including singlet oxygen ($^1O_2$), hydrogen peroxide (H_2O_2), and hydroxyl radical ($^{\bullet}OH$). Early work from Gorka *et al*.[61] and Henrichs and co-workers[67] suggested that the formation of carbonyl products is most consistent with a mechanism involving $^1O_2$-mediated dioxetane formation followed by cycloreversion. This hypothesis has been invoked in subsequent studies. In order to elucidate the mechanism, recent investigations have systematically compared the outcomes of direct photolysis with those following exposure to selected ROS. These experiments revealed that, among the four conceivable cleavage sites along the cyanine polyene, carbon–carbon bond cleavage occurs exclusively at two specific positions[68,69] (Fig. 2). Furthermore, this cleavage is induced exclusively by $^1O_2$, whether generated chemically or *via* independent photosensitization, and not by another candidate ROS such as H_2O_2 or $^{\bullet}OH$.

The photooxidative cleavage of cyanines transcends conventional photobleaching to serve as a versatile molecular tool in biomedical research. The intrinsic NIR absorption and emission profiles of these dyes facilitate deep tissue penetration and minimize background autofluorescence, thereby establishing a robust optical foundation for *in vivo* applications. Concurrently, the cleavage of the conjugated polyene backbone results in fluorescence quenching, a property that can be strategically harnessed to design activatable probes for the sensitive detection of specific biomarkers. Furthermore, this cleavage event can be coupled with the release of caged therapeutic payloads, enabling spatiotemporally controlled drug activation precisely at target sites. Notably, this reaction is highly pertinent to photodynamic therapy (PDT), as the same photoirradiation that drives cyanine photooxidation also generates reactive oxygen species to elicit photocytotoxic effects, thus furnishing a molecular rationale for integrated theranostic platforms. Collectively, subsequent imaging and antitumor applications are predicated upon this core mechanism, culminating in a coherent scientific narrative that bridges fundamental photochemical properties with translational biomedical functions.

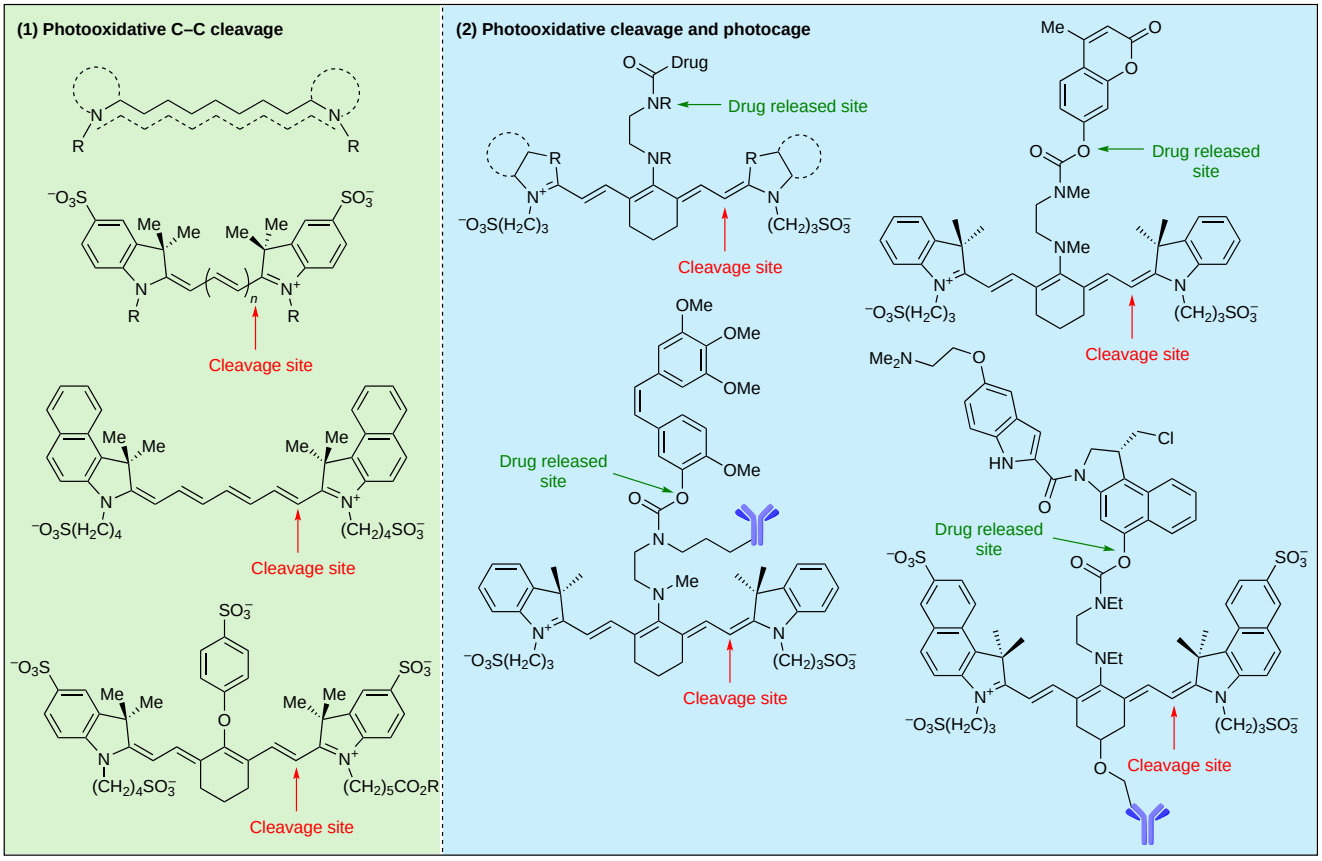


Figure 2. Representative structure of cyanines for photooxidative cleavage.

Table 2. Comparison of cyanine dyes with different polymethine chains for photooxidation

Cyanine type	Absorption/emission wavelength, nm	Tissue penetration depth	Photooxidation efficiency	Photostability	Clinical translation basis	Core limitations	Refs
Heptamethine cyanine	~700–900 (NIR-I)	Moderate (mm level)	High	Poor	High (indocyanine green approved for clinical use)	Strict oxygen dependence, reduced efficiency in hypoxic solid tumors	61
Pentamethine cyanine	~550–700	Shallow	Medium	Medium	Low	Insufficient tissue penetration for deep lesions	68
Trimethine cyanine	~400–550 (visible light)	Very shallow	Low	High	Medium	Strong background auto-fluorescence, low *in vivo* imaging signal-to-noise ratio	69

Among cyanine dyes, heptamethine derivatives bearing a seven-carbon polyene chain are the most extensively employed, because of their NIR absorption and emission maxima (*ca.* 700–900 nm) and comparatively high photooxidation efficiency (Table 2). In contrast, pentamethine and trimethine analogs exhibit shorter wavelength profiles, which afford limited tissue penetration but confer enhanced photostability.[70,71] With regard to biocompatibility, most clinically approved cyanine dyes, such as indocyanine green, have demonstrated acceptable *in vivo* safety. However, the small-molecule fragments generated upon cleavage may pose metabolic toxicity risks, warranting further toxicological assessment. A major intrinsic limitation of this photooxidative system lies in its strict oxygen dependence, as the reaction consumes $^1O_2$ as a key reactant. Consequently, the hypoxic microenvironment prevalent in solid tumors markedly diminishes the reaction kinetics, thereby compromising the overall antitumor efficacy. Moreover, the finite penetration depth of excitation light within biological tissues remains a critical challenge, particularly as conventional visible-light sources are inefficient for activating lesions located in deep-seated tissues.

2.3. Polymerization: simulation of biomacromolecules to fabricate functional supramolecular

Synthetic polymers have been extensively employed in biomedical applications due to the ability to precisely tailor their physicochemical properties and enhance their biocompatibility. Whilst natural polymers, which are derived from cells, frequently demonstrate inadequate mechanical and physical performance, synthetic polymers offer a more controllable and customizable platform. However, they can also carry risks such as immune clearance and influences on protein conformation. These devices can be designed with specific functionalities and distinct characteristics to meet the demands of advanced biomedical

Table 3. Comparison of typical intracellular polymerization systems.

Polymerization type	Trigger mode	Biocompatibility	Spatiotemporal controllability	*In vivo* application difficulty	Core limitations	Refs
Free radical polymerization	Light/Redox	Moderate	High (light control)	Medium	Monomer cytotoxicity, non-specific free radical damage	72
Oxidative polymerization	Endogenous ROS	Moderate	Low (endogenous stimulus)	Medium	Poor tumor-normal selectivity, difficult reaction degree control	73
Photo-initiated polymerization	External light	Good	Excellent	Medium	Limited light penetration depth, potential photodamage	74
Bioorthogonal polymerization	Complementary reactive groups	Excellent	Moderate	High	High reagent cost, complex monomer synthesis	75

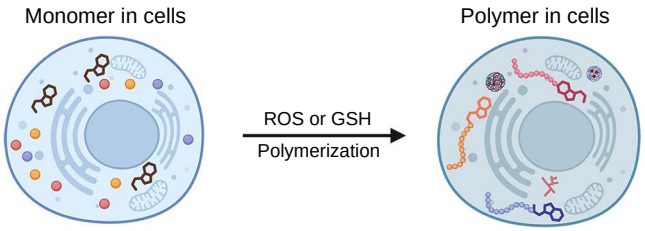


Figure 3. Schematic illustration of cell-mediated *in situ* polymerizations. GSH is intracellular glutathione and ROS are a type of high-reactive oxygen compound that is produced within cells as a result of oxygen metabolism.

uses. An emerging and promising approach in this field is intracellular polymerization, which demonstrates remarkable chemical diversity and efficiency (Fig. 3). Inspired by natural biosynthetic pathways, polymerization within living cells represents a powerful and versatile strategy for modulating cellular behavior and function (Table 3).

Free radical polymerization is considered to be one of the most widely utilized polymerization techniques. The process is comprised of three fundamental steps: initiation, propagation, and termination.[72,73,76,77] The process of initiation entails the generation of a reactive free radical species from an initiator through light, heat, or redox reactions. Subsequently, the radical reacts with vinyl monomers to begin chain formation. During propagation, the polymer chain undergoes successive monomer additions without undergoing alteration to its radical center. Termination occurs when two growing chain radicals combine or couple, or through disproportionation. A significant advantage of free radical polymerization is its compatibility with a wide range of media, including aqueous environments. This renders it especially well-suited for implementation within living systems, allowing active control over polymer characteristics such as molecular weight, polydispersity, and end-group functionality. This, in turn, supports biocompatibility at the cellular level.

In addition to radical polymerization, oxidative polymerization offers another route to achieve intracellular polymerization under physiological conditions. This process occurs in monomers with high oxidation tendency and strong electron-donating properties.[78,79] The reaction is driven by oxidizing agents or applied potentials, which remove electrons from the monomers. This process generates cationic or cation radical sites that initiate polymer chain growth. Despite its high specificity with regard to the mechanism, conventional oxidative polymerization is unable to distinguish between healthy and diseased cells, which can result in non-selective cytotoxic effects. It is important to note that the complex tumor microenvironment contains various upregulated enzymes, signaling molecules, and ROS.[80,81] These biomarkers provide opportunities to design polymerization systems that are tailored to respond specifically to tumor conditions. It has been demonstrated that ROS, in particular, function as critical reactive intermediates in the context of cancer cell activity.[82–84] The utilization of ROS as endogenous oxidizing agents has been demonstrated to facilitate the selective induction of oxidative polymerization within tumor cells. This approach enables the development of targeted polymerization-based platforms with tailored antitumor effects, enhancing specificity and reducing off-target harm.

Despite its expanding biomedical applications, intracellular polymerization technology is confronted with several practical challenges that hinder its clinical translation.[85,86] First, the cytotoxicity of both monomers and initiators constitutes a major concern: most vinyl monomers exhibit appreciable toxicity at elevated concentrations, and the free radicals generated during polymerization may cause nonspecific damage to intracellular biomolecules, including proteins and nucleic acids. Second, issues related to metabolic clearance and long-term accumulation arise because the synthetic polymers formed *in situ* are typically resistant to degradation by endogenous enzyme systems; their persistent retention within cells or organisms can potentially trigger chronic inflammatory or immunogenic responses. Third, the limited controllability *in vivo* further complicates the application, as the heterogeneous intracellular microenvironment and uneven monomer distribution lead to substantial intercellular variability in the degree of polymerization, thereby undermining the uniformity of therapeutic outcomes. At present, the majority of studies remain confined to *in vitro* cellular validation, indicating that considerable efforts are still required before clinical implementation becomes feasible.

2.4. Other reactions in living systems

In addition to the above-mentioned precision-engineered chemical reactions, living systems host a diverse array of other chemical transformations that expand the toolbox of synthetic biology and biomaterials engineering. These include microbe-assisted fabrication of bacterial cellulosic hybrids,[87] which leverage microbial metabolism to produce structurally robust cellulose networks; Schiff base reactions between amino groups and aldehyde groups,[88] which enable effective conjugation under physiological conditions; *in situ* synthesis of covalent organic frameworks (COFs),[89] allowing the construction of

ordered porous structures directly within biological environments; and living cell-mediated self-assembly,[90] where cells actively guide the organization of exogenous or endogenous building blocks into functional architectures. Beyond these, Zhang and co-workers[22] developed a photoswitchable compound capable of achieving real-time, precision opto-control, enabling site-specific inhibition of microtubule polymerization and spatiotemporal regulation of organelle dynamics in live cells. Meanwhile, Roelfes and co-workers[91] established a canonical enzyme-catalyzed reaction using an artificial enzyme, which efficiently catalyzes the formation of a hydrazone product from biosynthetically produced benzaldehydes in *E. coli*, thereby demonstrating the feasibility of integrating non-natural biocatalysis into microbial hosts. Despite the elegance and innovation of these approaches, they share a common limitation, *viz.*, a lack of practical bio-applications. Translating these advanced chemical strategies into real-world biomedical or industrial contexts remains challenging, hindered by issues such as insufficient stability, low biocompatibility, limited scalability, and the difficulty of achieving precise spatiotemporal control in complex living organisms. Future efforts should prioritize bridging this gap by optimizing reaction conditions, enhancing system robustness, and validating performance in disease models or bioproduction settings.

3. Biomedical applications of chemical reactions *in situ*

3.1. Regulation of cellular behavior

3.1.1. Protein — mediated cell surface engineering

Proton-coupled electron transfer (PCET) is a fundamental reaction mechanism in chemistry involving the coordinated transfer of a proton (H^+) and an electron (e^-) between reactants, either simultaneously or in a closely concerted manner.[44,92] This process is of paramount importance in a multitude of numerous redox reactions, where the oxidation of one species is coupled with the reduction of another.[93] The concurrent movement of protons and electrons, facilitated by PCET, stabilizes reaction intermediate and reduces the activation energy barrier, thereby enhancing reaction efficiency. It is imperative to acknowledge the pivotal function of the subject in a multitude of chemical and biological processes. Aromatic amino acid residues in proteins, such as tyrosine (Tyr), possess significant potential as one-electron redox mediators. However, these elements are frequently embedded within the protein structure, a property that often results in the production of low levels of intrinsic oxidation signals and consequently renders them difficult to detect efficiently.[94,95] Huang and co-workers[96] have demonstrated that tyrosine residues in cofactor-free proteins can mediate controlled radical polymerization under 405 nm light. This approach is based on a PCET mechanism, in which the excited-state TyrOH* residue acts as a photoinitiator, interacting with monomers or chain transfer agents (CTAs) to drive photopolymerization in biologically relevant aqueous solutions. The strategy is reliant upon the utilization of 405 nm short-wavelength light excitation, which possesses limited tissue penetration depth. At present, this is only suitable for superficial cells or *in vitro* cell engineering; the *in vivo* application of this strategy to deep tissue necessitates the matching of longer-wavelength light sources.

The employment of this strategy has resulted in the successful synthesis of a series of polymers, characterized by meticulously regulated molecular weights and minimal polydispersity. As illustrated in Fig. 4*a*, the system has been applied to a variety of proteins, including bovine serum albumin (BSA), human serum albumin (HSA), Lysozyme, ribonuclease A (RNase-A), and glyphosate oxidoreductase (Gox), with multiple monomers (such as 2-methoxyethyl acrylate, *N*-isopropyl acrylamide, 4-acryloylmorpholine, *etc.*). The developed polymerization platform demonstrates favorable biocompatibility. It has been demonstrated that this process facilitates the synthesis of non-natural polymers both on the surface and within the interior of yeast cells (see Fig. 4*b*). This, in turn, enables the modulation of cell surface hydrophobicity and agglutination behavior. This work provides a versatile and efficient method for functionally modulating living organisms *in vitro* and *in vivo* through the synthesis of diverse non-natural polymers. It is anticipated that future applications of protein-initiated photopolymerization, exploiting aromatic amino acid residues such as tyrosine, will facilitate the integration of cofactor-free proteins with controlled radical polymerization techniques. This approach is also poised to address key challenges in intra-organism polymerization and the synthesis of bioinspired living materials.

3.1.2. Functionalization of biomimetic catalytic surfaces

Cell membrane acts as a barrier for cell communication, which mainly controls the behavior of cells and modulates cellular interactions. The functionalization of cell surfaces has emerged as a powerful strategy for modulating cellular behavior and extending cellular functions beyond their natural biological limits.[97] Wang and co-workers[98] developed a novel *in situ* polymerization approach to modify cell surfaces with conjugated polymers, enabling precise regulation of cellular activity. The deposition of bio-Pd nanoparticles (NPs) on cells was facilitated by the utilization of the negative charge present on the cell surface (Fig. 5*a*). This process occurred subsequently to the reduction of the surface associated with enzymes or reductants. Subsequent *in situ* polymerization, catalyzed by the bio-Pd NPs, could be readily monitored using fluorescence imaging. In addition to displaying strong antibacterial activity against *E. coli*, the photoactive conjugated polymers formed *in situ* were shown to enhance adenosine triphosphate (ATP) synthesis in *C. pyrenoidosa* by broadening light absorption and promoting cyclic electron transport (see Fig. 5*b*). This bio-Pd-catalyzed polymerization strategy opens a new avenue for cell surface engineering, offering a means to regulate cellular functions through the synthesis of functional polymers *in situ* for tailored biological applications.

Alexander and co-workers[99] developed a copper-mediated radical polymerization system that enables the *in situ* synthesis of synthetic monomers directly on bacterial cell surfaces, leveraging the intrinsic redox machinery of the bacteria (Fig. 6*a*). This approach produces polymers that function as self-selective binding agents, capable of recognizing and binding to specific cell types. Moreover, the method allows fluorescent reporters to be directly grafted onto the polymers at the bacterial surfaces, facilitating both rapid pathogen binding and simultaneous real-time visualization (see Fig. 6*b*). As a result, this strategy offers a powerful platform for the swift, concurrent detection and imaging of pathogenic cells. This work is principally a conceptual demonstration of cell surface functionalization, with no immediate therapeutic applications. Its potential value lies in the engineering modification of probiotics or industrial microbial strains and the construction of pathogen detection platforms, for which further expansion of application scenarios is required.

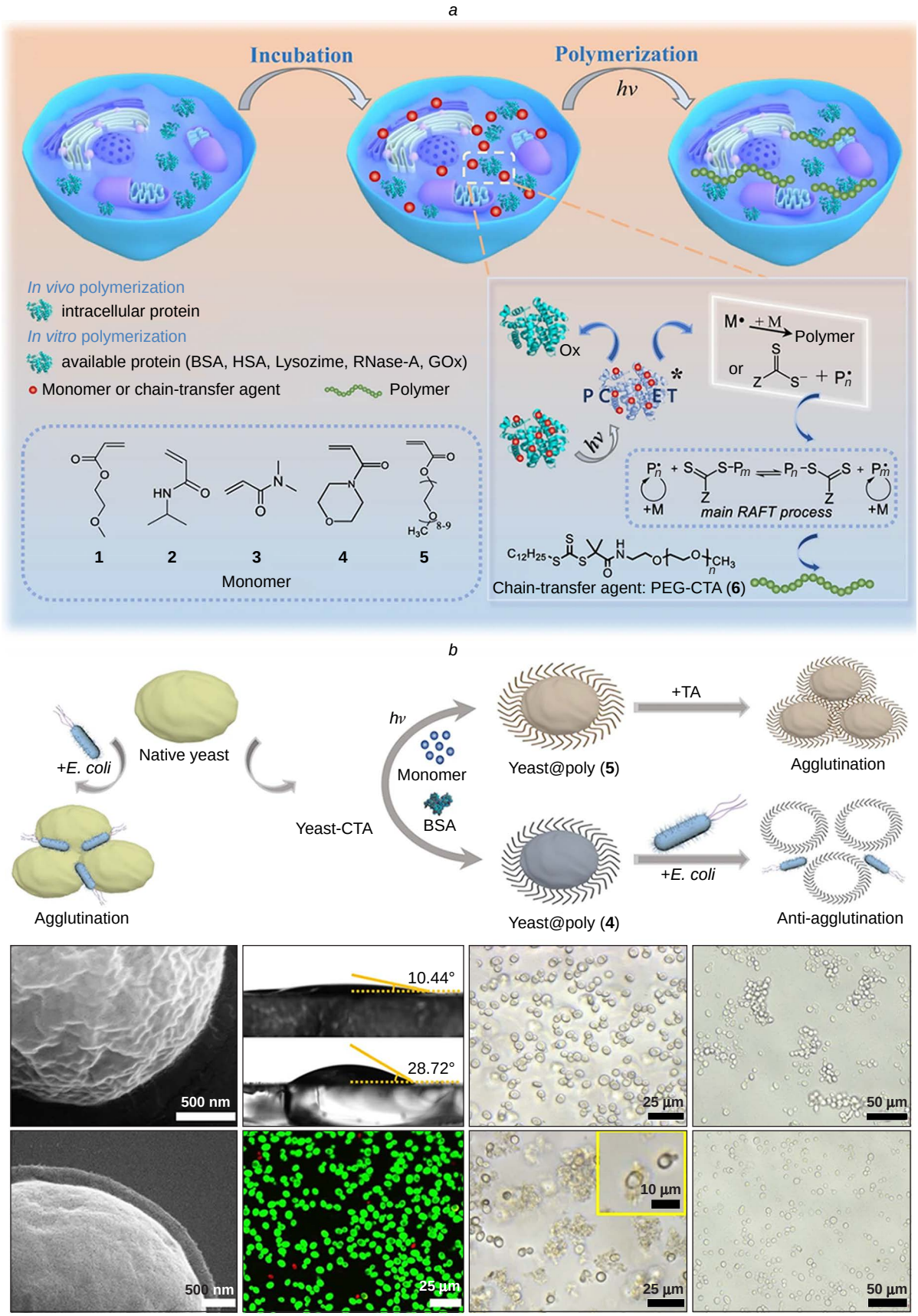


Figure 4. A schematic representation of tyrosine-containing cofactor-free protein mediated radical photopolymerization *in vitro* and *in vivo* (*a*). BSA-mediated reversible addition-fragmentation chain-transfer (RAFT) photopolymerization on the surface of yeast cells for agglutination/anti-agglutination behavior manipulation (*b*). TA is tannic acid, yeast@poly(4,5) is the yeast modified by poly(4,5) formed by monomers 4 or 5, respectively. Reproduced with permission from Huang and co-workers.[96] Copyright 2023, Springer Nature.

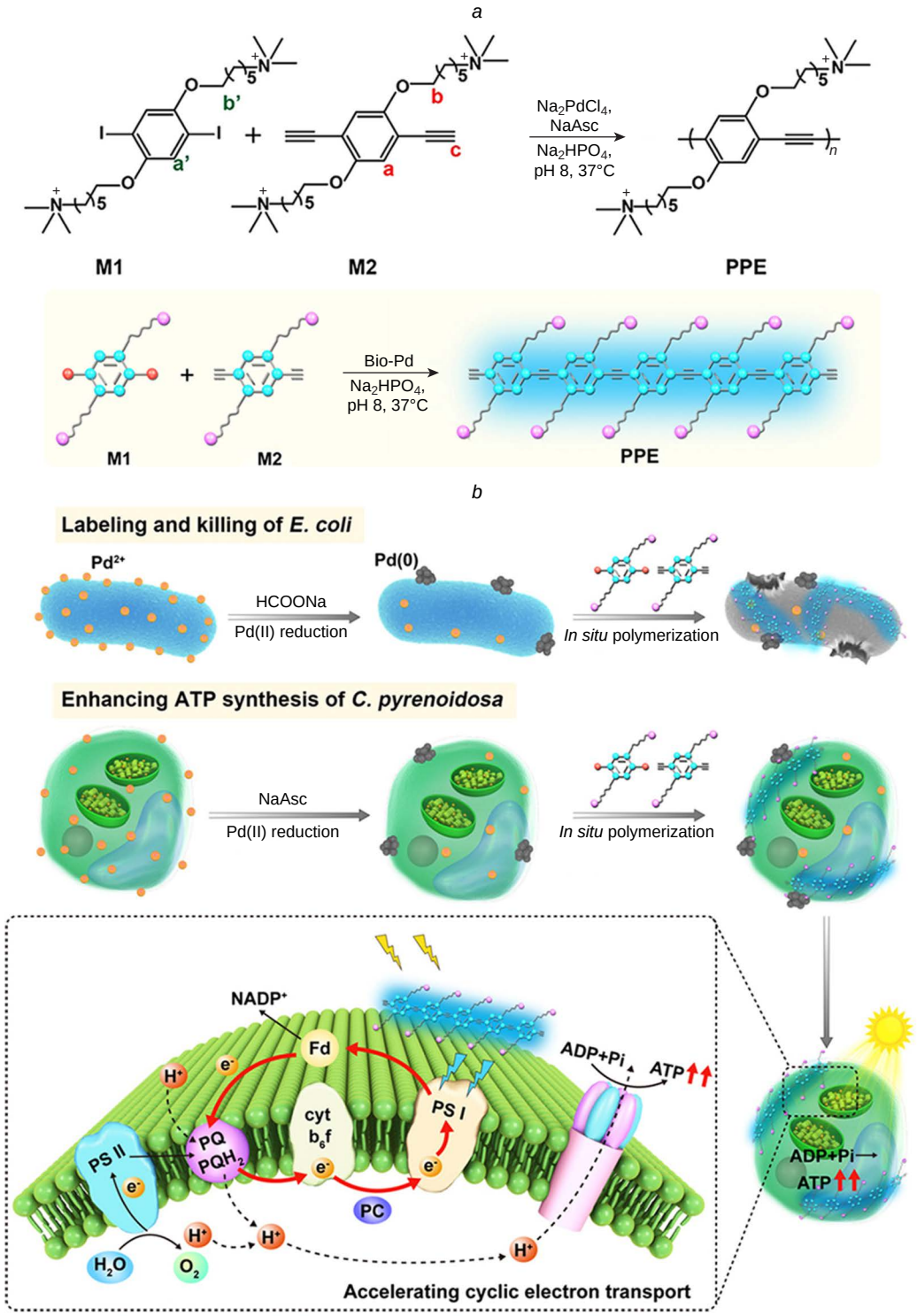


Figure 5. Synthesis of poly(phenyleneethynylene) (PPE) through bio-Pd catalyzed Sonogashira polymerization (*a*). *In situ* synthesis of PPE on the cell surface and its antibacterial activity against *E. coli* and improvement of ATP synthesis in *C. pyrenoidosa* (*b*). NaAsc is sodium ascorbate. ADP + Pi = adenosine diphosphate + phosphoric acid. Reprinted with permission from Wang and co-workers.[98] Copyright 2021, John Wiley and Sons.

3.1.3. Intracellular polymerization regulates the cytoskeleton

Bradley and co-workers[74] reported an innovative strategy for the direct synthesis of unnatural polymers within living cells *via* free radical photopolymerization in (Fig. 7*a*). Utilizing a suite of biocompatible acrylic and methacrylic monomers, thereby enabling the light-triggered generation of synthetic macromolecules in the intracellular space. The formation of polymers *in situ* provides a versatile platform for physical manipulation, tracking and controlling fundamental cellular behaviors, such as the modulation of cytoskeletal dynamics and impairing cellular motility (Figs 7*b*, 8*a–d*). This methodology has the potential to significantly expand the toolkit of biocompatible chemistries

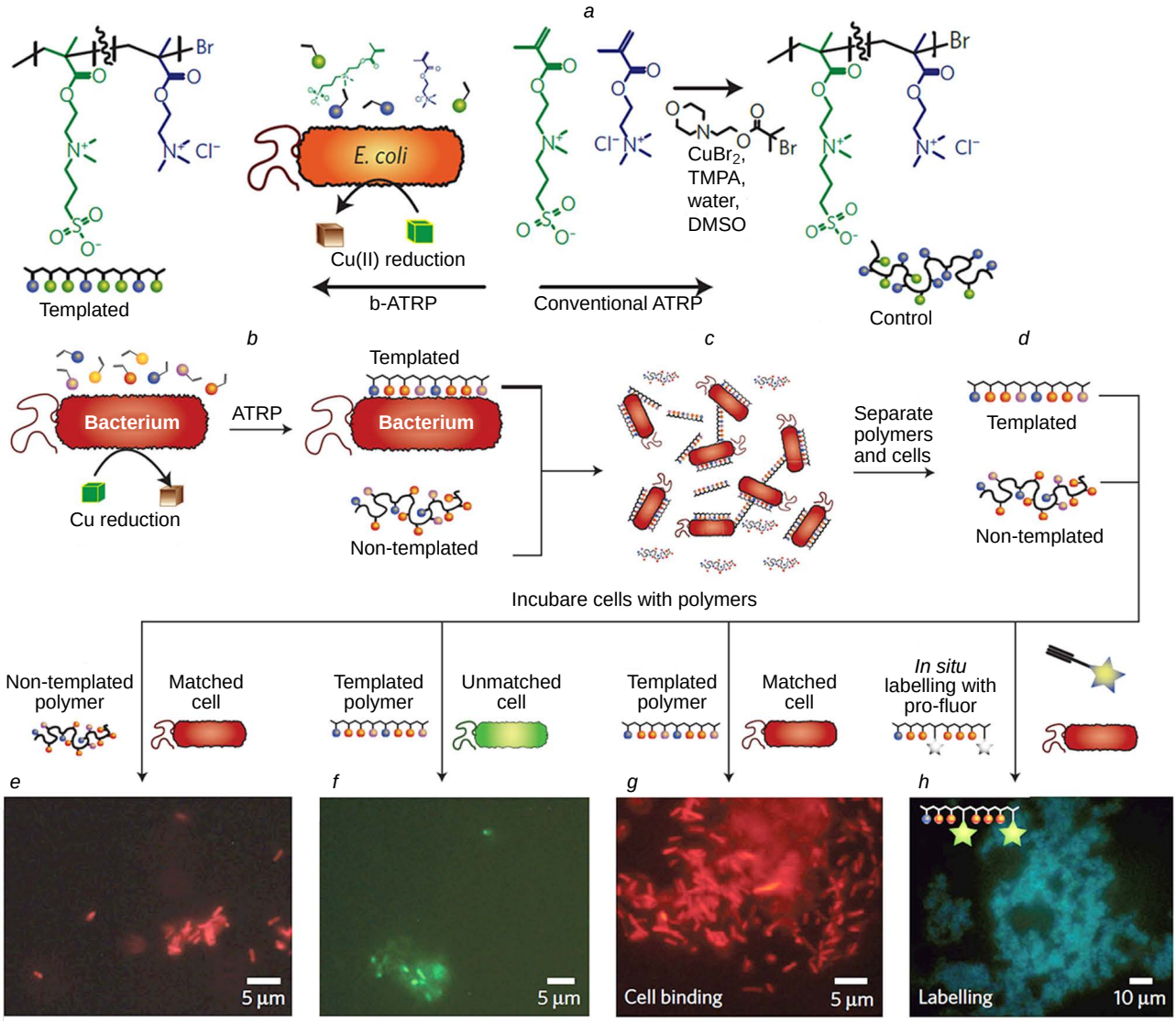


Figure 6. Schematic of the templating process (*a*). Schematic of the bacteria-instructed synthesis process: Bacteria induce polymerization in monomer-catalyst suspensions (*b*) to generate a synthetic extracellular matrix of polymers (*c*). Recovery of polymers from the suspensions leads to two fractions (*d*), with polymer obtained from the aqueous phase suspension around the bacteria denoted conceptually as non-templated and a second fraction obtained from a wash of the cell surfaces denoted as templated. Incubation of polymers with bacteria results in low binding of cells for which the polymer is non-templated (*e*), or where a polymer templated with one cell type (shown in red) is incubated with a cell (shown in green) of another type (*f*). Addition of a polymer, templated by one cell type, with its own 'matched' cell population results in the formation of large polymer cell clusters, as the templated polymers sequester the bacteria that 'instructed' their formation with high affinity (*g*). The same reducing environment at bacterial surfaces that aid the polymer synthesis can also be used to label the cells *in situ via* pro-fluorescent markers, which react with cell-surface bound polymers containing 'clickable' residues (*h*). TMPA is trimethyl phosphonoacetate, ATRP is atom-transfer radical polymerization, b-ATRP is bacteria-mediated ATRP. Reproduced with permission from Alexander and co-workers.[99] Copyright 2014, Springer Nature.

suitable for the intracellular environment, moving beyond small molecules to include synthetic macromolecular structures. The potential efficacy of this approach stems from two key factors. Firstly, it offers high spatiotemporal precision through light control and secondly, it provides a wide range of materials through radical polymerization. Further exploration into the domain of intracellular polymerization has the potential to yield significant advances, paving the way for developing novel biohybrid systems, engineered cellular functions, and novel therapeutic modalities based on direct physical and chemical intervention inside the cell. The 365 nm ultraviolet light employed in this system has been shown to cause photodamage to cells, with long-term irradiation having the potential to induce DNA damage. This highlights the necessity for further optimization of biocompatibility. Additionally, the spatial precision of intracellular polymerization is inadequate, making it challenging to achieve regulation at the sub-organelle level. The long-term biological effects of synthetic polymers retained in cells are also lacking systematic safety data, which is a significant concern.

In situ polymerization for cell behavior regulation provides a novel approach for cell engineering and synthetic biology, yet there are clear gaps in the field. Firstly, the majority of strategies rely on short-wavelength light excitation, which is unable to meet the requirements for *in vivo* application to deep tissue. Secondly, functional regulation is still limited to basic phenotypes such as adhesion and migration, with few studies on complex physiological functions such as cell differentiation and

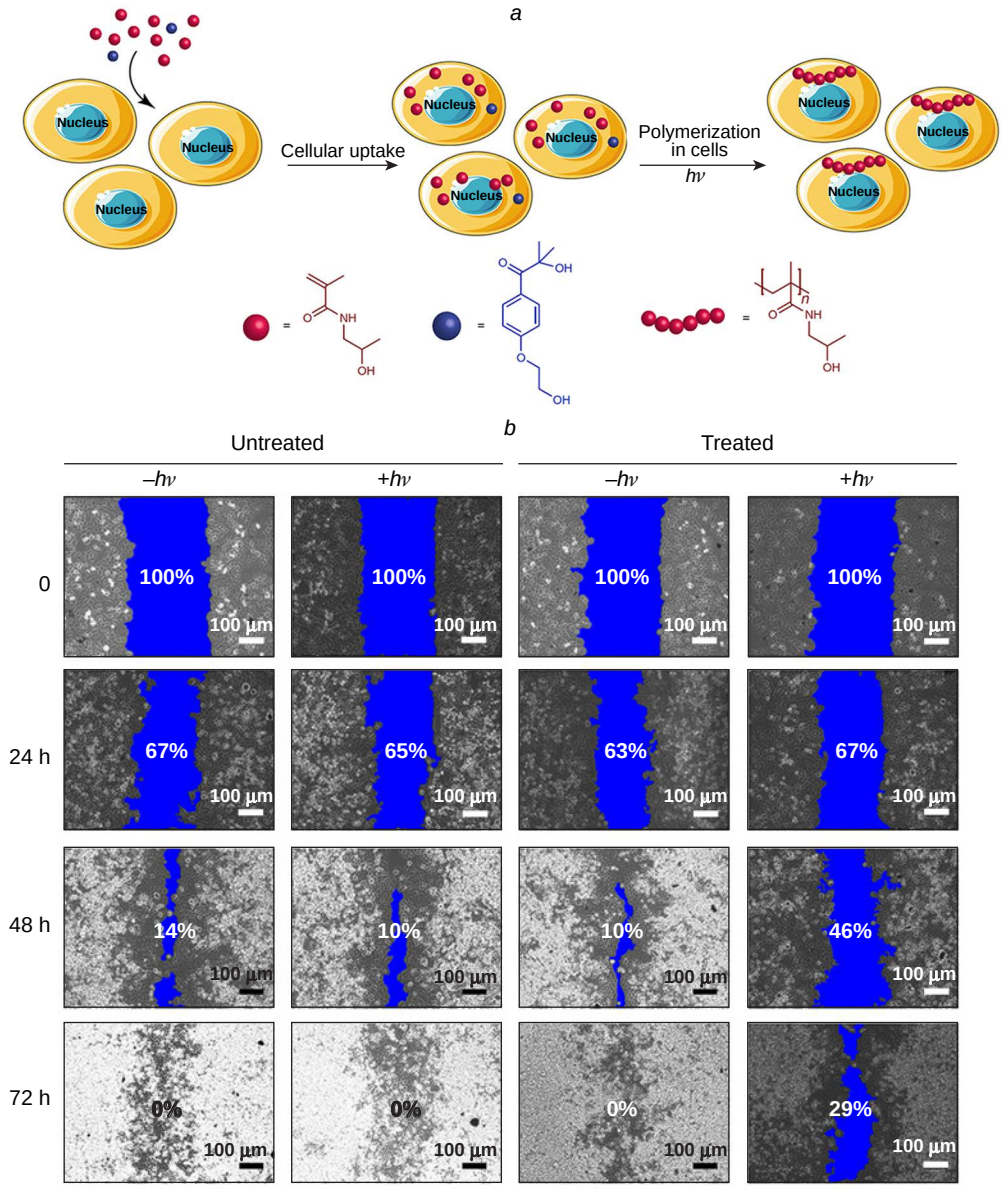


Figure 7. Generic strategy for polymerization inside living cells. The monomer *N*-(2-hydroxypropyl) methacrylamide (HPMA) and the initiator Irgacure 2959 were added to the cell culture, with photopolymerization initiated by illumination at 365 nm (*a*). Cell migration was determined by a wound-healing assay of HeLa cell monolayers. HeLa cells were plated in Dish. Cells were treated with HPMA (50 mM) and Irgacure 2959 (2 mM) for 4 h, followed by illumination at 365 nm for 5 min. 'Wounds' were created and 'wound closure' was monitored by bright-field microscopy at 24, 48 and 72 h and compared to untreated and treated cells without illumination. Wound areas were measured using ImageJ and are colored in blue. The experiments were independently repeated three times, with similar results (*b*). Reprinted with permission from Bradley and co-workers.[74] Copyright 2019, Springer Nature.

signal transduction. Thirdly, there is a lack of systematic verification of the biosafety of long-term polymer retention in cells.

3.2. Fluorescence imaging

3.2.1. Intracellular synthesis of luminescent substrates

As is well established, the luciferin-luciferase system has been widely adopted for bioluminescence imaging across diverse biological processes.[100] However, its performance can be limited by the relatively low chemical stability of its natural substrate, *D*-luciferin, which is susceptible to degradation under acidic conditions, in the presence of oxygen, and upon exposure to light.[100–103] In order to address this limitation, Liang and co-workers[104] rationally designed two chemically stable precursor molecules, CBT-*D*-cystine-CBT (**D-1**) and CBT-*L*-cystine-CBT (**L-1**) (where CBT is 6-amino-2-cyanobenzothiazole), for the intracellular synthesis of active aminoluciferin analogs, *D*-AmLH$_2$ and *L*-AmLH$_2$. As illustrated in Fig. 9 *a*, the proposed mechanism involves the cellular uptake of **D-1** or **L-1**, followed by the reduction of their disulfide bonds *via* GSH. This reduction exposes reactive 1,2-aminothiol groups, which undergo rapid condensation with the cyano groups to form a linear luciferin oligomer (referred to as 1-oligomer). Subsequently, intracellular proteases catalyze the hydrolysis of this oligomer, selectively releasing the final product, either *D*-AmLH$_2$ or *L*-AmLH$_2$, which then serves as a substrate for bioluminescence generation. **D-1** and **L-1** were successfully applied for bioluminescence imaging in fLuc-transfected MDA-MB-231 cells and were

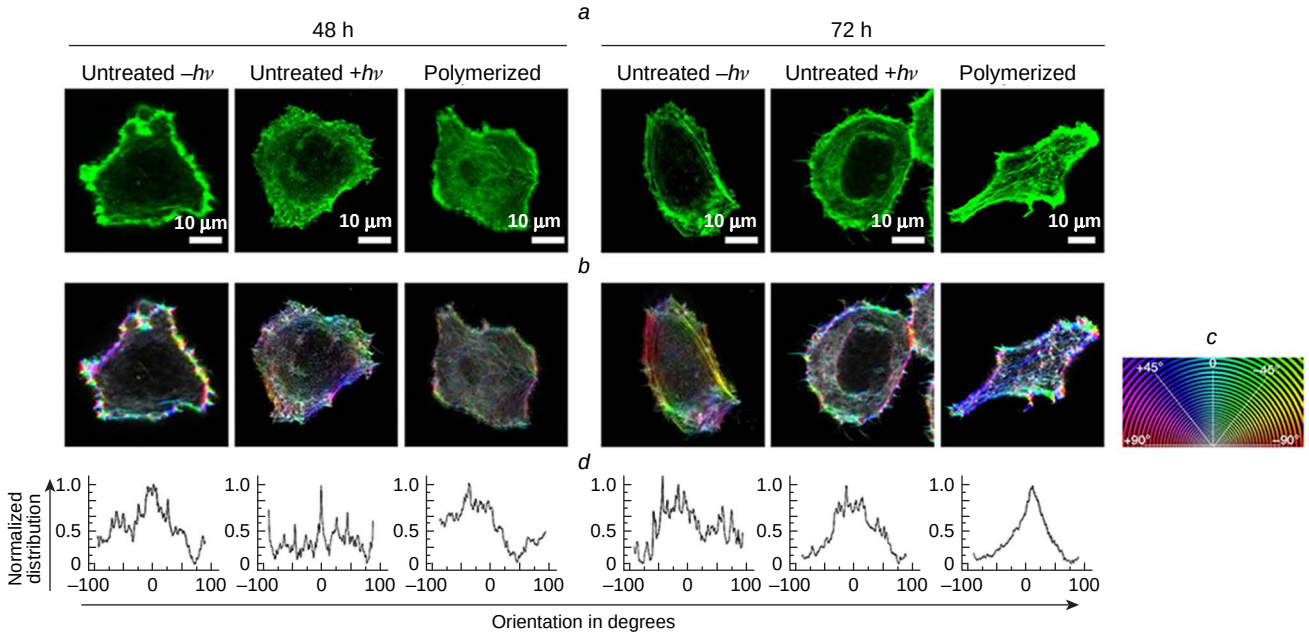


Figure 8. Actin cytoskeleton organization was altered in polymerized HeLa cells. Untreated cells, with and without illumination, and polymerized cells (incubated with 50 mM HPMA and 2 mM Irgacure 2959 for 4 h, followed by 5 min at 365 nm) were stained for actin filaments after 48 and 72 h (*a*). Corresponding orientation plots for actin staining (*b*), where the different colors indicate different orientations of actin filaments, as per the given color map (*c*), and the microdomain distributions for actin filament orientations (as measured by ImageJ) (*d*). The experiments were independently repeated three times, with similar results. HPMA is *N*-(2-hydroxypropyl) methacrylamide. Reprinted with permission from Bradley and co-workers.[74] Copyright 2019, Springer Nature.

successful in tumor-bearing nude mice. The results of the study demonstrated that both precursors were effectively converted into the active luciferin form within biological systems, resulting in the production of detectable bioluminescence signals. It is worth noting that, in both cellular and animal models, treatment with **L-1** yielded somewhat stronger bioluminescence signals compared to **D-1**, as shown in Fig. 9 *b*,*c*. This discrepancy may be indicative of stereoselective variations in cellular processing or activation efficiency between the two enantiomeric forms. It is evident that the enhanced stability and successful intracellular conversion of these precursor molecules render them a promising alternative to conventional *D*-luciferin. It is anticipated that this will enhance the utility and reliability of bioluminescence imaging in applications where substrate instability has previously posed a significant constraint. The *in vivo* conversion efficiency of precursors remains limited, and the bioluminescence intensity is lower than that of natural luciferin, which has a detrimental effect on the sensitivity of *in vivo* imaging. Furthermore, the metabolic pathway of oligomer intermediates and the potential immunogenicity of the process are not yet fully elucidated. The absence of tumor-targeting modification of precursors results in non-specific activation in normal tissues, which has a negative impact on the imaging signal-to-noise ratio.

3.2.2. Reductive activation polymerization imaging

In a related approach, Rao and co-workers[105] designed a novel small-molecule scaffold based on a carbohydrate linker and the well-established CBT-cysteine condensation reaction. This scaffold is engineered to undergo rapid polymerization upon encountering specific physiochemical changes, such as a reductive microenvironment, forming what is described as a pseudopolysaccharide structure. As depicted in Fig. 9 *d*,*e*, the construct was synthesized by linking the CBT group to the C-6 position of a glucosamine unit *via* a click reaction, while a cysteine residue was attached to the C-2 amine *via* a peptide linker. In order to facilitate visualization, the researchers conjugated an IR800 dye as an imaging moiety, creating fluorescent probes 1 and 2. These probes allowed the assessment of both fluorescence and photoacoustic properties, facilitating dual-modality tracking. A pivotal challenge that this work sought to address was the real-time detection of polymerization within living animals. The team successfully demonstrated *in situ* polymer formation triggered by reductive activation in mouse models by employing combined fluorescence and photoacoustic (PA) imaging. This multimodal imaging strategy not only confirmed the responsiveness of the system but also provided spatial and temporal insights into the polymerization process *in vivo*. It is anticipated that this stimuli-responsive scaffold will exhibit considerable potential for adaptation to other tumor-specific triggers, such as enzyme activation. Extending the system in this direction could enhance its selectivity for tumor microenvironments and broaden its applicability in diagnostic imaging and targeted therapeutic delivery. The system demonstrates a response to the reductive microenvironment, exhibiting incomplete tumor specificity. It has been observed that normal cells with high GSH levels (such as hepatocytes and renal cells) are capable of producing non-specific signals, thereby affecting imaging specificity. Furthermore, the metabolic clearance pathway of the polymer formed *in situ in vivo* remains unclear, and the safety of long-term retention in the body requires further verification.

3.2.3. Bioorthogonal polymerization for artificial organelle imaging

Zhang and co-workers[75] reported an innovative intracellular polymerization strategy that leverages bioorthogonal click

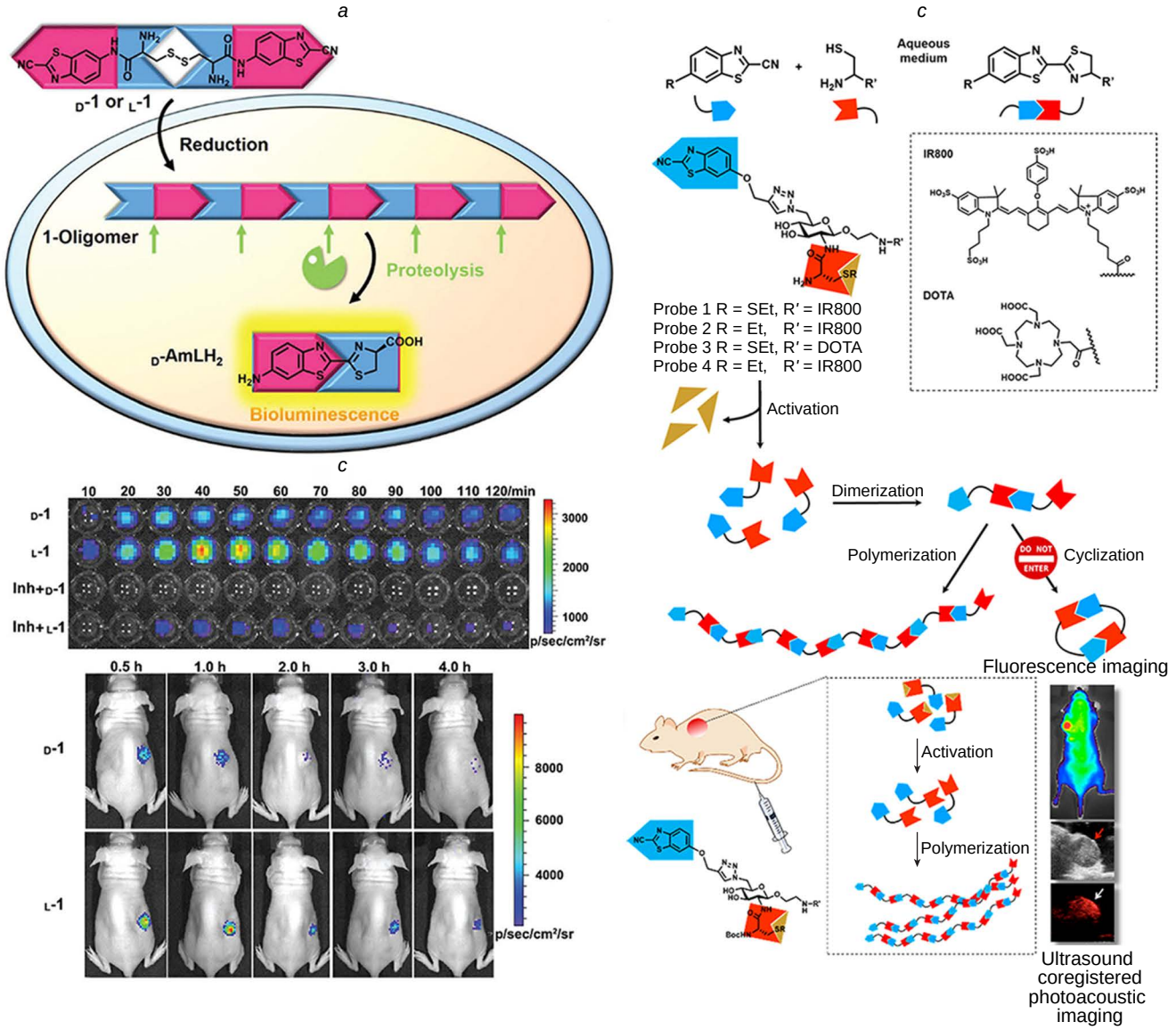


Figure 9. Chemical structure of **D-1** or **L-1** and schematic illustration of their intracellular reduction-controlled condensation to form linear oligomer and subsequent proteolysis of the oligomer to yield *D*-amino luciferin for bioluminescence generation (*a*). Time-course bioluminescence images of fLuc-transfected MDA-MB-231 cells incubated with 25 mM D^{-1} (top row), **L-1** (second row), pretreated with protease inhibitor then **D-1** (third row), or pre-treated with protease inhibitor then **L-1** (bottom row) acquired at indicated time points in a serum-free culture medium at 37 °C (*b*). Time-course bioluminescence imaging of nude mice xenografted with fLuc-transfected MDA-MB-231 tumor cells after intraperitoneal injection of 17.8 mmol kg^{-1} **D-1** (top row) or **L-1** (bottom row) at 2.5 mM in saline acquired at different time points (*c*). Reproduced with permission from Liang and co-workers.[104] Copyright 2017, Royal Society of Chemistry. Probes undergo polymerization upon reductive activation for fluorescent and photoacoustic imaging: Condensation reaction between cyanobenzothiazole and cysteine (*d*). Probes 1 and 3 undergo polymerization upon reductive activation. Control probes 2 and 4 remain as monomers under the same conditions (*e*). Reproduced with permission from Rao and co-workers.[105] Copyright 2020, American Chemical Society.

chemistry for monomer conjugation. This enables the efficient *in situ* construction of three-dimensional crosslinked 'polymeric artificial organelles' within living host cells. To achieve this, two complementary monomers were designed and synthesized, designated as 1 and 2 (Fig. 10). Each monomer is characterized by a tribranched core, which is functionalized with three reactive groups, either tetrazines (represented by blue hemispheres) or norbornenes (red hemispheres). Each monomer is also equipped with a selective cell-penetrating peptide (AKRGARSTA, indicated by green arrows), which facilitates facilitate targeted cellular entry. Guided by the IEDDA reaction, a bioorthogonal click chemistry known for its fast kinetics and biocompatibility, the team selected 3-methyl-6-phenyl-1,2,4,5-tetrazine and norbornene as the mutually reactive pair for intracellular polymerization. The incorporation of the selective cell-penetrating peptide ensured that monomers were preferentially internalized by target MDA-MB-231 cells, while showing minimal uptake in control HK-2 cells, demonstrating cellular specificity. In contrast to conventional nanomaterials, which are frequently sequestered and degraded in lysosomes, only a minor fraction of these monomers or the subsequently formed polymeric organelles localize to lysosomal compartments. This favorable intracellular distribution exerted negligible effects on cell viability. Once inside the cell, the bioorthogonal reaction between the tetrazine and norbornene groups drove the formation of submicrometer-sized, stable 3D crosslinked particles. These

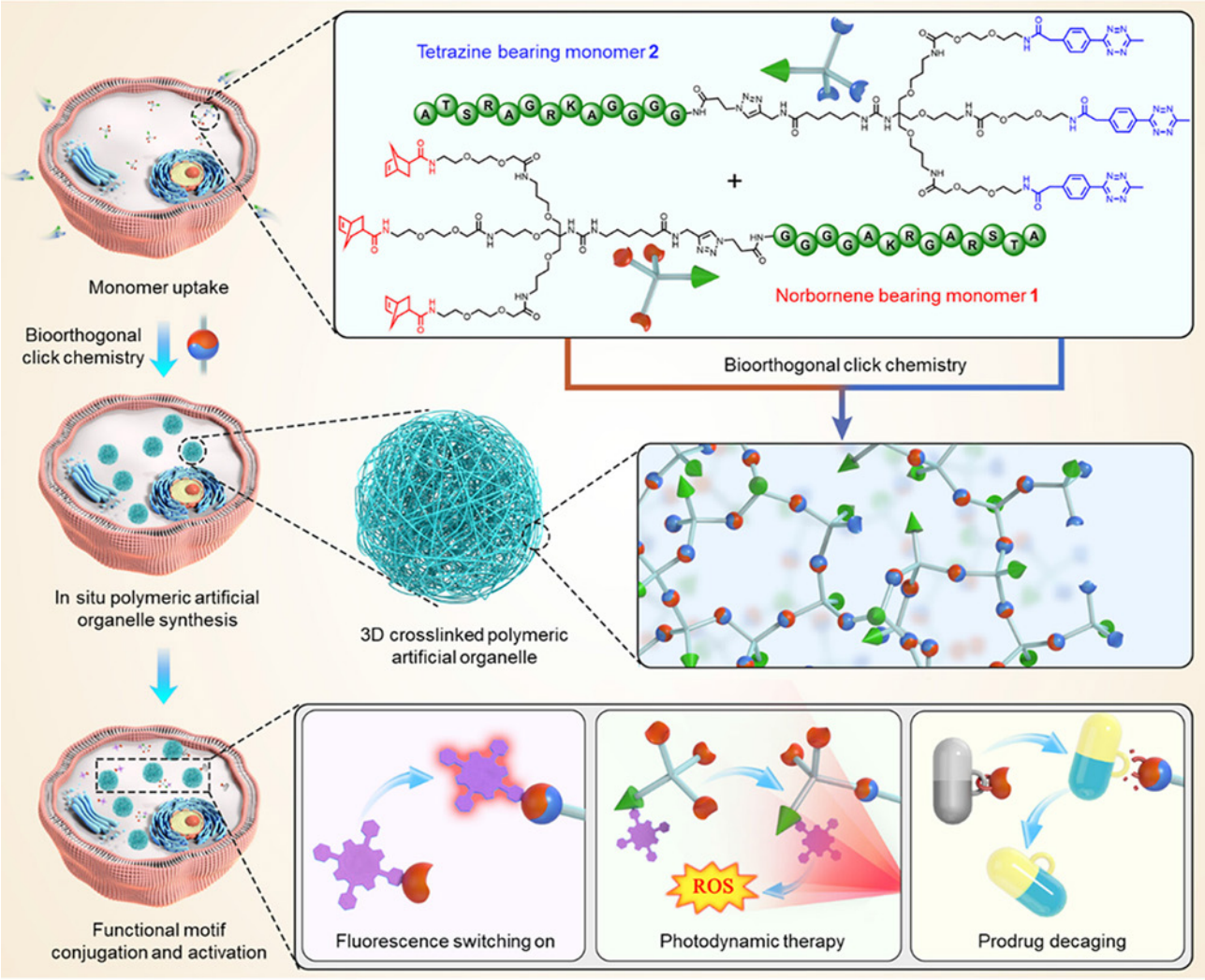


Figure 10. Overview of the polymeric artificial organelle synthesis in cells to enable the incorporation of unnatural functionalities that mediate a range of chemistries. Reproduced with permission from Zhang *et al*.[75] Copyright 2025, American Chemical Society.

polymeric artificial organelles significantly enhanced the intracellular retention and stability of the functional components, thereby enabling a suite of unnatural cellular functions. For instance, a fluorophore that was initially quenched due to aggregation in aqueous environments became activated upon polymerization. Furthermore, the platform allowed for the conjugation of a photosensitizer for photodynamic therapy (PDT) and the controlled release of a caged prodrug for chemotherapy, demonstrating its multifunctional utility. This work establishes a novel and robust methodology for fabricating stable artificial organelles inside living cells, opening new avenues for advanced engineering functions into biological systems. It has the potential to significantly advance applications in synthetic biology, cell engineering, and the development of living robotic systems. The synthesis process of tribranched monomers is complex, with a low total yield and high cost, which makes large-scale preparation difficult. Furthermore, the long-term intracellular fate of artificial organelles and their impact on the function of normal organelles, such as mitochondria and the endoplasmic reticulum (ER), require further clarification. In addition, the targeting specificity of cell-penetrating peptides is limited, and normal cells also have a certain degree of uptake.

3.2.4. Metal-catalyzed fluorogenic reactions

Mascareñas and coworkers[106] have reported the first examples of intracellular synthesis of 2-substituted indoles from *ortho*-azido styryl arenes, successfully converting exogenous substrates into valuable synthetic products *via* visible-light photocatalysis. Through the judicious alignment of excitation sources with suitable photocatalysts, a substantial enhancement in ratio of the catalyzed to non-catalyzed photochemical processes was achieved (Fig. 11 *a*). It is noteworthy that a photocatalyst derived from Eosin Y, designated Eosin-cRGD, produced markedly stronger fluorescence inside HeLa cells compared to MCF7 cells, which express lower levels of integrins. These observations confirm the potential of this strategy for selective imaging of specific cancer cell populations, pointing toward promising applications in precision medicine. Eosin Y photosensitizers have been shown to possess a rapid photobleaching rate, resulting in the evident decay of signal during prolonged imaging procedures. The imaging depth is constrained by the penetration of visible light, which is only adequate for superficial tissue analysis or cell-level research. Moreover, the metabolic toxicity of indole products in organisms has not been the subject of sufficient long-term evaluation data.

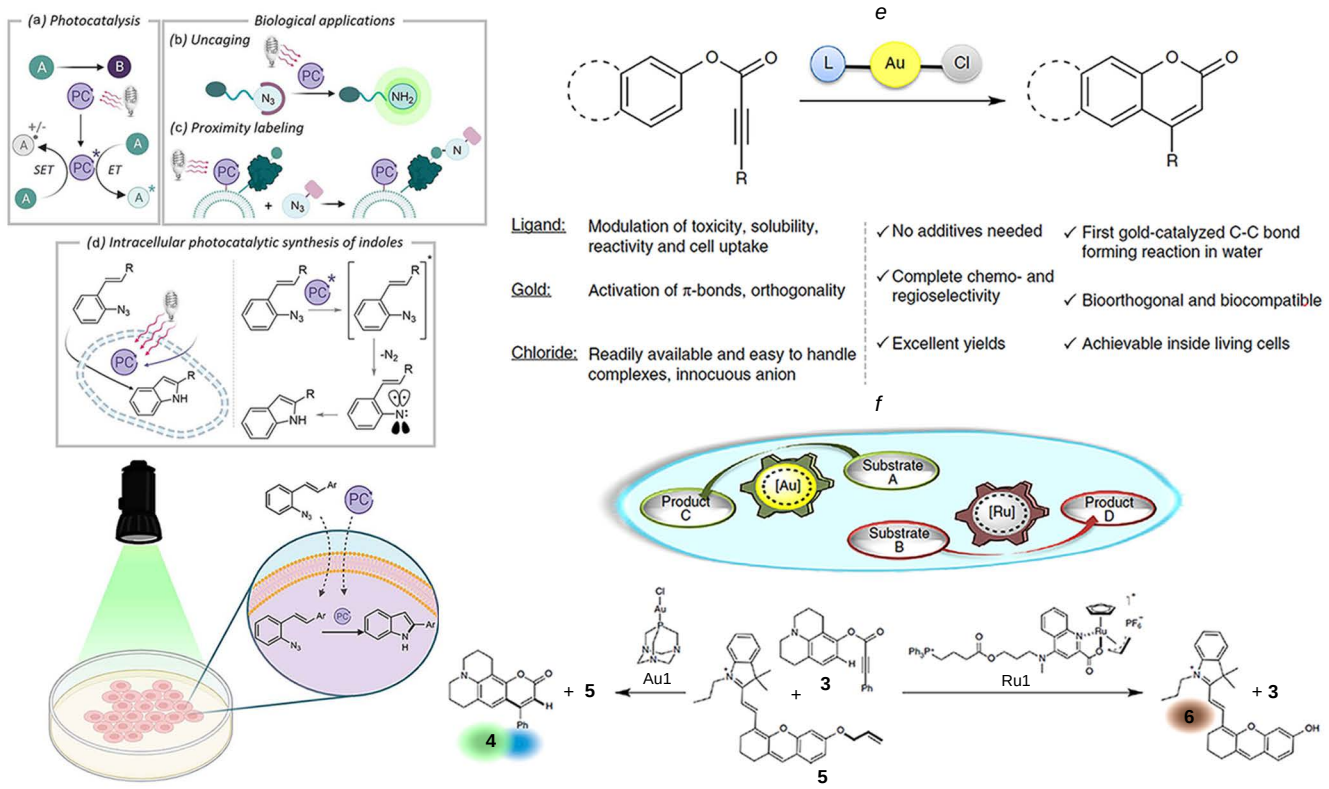


Figure 11. Outline of direct photocatalytic activation mechanisms (*a*). Schematic representation of photobiological applications of aryl azides (*b*, *c*). This work: Photocatalytic synthesis of indoles in cells and schematic outline of a putative mechanism (*d*). Reproduced with permission from Mascareñas and co-workers.[106] Copyright 2024, American Chemical Society. Concurrent Au(I) and Ru(II) catalysis and intracellular transformations: Gold-chloride complexes as ligand-tuned, water-activatable precatalysts, and proposed gold-promoted carbocyclization (*e*). Mutually orthogonal, and bioorthogonal, gold and ruthenium catalysis inside living cells (*f*). Reproduced with permission from Mascareñas and co-workers.[107] Copyright 2018, American Chemical Society.

Furthermore, it was also demonstrated that readily accessible and ligand-tunable gold(I)-chloride complexes can drive efficient hydroarylation reactions in complex aqueous media, including within living mammalian cells.[107] In contrast to conventional gold(I) catalysis performed in organic solvents, this C–C bond-forming cyclization in water does not require chloride scavengers, a crucial advantage for implementing such chemistry under physiological conditions. The reaction is characterized by its biorthogonal nature, biocompatibility, and the capacity to occur within living cells (see Fig. 11 *b*). While the gold-promoted transformation constitutes a significant expansion of the life-compatible reaction toolbox, it can be performed in parallel with another metal-mediated process inside cells, such as a ruthenium-catalyzed deallylation. This capacity to execute multiple designed catalytic reactions within living systems opens new avenues for biological intervention and is particularly intriguing from a fundamental perspective, paving the way toward engineered metal-based artificial metabolic networks. The pharmacokinetic behaviors of gold and ruthenium catalysts in cells are significantly different, which complicates the achievement of synchronous and optimal catalytic efficiency. Furthermore, the long-term accumulation of noble metals in the body has the potential to induce oxidative damage and organ toxicity. Additionally, the orthogonality of the dual catalytic system is susceptible to cross-interference in the complex intracellular environment.

Do and co-workers[108] demonstrated that unprotected organoiridium complexes can effectively promote transfer hydrogenation within living cells, using aldehyde-functionalized Bodipy derivatives as fluorogenic substrates (Fig. 12 *a*,*b*). This work provides compelling evidence that the catalytic reaction occurs intracellularly rather than in the extracellular environment. As described in Fig. 12 *c*–*i*, the following observations are particularly salient in substantiating this conclusion: the development of Bodipy-OH fluorescence specifically within the cytoplasm; the retention of the iridium catalyst inside the cells; and the essential requirement of endogenous reduced nicotinamide adenine dinucleotide (NADH) (or its phosphorylated analog, NADPH) for the reduction of the aldehyde group. This study presents a simple, additive-free, and non-toxic catalytic system that is straightforward to implement and readily scalable. Consequently, it provides a versatile new tool for the chemical biology toolkit. This advance has the potential to pave the way for the development of innovative biotechnological applications, such as detoxifying cytotoxic aldehydes associated with neurodegenerative diseases and the facilitation of novel intracellular bioconjugation strategies. Iridium complexes have been observed to lack precise targeting of intracellular distribution, and it has been demonstrated that normal cells will also produce non-specific signals, which has the effect of reducing imaging specificity. Furthermore, the metabolic clearance of noble metals *in vivo* is slow, and long-term toxicity data are missing. In addition, the applicable range of catalytic substrates is narrow, and it is difficult to expand to more functional molecules for multiscenario imaging.

In situ reaction-based fluorescence imaging strategies have been demonstrated to overcome the limitations of traditional pre-synthesized probes with regard to signal-to-noise ratio and retention time. However, there are still common bottlenecks: It is imperative that activation specificity is improved. The

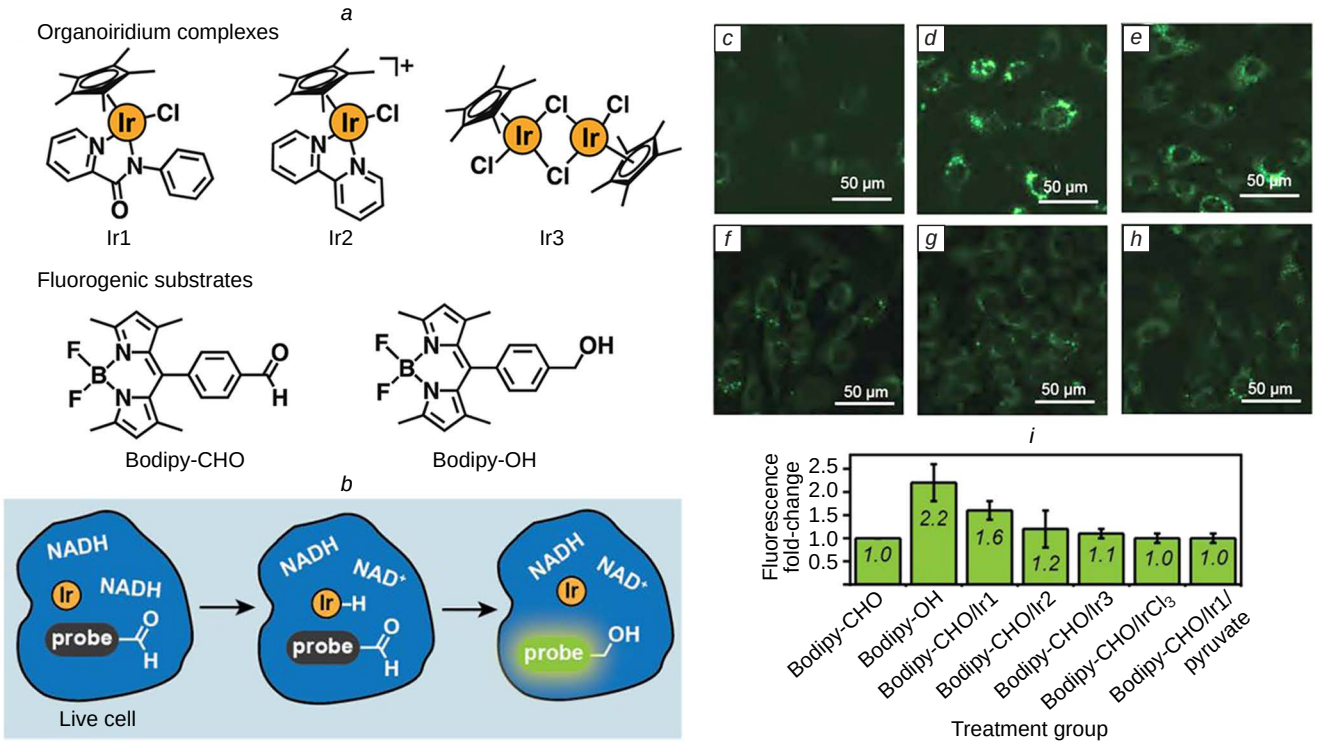


Figure 12. Iridium complexes and fluorogenic substrates used in cell studies (*a*). Proposed reaction of a fluorogenic aldehyde probe inside cells treated with Ir catalysts (*b*). Fluorescence confocal microscope images (40×) of NIH-3T3 cells treated with Bodipy-CHO (30 μM) (*c*); Bodipy-OH (30 μM) (*d*); Bodipy-CHO (30 μM)/**Ir1** (20 μM) (*e*); Bodipy-CHO (30 μM)/**Ir3** (10 μM) (*f*); Bodipy-CHO (30 μM)/$IrCl_3$ (20 μM) (*g*); and Bodipy-CHO (30 μM)/**Ir1** (20 μM)/sodium pyruvate (10 mM) (*h*). The plot in part *i* shows the fold-change in fluorescence of cells in different treatment groups relative to that observed in the Bodipy-CHO only treated cells. The fold-change values are the average measurements obtained from triplicate duplicate experiments, and the error bars show the standard deviation from the mean. Reproduced with permission from Do and co-workers.[108] Copyright 2017, American Chemical Society.

majority of probes are reliant upon single stimulus responses, and non-specific activation in normal tissues is pronounced, resulting in elevated background signals. Furthermore, there is an absence of quantitative capability. The quantitative relationship between the degree of *in situ* reaction and signal intensity remains to be elucidated, which is not conducive to accurate diagnosis and dynamic monitoring of disease progression. Insufficient tissue penetration: The majority of excitation light sources operate within the visible light spectrum. This capacity is limited to superficial tissue imaging and is inadequate for addressing the requirement for deep lesion imaging. Additionally, there is a lack of clarity regarding metabolic safety concerns. The long-term metabolic pathways and potential toxicity of reaction products and catalysts in organisms have not been systematically verified, which restricts clinical translation.

3.3. Antitumor research

Although nano-drug delivery systems have significantly optimized the pharmacokinetic properties and safety profile of anti-tumor drugs,[109] *in situ* chemical reactions are an emerging tumor treatment strategy, due to their targeted activation and local enrichment advantages. According to trigger mechanism and reaction type, representative antitumor strategies are divided into four categories: endogenous microenvironment-triggered polymerization, light-triggered *in situ* reactions, metal-catalyzed prodrug activation, and bioorthogonal polymerization therapy. To facilitate systematic comparison, the core parameters of representative strategies are summarized in Table 4.

PET-RAFT is photoinduced electron/energy transfers reversible addition – fragmentation chain transfer

3.3.1. Endogenous microenvironment-triggered polymerization

Natural biopolymers, including proteins, nucleic acids, polysaccharides and lipids, can be synthesized *in situ* within living organisms through a series of precisely regulated enzymatic and genetic mechanisms. This controlled *in situ* synthesis enables their intricate assembly into complex structures with specific functions, which are fundamental to virtually all biological activities. These biopolymers function as vital components in various aspects of cellular processes, including cellular architecture, molecular recognition, information storage and transmission, catalysis, and energy conversion. The capacity for these proteins to be synthesized as required and to be spatially organized within cells or tissues highlights their pivotal function in growth, development, adaptation, and homeostasis. Moreover, the study of these natural synthesis processes provides key insights for the development of advanced biomimetic materials and synthetic biology applications. Herein, an innovative strategy for the *in situ* biosynthesis of a functional conjugated polymer specifically within the TME was developed.[110] This approach capitalizes on the overexpression of hydrogen peroxide that is characteristic of the TME. Upon co-injection of horseradish peroxidase (HRP), H_2O_2 is catalyzed to generate hydroxyl radicals (•OH). These radicals then initiate the polymerization of a carefully designed, water-soluble aniline dimer derivative, *N*-(3-sulfopropyl) 4-aminodiphenylamine

Table 4. Comparison of efficacy and translational potential of typical *in situ* reaction antitumor strategies

Representative strategy	Reaction type	Trigger mode	Tumor model	Tumor inhibition rate	Main safety performance	Administration route	Clinical translation potential	Core basis for translation rating	Refs
TME-responsive polyaniline polymerization	Oxidative polymerization	Endogenous H_2O_2+HRP	Mouse xenograft	~60–70%	Low systemic toxicity	Intratumoral injection	Medium	NIR-II imaging guidance supports translation; exogenous enzyme carries immunogenic risk	110
Te-mediated oxidative polymerization	Oxidative polymerization	Endogenous ROS	HepG2 xenograft	~75%	Mild body weight change	Intravenous injection	Medium	High endogenous trigger selectivity; tellurium metabolic toxicity to be verified	111
PET-RAFT intracellular polymerization	Radical polymerization	Visible light	MDA-MB-231/4T1	~70–80%	Light-dependent toxicity	Intravenous injection	Medium	Prominent spatiotemporal controllability; limited by light penetration depth	112
Hypoxia-initiated supramolecular polymerization	Radical polymerization	Tumor hypoxia	4T1 xenograft	~80%	High tumor selectivity	Intravenous injection	Medium-low	Complex supramolecular system; cucurbituril safety to be verified	113
Light-triggered hydrogel PDT-immunotherapy	Photopolymerization+PDT	660 nm light	Mouse tumor model	~90% (combined immunotherapy)	Good local safety	Intratumoral injection	High	Local administration with mature PDT basis; repeated stimulation enhances immune response	114
DFY peptide polymerization immunotherapy	Enzymatic oxidative polymerization	Tyrosinase	Melanoma model	Prolongs survival by ~40%	Good bio compatibility	Transcutaneous administration	High	Endogenous enzyme trigger with safe peptide raw materials; validated in minipig models	115
Cu-catalyzed prodrug activation	CuAAC click reaction	Intracellular GSH reduction	HeLa xenograft	~60%	Potential copper toxicity	Intravenous injection	Low	Metal safety risk; non-specific uptake by reticuloendothelial system	116
Schiff base intracellular polymerization	Condensation polymerization	Exogenous monomer+catalyst	Cell line/xenograft	~70%	Certain normal cell toxicity	Intracellular delivery	Low	Poor tumor selectivity; scandium catalyst has non-specific toxicity	88

Note. PET-RAFT is photoinduced electron/energy transfers reversible addition−fragmentation chain transfer.

(SPA), directly at the tumor site, transforming it into polySPA (PSPA) nanoparticles. A key advantage of this *in situ* polymerization is the transition of the material's size from small molecular precursors to larger polymeric nanostructures, which significantly enhances the local accumulation and retention of PSPA within tumors due to the enhanced permeability and retention (EPR) effect. The resulting PSPA, a conjugated polymer, demonstrates notable NIR-II absorption properties. The property was harnessed for tumor-specific NIR-II PA imaging and effective photothermal therapy, thereby improving the precision and efficacy of tumor theranostics. This work establishes a pioneering method to exploit TME-activated biochemical reactions for the localized synthesis of functional polymers, offering a promising pathway to address key challenges in targeted cancer treatment and diagnosis. This strategy necessitates the concurrent delivery of HRP enzyme and monomer, yet the extent to which intratumoral distribution of these components is uniform remains challenging to regulate. The disparate distribution of H_2O_2 within the tumor engenders considerable heterogeneity in the degree of polymerization, thereby exerting an influence on the uniformity of the therapeutic effect. Moreover, the administration of exogenous HRP carries a potential immunogenic risk, a factor that serves to limit the feasibility of repeated administration.

In a complementary study, Li and co-workers [88] demonstrated that chemical reactions, specifically the Schiff base reaction, can be performed within living cells to synthesize sophisticated polymeric structures. As shown in Fig. 13*a*, they employed molecular engineered monomers that undergo intracellular polymerization, forming a hollow covalent organic polymer (HCOP). The synthesis process entails a dynamic sequence of growth, hollowing, dissolution, and recondensation, culminating in the formation of woolen-ball-like morphologies. This direct intracellular polymerization strategy circumvents the difficulties associated with internalizing pre-formed large particles, thereby improving the cellular uptake and bioavailability of the micro-sized HCOP. The resulting HCOP, characterized by a specific porous architecture and a large surface area, actively interfaces with cellular components. This results in significant perturbations to key physiological activities, leading to reduced cellular motility, mitochondrial dysfunction, and the induction of apoptosis and necroptosis (see Fig. 13*b–e*). This work introduces a novel modality in cell biology and therapeutics, showcasing how artificially mediated intracellular synthesis can be used to construct bioactive materials that directly modulate cellular fate from within. Collectively, these two studies highlight the transformative potential of *in situ* synthesis strategies within biological systems, one leveraging endogenous pathological cues especially TME and the other deploying exogenous artificial chemistry inside cells. Both approaches enable the localized generation of functional polymeric materials with enhanced therapeutic precision and biological activity, opening new frontiers for advanced biomedical applications. The system under discussion necessitates the concurrent delivery

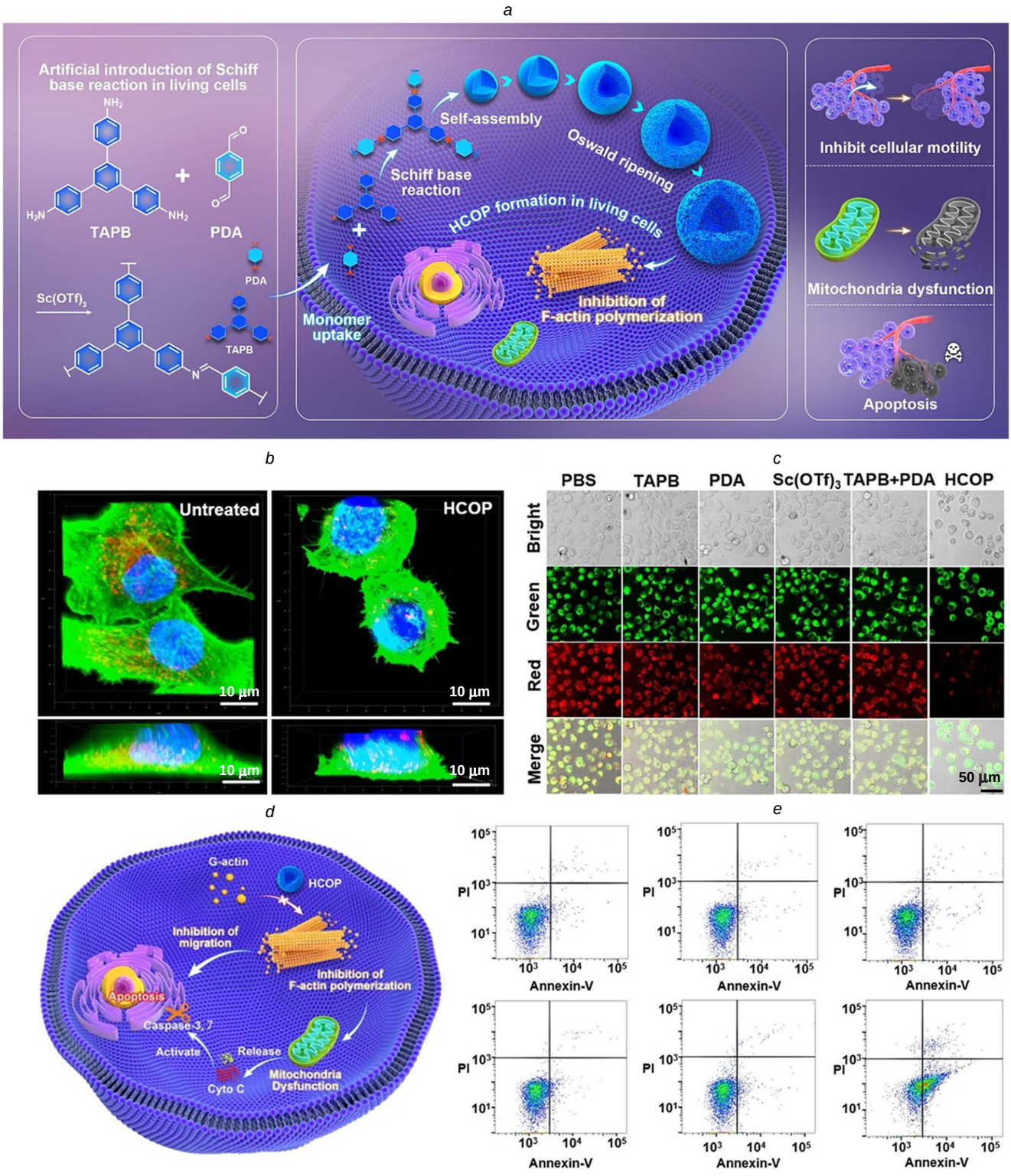


Figure 13. Artificial introduction of Schiff base reaction in living cells for *in situ* synthesis of HCOP (*a*). Intracellular generation of HCOP induces mitochondria dysfunction and programmed cell death: confocal fluorescence images of untreated cells and HCOP-generated cells stained for actin filaments (green), cell nucleus (blue) and mitochondria (red). The cells were treated with TAPB (120 μM) for 0.5 h, followed by treatment with PDA (120 μM) and $Sc(OTf)_3$ (120 μM) for 6 h, then stained for actin filaments, cell nucleus and mitochondria (*b*). Confocal fluorescence images of mitochondrial membrane potential (*c*). Mechanism of HCOP-induced cell deat (*d*). Degree of apoptosis and necroptosis induced by intracellular generation of HCOP as determined by flow cytometry; apoptosis: annexin-V-positive and PI-negative; necroptosis: PI-positive (*e*). TAPB is 1,3,5-triaminobenzene, PDA is *p*-phenylenedicarbaldehyde. Reproduced with permission from Li and co-workers.[88] Copyright 2023, John Wiley and Sons.

of two monomers and a scandium catalyst, a process which is notable for its elevated level of complexity in terms of administration. The catalyst $Sc(OTf)_3$ has been observed to demonstrate non-specific toxicity and an inadequate degree of tumor selectivity, a property which renders it susceptible to causing damage to normal tissues. Furthermore, the time and

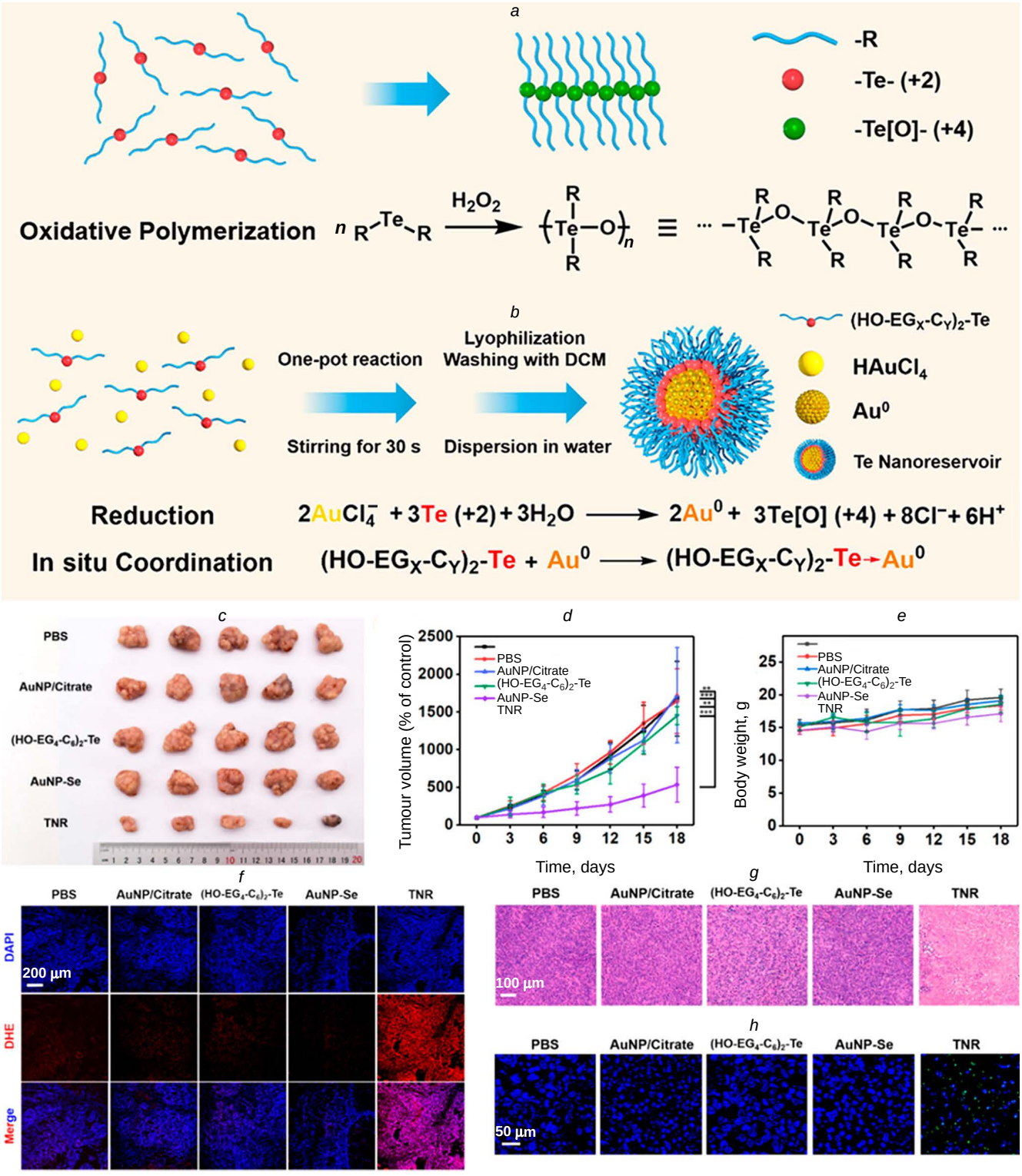


Figure 14. Synthesis and characterization of Te nanoreservoirs (TNRs) for oxidation polymerization: Oxidative polymerization of Te-containing molecules (*a*), Synthetic process of Te nanoreservoirs (*b*). Intracellular oxidative polymerization for *in vivo* cancer treatment: Digital photographs of tumors in each group (*c*). Relative tumor growth curves of HepG2-tumor-bearing mice ($n = 5$) after intravenous (i.v.) injection of PBS (control group) or various agents as indicated (*d*). Changes in body weights of HepG2-tumor-bearing mice in different groups during the treatment (*e*). Confocal fluorescence images of tumor slices collected at 24 h after i.v. injection of various agents and stained with a ROS probe, DHE (*f*). Images of H&E-stained tumor slices from various groups (*g*). Confocal fluorescence images of tumor slices from different groups by terminal deoxynucleotidyl transferase mediated dUTP nick-end labeling (TUNEL) staining (*h*). PBS is phosphate-buffered saline, DHE is Dihydroethidium. Reproduced with permission from Xu and co-workers.[111] Copyright 2021, American Chemical Society.

degree of intracellular polymerization are challenging to regulate with precision, and the controllability of the treatment is deemed to be insufficient.

Xu and co-workers[111] have reported a novel strategy for conducting ROS-triggered polymerization within living cells, leveraging the unique coordination capability and ultra-sensitive

oxidative responsiveness of organotellurium compounds. As depicted in Fig. 14*a*,*b*, the resultant tellurium-oxygen (Te–O) polymers selectively interact with cellular antioxidant defenses *via* interactions between Te(IV) and selenoproteins. This interaction locally suppresses antioxidant activity, thereby preserving the elevated ROS levels required to sustain the polymerization process. It is important to note that, due to intrinsic biochemical differences, particularly the elevated baseline ROS status in malignant cells, the polymerization reaction occurs preferentially within cancer cells rather than in healthy ones. This selectivity enables the targeted induction of apoptosis in cancerous cells, thus providing a potential therapeutic strategy. The validity of this approach has been demonstrated through a combination of *in vitro* experimentation at the cellular level and *in vivo* investigation using animal models (see Fig. 14*c*–*h*). A significant advantage of this method is its operational simplicity and biocompatibility; it does not require high monomer concentrations or external physical or chemical stimuli. Instead, polymerization is autonomously initiated and sustained by the inherent biochemical microenvironment of the target cells. This work considerably expands the toolbox for intracellular polymerization and opens new avenues for selectively modulating cell behavior in living systems, with promising implications for targeted cancer therapy and fundamental cell biology research. The *in vivo* metabolism and long-term toxicity of organotellurium compounds have not yet been the subject of a systematic toxicological evaluation. The difference in ROS level between normal cells and tumor cells is limited, and there is a certain risk of off-target effect. In addition, there is a lack of quantitative monitoring methods for the degree of polymerization *in vivo*, which makes it difficult to dynamically evaluate the treatment process.

Wang and co-workers[113] developed an innovative supramolecular system that utilizes the tumor's unique reducing microenvironment to trigger targeted intracellular polymerization for cancer therapy. This basis of this system is a host-guest complex formed between cucurbit[7]uril (CB[7]) and a perylenediimide derivative (PDI), denoted as PDI+2CB[7]. Within the hypoxic and reductive conditions of the tumor, this complex undergoes reduction to generate stable, delocalized free radical anions. Crucially, CB[7] plays a pivotal role in stabilizing these reactive species, preventing their premature deactivation and enabling them to function as efficient initiators within the cellular milieu. Subsequently, the stable radicals initiate a free radical polymerization reaction with the co-delivered, biocompatible monomer 2-hydroxyethyl methacrylate (HEMA). This hypoxia-initiated supramolecular free radical system has been shown to successfully carry out intracellular polymerization within 4T1 cancer cells (Fig. 15). The rapid formation of poly(HEMA) networks *in situ* acts as a direct physical intervention, causing severe disruption to critical cellular structures, including the cytoskeleton and various organelles. This process of intracellular materialization leads to a significant suppression of tumor cell metabolism and function,

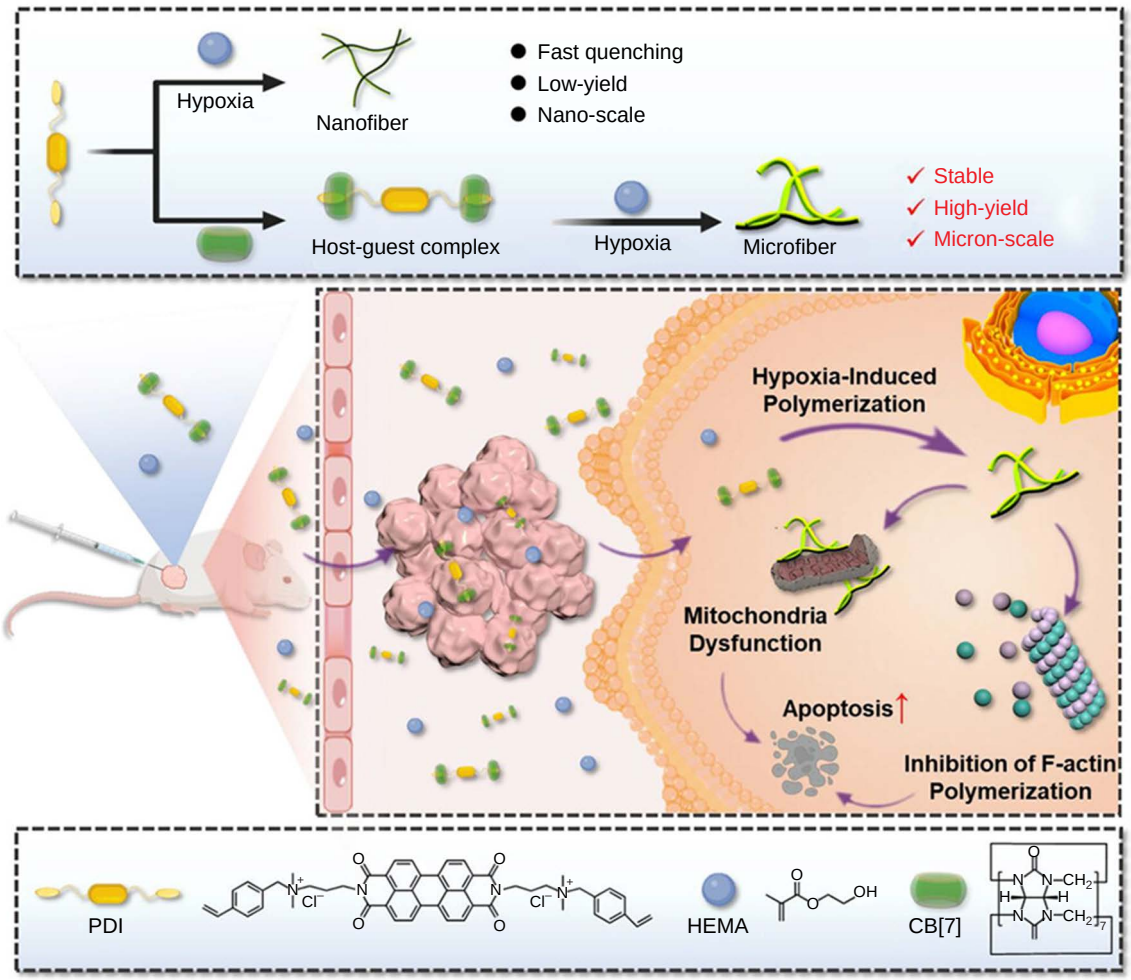


Figure 15. Schematic illustration of intracellular polymerization induced by supramolecular radical anions in a hypoxic tumor microenvironment. Reproduced with permission from Wang and co-workers.[113] Copyright 2025, American Chemical Society.

resulting in a potent antitumor effect. Importantly, due to the specific activation of the system by pathological tumor conditions (hypoxia/reduction), healthy tissues with normal redox states remain unaffected. These results result in a high therapeutic selectivity without observable systemic toxicity. This study establishes a novel paradigm, demonstrating that supramolecularly stabilized, endogenous stimulus-responsive radicals can be harnessed to drive controlled polymerization reactions inside diseased cells. This approach has been demonstrated to achieve selective and effective tumor inhibition through a non-chemotherapeutic, physically disruptive mechanism. It thus offers a promising new avenue in precision cancer treatment. This strategy is only effective in response to a hypoxic microenvironment, with limited efficacy in tumors exhibiting normal oxygen content. The supramolecular system demonstrates inadequate stability during blood circulation, leading to premature dissociation and, consequently, a reduction in tumor targeting efficiency. Furthermore, the *in vivo* safety and immunogenicity of the host molecule, cucurbituril, require validation in large animals.

Zhao and co-workers[117] developed a nanocompartment-confined strategy that has been successfully utilized to realize a broad spectrum of polymerization within living systems. This approach utilizes engineered nanocompartments to create a spatially confined microenvironment for reactions. Confinement has been demonstrated to result in elevated local concentrations of monomers, thereby substantially augmenting and significantly increasing the polymerization rate through the enhancement of effective monomer collisions (Fig. 16*a*). Furthermore, compartmentalization sequesters the active polymerization process, shielding it from potential interference by cellular components and mitigating the influence of the generated polymers on normal cellular functions. This strategy has been demonstrated to enhance dramatically enhances the feasibility and efficiency of conducting artificial polymerizations in living systems. Experimental findings have validated that the nanocompartment-confined design enhances not only reaction efficiency and control but also facilitates multiple types of polymerizations that were previously challenging to achieve in biological environments. A key application of this platform was demonstrated in the context of cancer therapy. The product of this process, through endogenous oxidative polymerization confined within nanocompartments, could harvest light to produce heat, effectively ablating tumor cells and activating a potent photothermal immunotherapy (PTI) response (see Fig. 16*b*). The confinement effect was determined to be a critical factor in the therapeutic efficacy of the treatment. In comparison with administrations employing free monomers, the

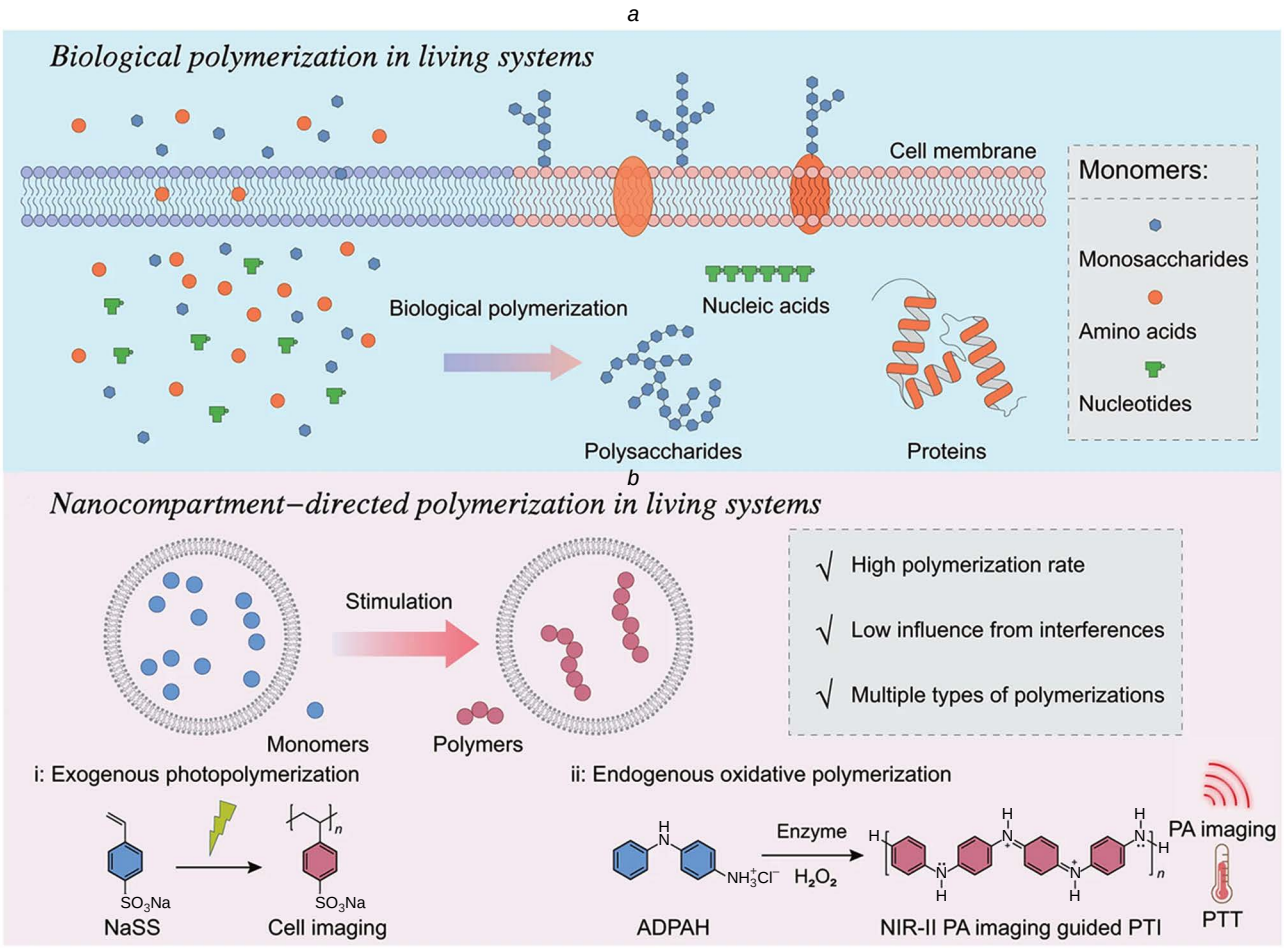


Figure 16. Schematic diagram of polymerization in living systems: Biological polymerization of monosaccharides, amino acids, and nucleotides for the synthesis of polysaccharides, proteins, and nucleic acids to constitute the elementary components, confer essential functionalities, and modulate the biological process (*a*). Nanocompartment-confined strategy to make a broad spectrum of polymerizations achievable in living systems: exogenous photopolymerization of the sodium salt of 4-styrenesulfonate (NaSS) and endogenous oxidative polymerization of *p*-aminodiphenylamine hydrochloride (ADPAH). NIR-II PA imaging second near-infrared photoacoustic imaging, PTI is photothermal immunotherapy, PTT is photothermal therapy (*b*). Reproduced with permission from Zhao and co-workers.[117] Copyright 2023, Springer Nature.

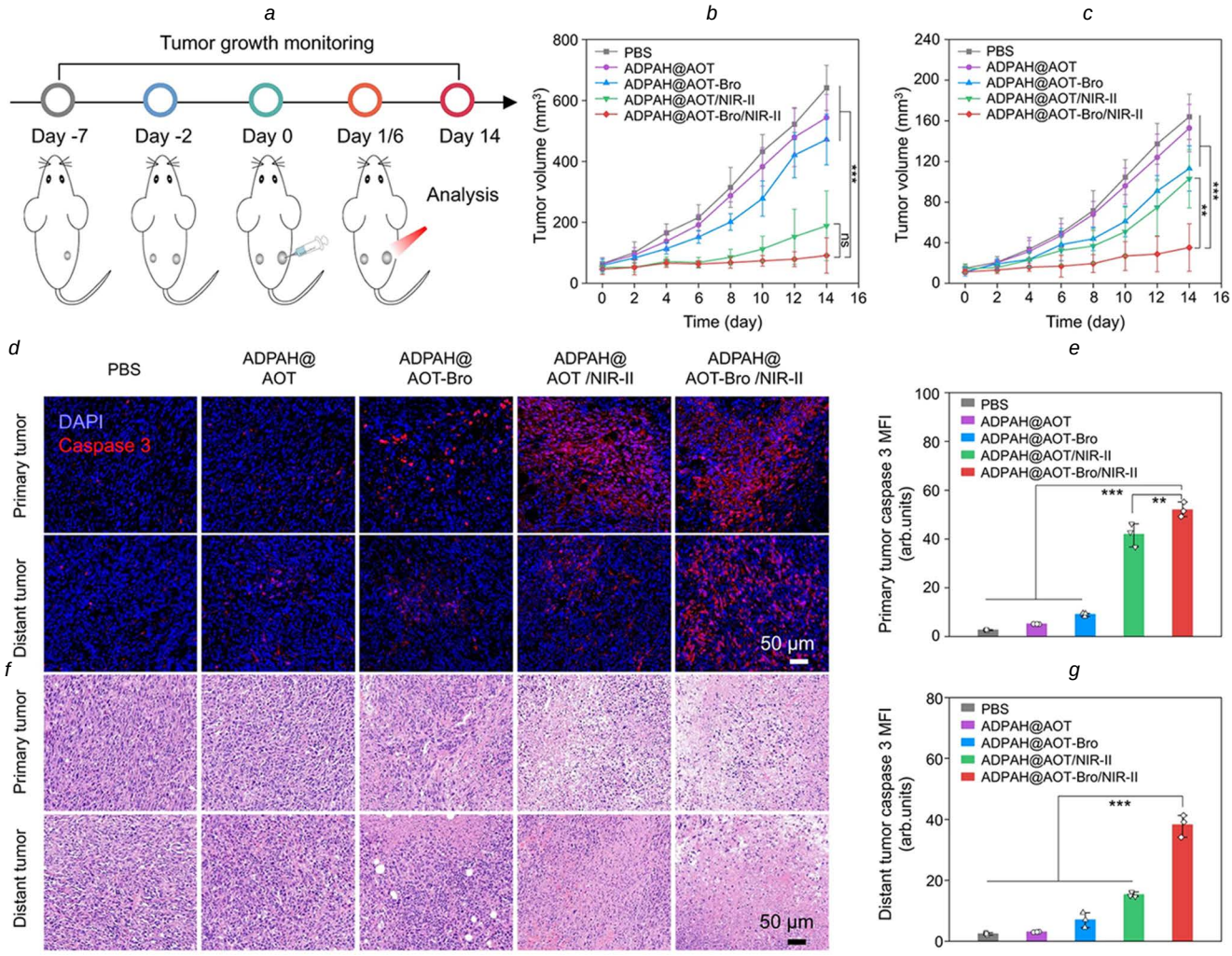


Figure 17. *In vivo* antitumor performance of ADPAH@AOT-Bro (AOT is sodium bis(2-ethyl-1-hexyl) sulfosuccinate): Schematic illustration of *in vivo* antitumor schedule (*a*). Tumor growth curves of primary (*b*) and distant (*c*) tumors in 4T1-tumor-bearing mice following various treatments (1064 nm, 5min, $n = 5$). Immunofluorescent images of active caspase-3 (red) in primary and distant tumor sections following various treatments (*d*). Quantification of expression level of active caspase-3 in primary (*e*) and distant (*f*) tumor sections from euthanized mice following various treatments ($n = 3$). H&E-stained images of the primary and abscopal tumor sections from euthanized mice following various treatments ($n = 3$) (*g*). Data were presented as mean ± SD. Reproduced with permission from Zhao and co-workers.[117] Copyright 2023, Springer Nature.

nanocompartment-based system elicited a 3.5-fold increase in temperature at the tumor site following ten minutes of second near-infrared (NIR-II) light irradiation. This enhancement illustrates the potential for significant dosage reduction and systemic toxicity mitigation. In summary, the nanocompartment-confined polymerization strategy effectively overcomes significant obstacles to synthetic polymerization in living systems. It facilitates the *in vivo* construction of polymers with diverse structures and functions, providing a universal and powerful platform for exploring polymerization biology and developing novel bio-hybrid therapeutic modalities. The penetration depth of nanocarriers in solid tumors is limited, and the coverage of deep tumor regions is difficult. The disassembly and release mechanism of the confined structure inside cells is not yet fully understood. Furthermore, the universality of this platform for different types of polymerization reactions needs to be expanded and verified (Fig. 17).

Zhang and coworkers[115] developed an innovative peptide-based tumor antigen-engineering platform for melanoma immunotherapy, centered on the Asp-Phe-Tyr (DFY) tripeptide. This system is predicated on the elevated expression of tyrosinase, a key melanogenic enzyme, within melanoma cells. Upon entering the cell, the DFY tripeptide undergoes tyrosinase-catalyzed oxidative polymerization, leading to its selective accumulation and the formation of poly(DFY) (pDFY) specifically in the target tumor cells (Fig. 18). Concurrently, the polymerization process, which is mediated by reactive quinone intermediates generated from tyrosine residues, facilitates a Michael addition reaction. This critical step covalently captures diverse, highly immunogenic endogenous proteins from cellular compartments such as the nucleus, mitochondria, and ribosomes. The substantial cross-linking and aggregation of cellular components result in a rapid, necrosis-like cell death process. Consequently, the tumor protein-cross-linked pDFY complexes are released from the disrupted cancer cells. The resulting fibrous aggregates possess a macromolecular structure that enhances their uptake by antigen-presenting cells (APCs), such as dendritic cells. The system's design is ingenious in its implementation of three key functions *in situ*. It utilizes covalent capture to collect a comprehensive array of tumor antigens,

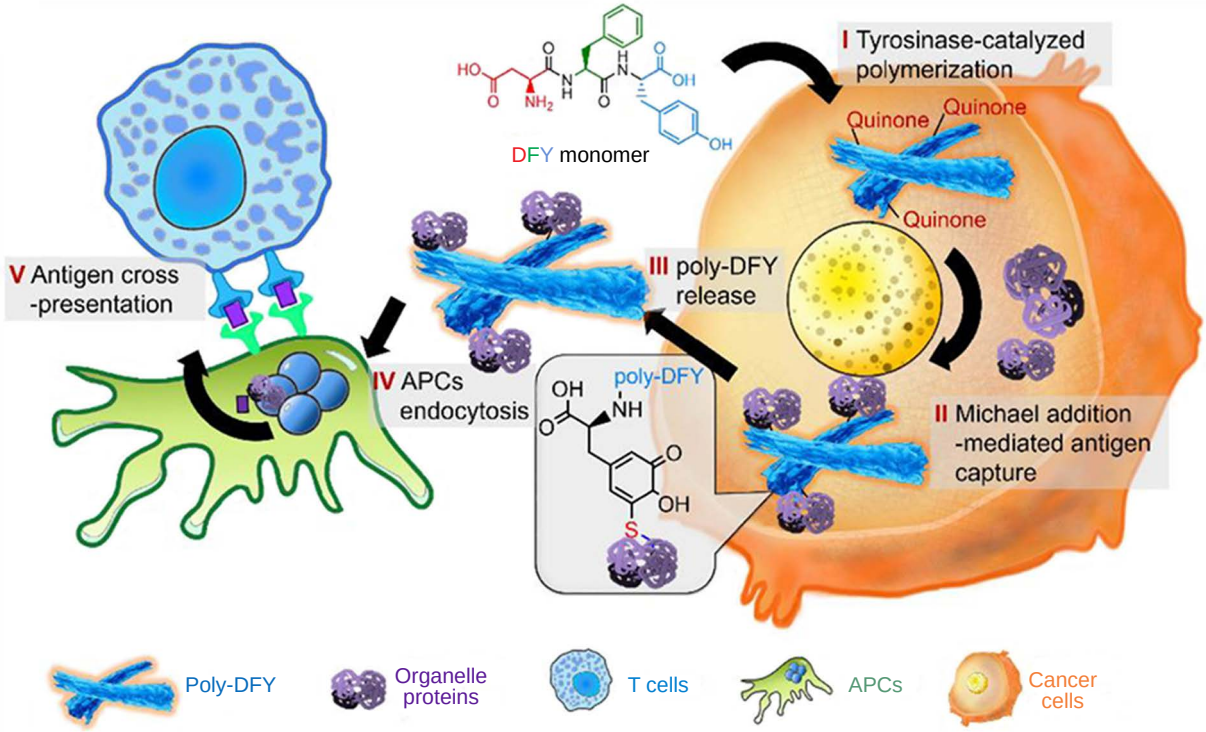


Figure 18. Schematic diagram for the working mechanism of DFY. This tripeptide is polymerized with tyrosinase in malignant melanoma cells. Michael addition between the quinone-rich structure of polymerized intermediates and sulfhydryl groups of cysteine residue captures intracellular proteins. The antigen-loaded microfibers with larger sizes are more likely to be engulfed by APCs. Reproduced with permission from Zhang and co-workers.[115] Copyright 2021, American Chemical Society.

subsequently packaging them into an aggregated form and delivering this antigenic payload to APCs with efficiency. The pDFY framework itself acts as an adjuvant, further boosting the ensuing immune response for systemic tumor elimination. This strategy has been demonstrated to be both highly efficacious and biocompatible in translational models. Transcutaneous immunotherapy with DFY has been shown to significantly prolong survival in tumor-bearing mice and has demonstrated promising results in minipig models. The study establishes a versatile and accessible platform for *in situ* antigen engineering, demonstrating how a simple peptide precursor can be transformed within the tumor into a potent immunogenic scaffold. This approach provides a compelling new direction for developing immunological materials that seamlessly integrate diagnostics and therapy by exploiting the tumor's own biochemical environment for personalized vaccine generation. It is important to note that the applicability of this strategy is restricted to cases of melanoma characterized by high tyrosinase expression, and the range of indications is limited. It is evident that tripeptides exhibit inadequate stability during blood circulation, rendering them susceptible to rapid degradation by proteases. Furthermore, the intensity of immune response exhibits significant inter-individual variability, and the uniformity of therapeutic effect is inadequate.

3.3.2. Light-triggered *in situ* antitumor reactions

Rao and co-workers[118] developed a novel *in situ* polymerization strategy to synthesize polymers directly within living cells using cell-permeable small-molecule monomers. As demonstrated in Fig. 19, this methodology is founded on a biocompatible polycondensation reaction between *L*-cysteine and CBT, which can be meticulously regulated through light irradiation to yield insoluble poly(luciferin) aggregates inside the cell. Notably, the study demonstrated that this intracellular polymerization process specifically activates the BiP-PERK-CHOP signaling pathway of the unfolded protein response (UPR). The resulting, unresolved ER stress subsequently initiates a form of regulated cell death consistent with paraptosis, a non-apoptotic cell death mode characterized by cytoplasmic vacuolation. Furthermore, the dying cells were found to release damage-associated molecular patterns (DAMPs), indicating the induction of immunogenic cell death (ICD), which can potentially stimulate antitumor immune responses (Fig. 20*a*–*i*). Collectively, these results demonstrate that *in situ* polymerization can effectively mimic the pathological accumulation of misfolded protein aggregates, thereby inducing potent proteotoxic stress and selective cancer cell death. This work presents an innovative therapeutic strategy that exploits the inherent vulnerability of cancer cells to proteostasis disruption, positioning intracellular polymerization as a powerful tool for both inducing cancer cell death and modulating the tumor immune microenvironment. The collective findings of these studies emphasize a transformative paradigm in biomaterials and therapy, namely the transition from the administration of pre-formed agents to the stimulation of their synthesis within the target biological milieu. These *in situ* polymerization strategies have been shown to achieve superior spatial precision, enhance local retention, and the ability to generate therapeutic effects directly from within cells. By harnessing or mimicking native and artificial biochemical processes, such approaches open promising avenues for developing highly specific and effective diagnostic and therapeutic platforms. Excitation light at 365 nm has been demonstrated to have minimal penetration depth into tissue, thus rendering it only suitable for superficial tumors. The immunogenic intensity of paraptosis remains a subject of debate,

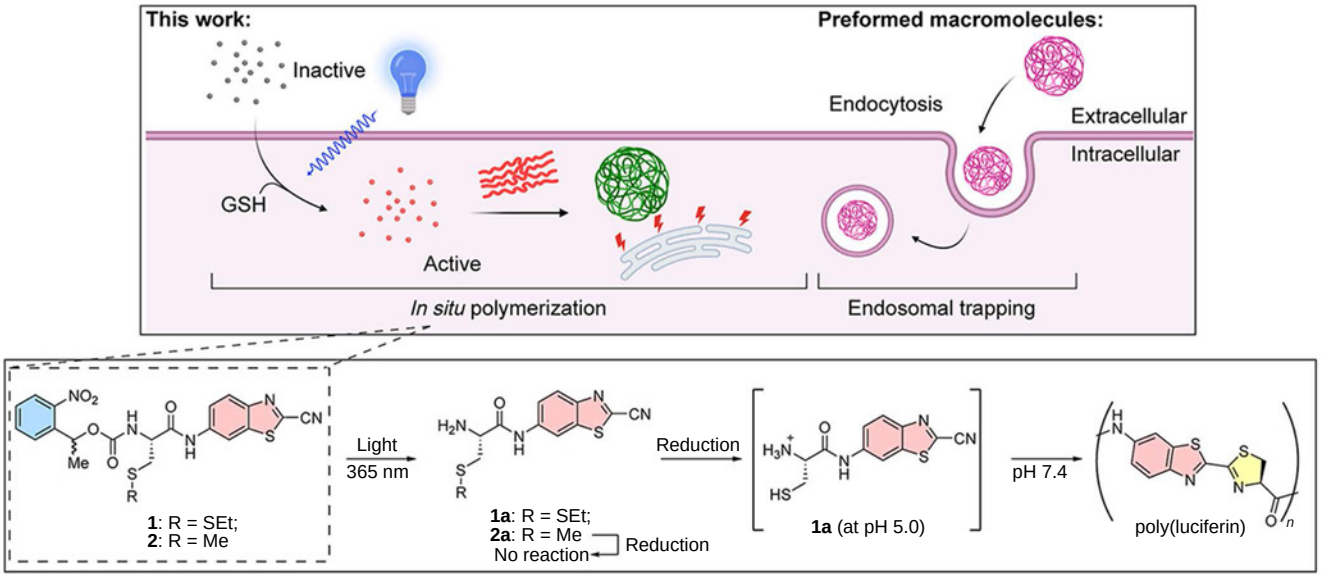


Figure 19. Scheme showing *in situ* polymerization in comparison to preformed macromolecules that suffer from endosomal trapping, and chemical structures and properties of monomers 1 and 2 (lower box). Reproduced with permission from Rao and co-workers.[118] Copyright 2025, American Chemical Society.

and the *in vivo* antitumor immune effect is thus far limited. Additionally, the spatial uniformity of light irradiation is challenging to regulate, resulting in an uneven polymerization degree in the tumor.

As demonstrated in Fig. 21 *a*, a novel photoactivatable prodrug system for cancer treatment has been developed, utilizing intracellular PET–RAFT polymerization.[112] In this approach, biocompatible monomers such as *N*,*N*-dimethylacrylamide (DMA) exhibit minimal inherent toxicity but become highly bioactive upon visible-light-mediated polymerization inside cells. The *in situ* formation of poly(DMA) within tumor cells has been shown to trigger multiple cytotoxic effects, including cell cycle arrest, induction of apoptosis and necroptosis, as well as marked suppression of cellular proliferation and motility (see Fig. 21 *b–f*). Notably, this intracellular polymerization strategy exhibited a substantial inhibitory effect on tumor growth and metastasis *in vivo*, thereby underscoring its therapeutic potential. The notion of utilizing monomers as 'prodrugs' that are selectively activated and polymerized only at illuminated target sites represents a promising new strategy in the field of oncology. This process facilitates the spatial regulation of the conversion of otherwise nontoxic precursors into bioactive polymeric agents, which are subsequently introduced directly within cancer cells. Consequently, intracellular polymerization establishes a novel therapeutic modality that combines precision, local activation, and potent cytostatic/cytotoxic outcomes, offering a versatile platform for targeted cancer intervention. The depth of visible light is limited, and deep tumors cannot be effectively activated. The long-term safety of monomers *in vivo* is not sufficiently data-driven, and the metabolic pathway of polymerization products remains opaque. Furthermore, the therapeutic window is narrow, and excessive light doses can easily cause normal tissue photodamage.

Beyond polymerization-based phototherapeutic strategies, nanocarrier-mediated *in situ* activation of photosensitizers constitutes another pivotal branch of light-triggered antitumor modalities. As systematically summarized in a recent review by Hong and Chang,[119] PDT, when used in combination with standard care treatments including chemotherapy, surgical resection and radiotherapy, can universally enhance tumor response rates, reduce recurrence risk and minimize treatment-related adverse effects across multiple malignancies such as lung cancer, breast cancer, cholangiocarcinoma and cervical cancer. These clinical and preclinical findings provide a strong translational rationale for developing *in situ* reaction-augmented PDT platforms with further improved tumor specificity and therapeutic efficacy.

Liu and coworkers[114] have developed a novel light-induced *in situ* hybrid hydrogel system designed to enable robust and sustained photodynamic immunotherapy against tumors. The system integrates a chlorin e6 (Ce6) photosensitizer, catalase (CAT), polymeric nanoparticles containing an immune adjuvant (RPNPs), and the cross linkable monomer poly(ethylene glycol) diacrylate (PEGDA). Upon red-light irradiation at the tumor site, the PDT process generates ROS, which serves a dual function: they induce direct tumor cell damage and simultaneously trigger a rapid polymerization reaction. This results in the light-triggered *in situ* gelation of the injected Ce6-CAT/RPNPs/PEGDA hybrid solution, forming a localized hydrogel depot directly within the tumor tissue (Fig. 22). A pivotal innovation of this approach is the hydrogel-enabled multiround PDT strategy. The formed gel functions as a reservoir, allowing for repeated light applications. It has been demonstrated that each round of PDT exerts a dual effect on tumor cells. In addition to directly eliminating them, the treatment also utilizes the tumor's retention of RPNPs as an adjuvant, thereby inducing the release of waves of tumor-associated antigens. This repeated simulation has been demonstrated to promote a potent and sustained antitumor immune response. When combined with systemic α-CTLA-4 checkpoint blockade immunotherapy, this localized treatment elicited a powerful systemic effect, effectively inhibiting the growth of untreated, distant abscopal tumors, highlighting its potential to control metastasis (Fig. 23). Moreover, a significant immune memory effect was observed in the treated mice, which resulted in long-term protection against subsequent rechallenge with cancer cells. The cited work underscores the therapeutic

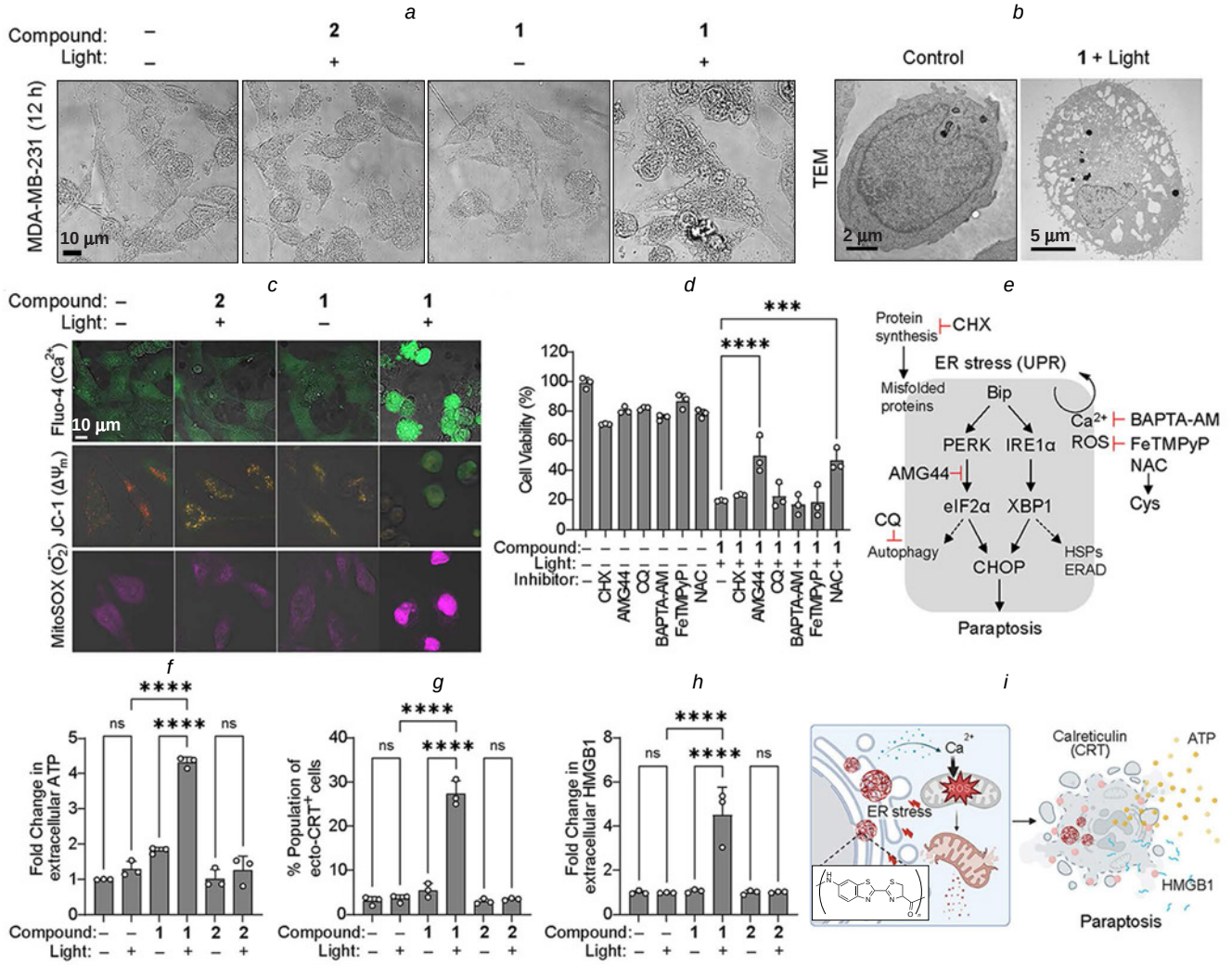


Figure 20. Intracellular luciferin polymerization induces paraptosis and immunogenic cell death: Brightfield images of MDA-MB-231 cells 12 h after being treated with 1 or 2 (10 μM) with or without irradiation. The treatment of 1 and light-triggered vacuolization (*a*). TEM images of the ultrastructure of MDA-MB-231 cells treated with DMSO or 1 (10 μM) with light (*b*). CLSM images of MDA-MB-231 cells treated with 1 or 2 (10 μM) with or without irradiation and stained with Fluo-4 AM (upper row), JC-1 (middle row), or MitoSOX Red (lower row) (*c*). Cell viability of MDA-MB-231 cells 24 h after being treated with 1 (10 μM) and light in the absence or presence of various inhibitors: CHX (2 μM), AMG44 (10 μM), CQ (2 μM), BAPTA-AM (2 μM), FeTMPyP (10 μM), and NAC (1 mM) (*d*). Schematic diagram of ER stress-induced paraptosis and mechanism of action of the tested inhibitors (*e*). Fold change in the ATP level in extracellular medium from 4T1 cells treated with 1 or 2 (10 μM) with or without irradiation (*f*). Percentage population of 4T1 cells analyzed by flow cytometry with surface-exposed calreticulin after being treated with 1 or 2 (10 μM) with or without irradiation (*g*). Fold change in HMGB1 abundance in extracellular medium from 4T1 cells treated with 1 or 2 (10 μM) with or without irradiation (*h*). Schematic illustration of intracellular polymer aggregates in inducing ER stress and disruption of calcium and mitochondria homeostasis that led to immunogenic paraptosis cell death (*i*). Reprinted with permission from Rao and co-workers.[118] CRT is calreticulin. CLSM is confocal laser scanning microscopy. TEM is transmission electron microscopy. Fluo-4 is Fluo-4 acetylmethyl ester (Fluo-4 AM) fluorescent probe that is frequently utilized for the detection of intracellular free calcium ions (Ca^{2+}). JC-1 is 5,5′,6,6′-tetrachloro-1,1′,3,3′-tetraethylbenzimidazole carbocyanine iodide, a specific probe for mitochondrial membrane potential. MitoSOX Red is a mitochondrial superoxide probe. CHX is cycloheximide, a substance that functions as a protein synthesis inhibitor. AMG PERK 44 is a highly selective PERK kinase inhibitor. BAPTA-AM is 1,2-bis(2-aminophenoxy)ethane-*N*,*N*,*N*′,*N*′-tetraacetic acid tetra(acetoxymethyl) ester. FeTMPyP is iron(III) tetrakis(*N*-methyl-4-pyridyl)porphyrin, has been identified as a potent catalyst for the decomposition of peroxynitrite ($ONOO^-$). NAC is *N*-acetylcysteine. Cys is *L*-cysteine. BiP is the binding immunoglobulin protein (Grp78), which is a protein that plays a role in the immune system. PERK is protein kinase R-like endoplasmic reticulum kinase. IRE1α is an enzyme known as inositol-requiring enzyme 1 alpha (IRE1α) that has been identified as a key player in the process. eIF2α′ is the initiation factor 2 alpha of eukaryotic origin. XBP1 is X-box binding protein 1. HSP is a heat shock protein. CHOP is C/EBP homologous protein. ERAD is ER-associated degradation. ATP is adenosine triphosphate. CRT (ecto-CRT) is calreticulin, also known as ecto-calreticulin. HMGB1 is High Mobility Group Box 1. Reproduced with permission from Rao and co-workers.[118] Copyright 2025, American Chemical Society.

advantage of coupling light-triggered *in situ* gelation with a rationally designed hybrid polymeric system. This approach signifies a strategy to surmount the limitations of single-session PDT by facilitating repeated, locally reinforced treatments that augment systemic immunotherapeutic outcomes. A platform of this nature has been demonstrated to enhance both local tumor control and the establishment of systemic antitumor immunity, thus holding significant translational promise, particularly for the treatment of solid tumors with existing or potential metastatic spread. This strategy is the purview of local administration and is only suitable for directly injectable solid tumors, which cannot be treated with distant metastatic foci. The operation of multiple

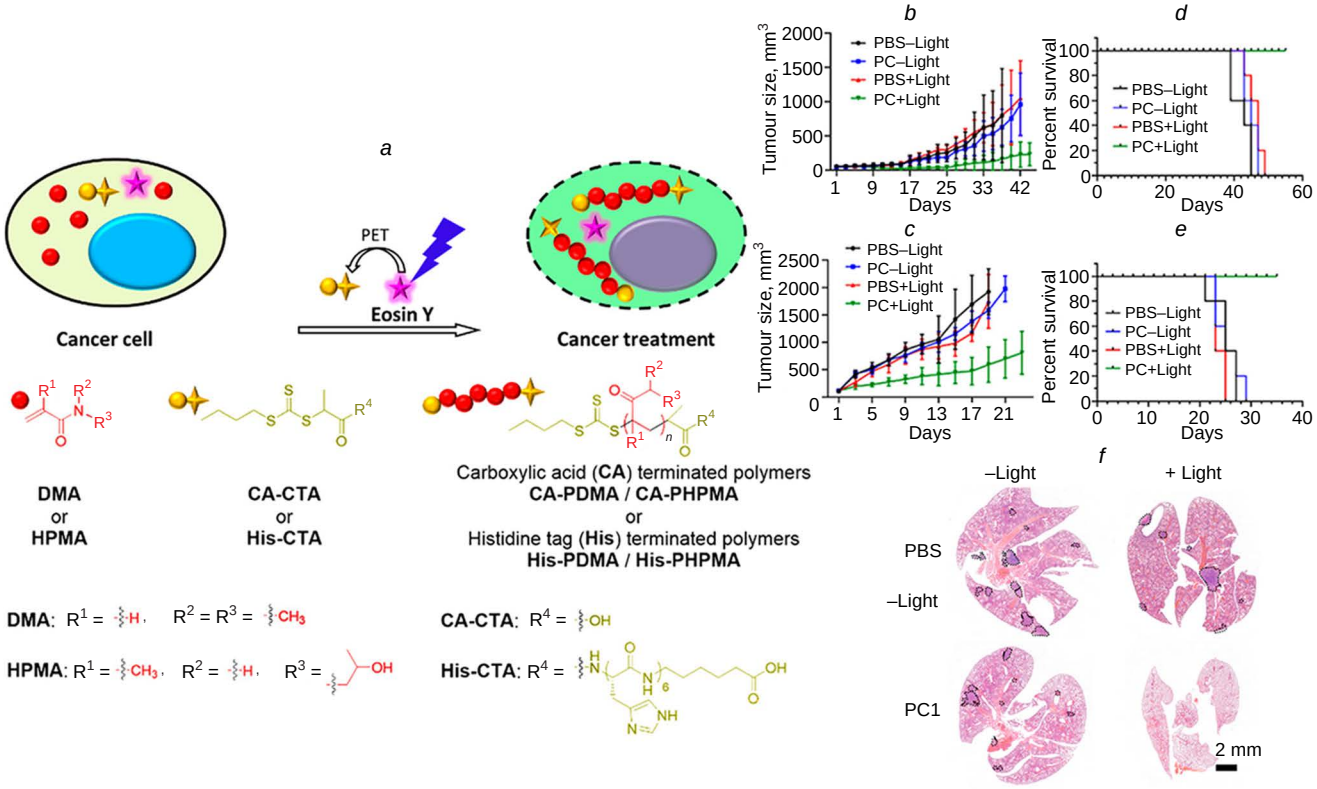


Figure 21. Schematic illustration of the intracellular polymerization (*a*). Survival and biosafety evaluation of intracellular polymerization: Tumor burdens (*b*) and survival curves (*c*) of MDA-MB-231-tumor-bearing BALB/c nude mice with various treatments ($n = 5$). Tumor burdens (*d*) and survival curves (*e*) of 4T1-tumor-bearing BALB/c mice with various treatments ($n = 5$). Mice were aged until moribund or the tumor volume reached 2000 mm^3. Representative H&E-stained whole lung sections of each group collected from the mice on day 19. Metastatic sites were highlighted by black dash lines (*f*). MDA-MB-231 is a human breast cancer cell line derived from a specimen of Metastatic Breast Cancer 231, as identified by the M.D.Anderson Cancer Center. Reproduced with permission from Geng and co-workers.[112] Copyright 2022, American Chemical Society.

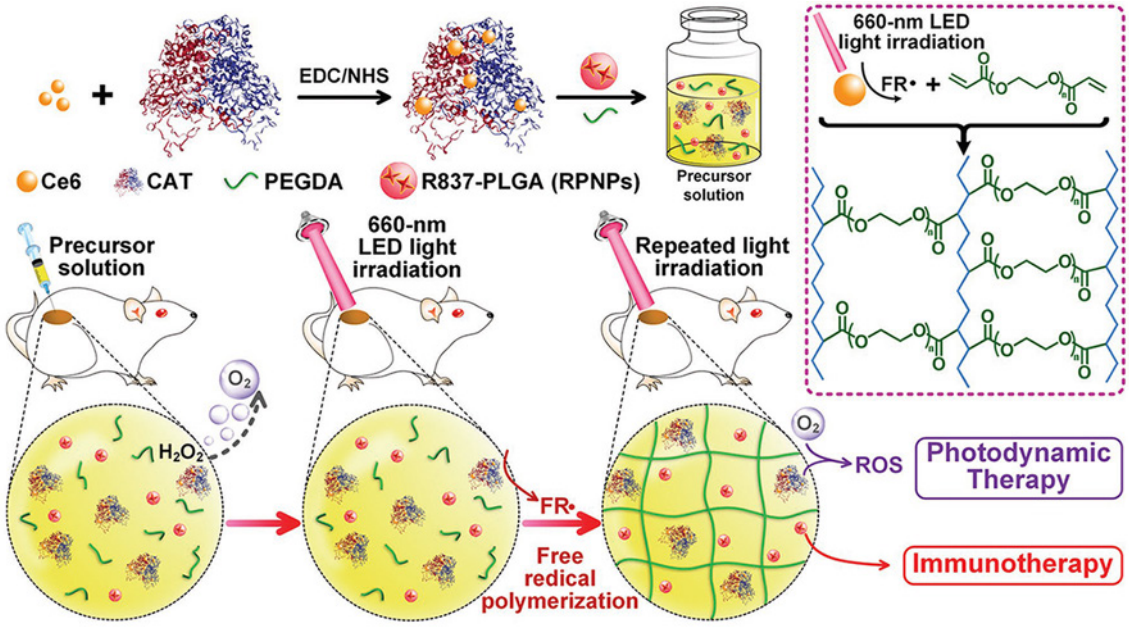


Figure 22. The scheme shows the light-triggered formation of Ce6-CAT/PEGDA hydrogel in tumor of mice. Reproduced with permission from Liu and coworkers.[114] Copyright 2019, John Wiley and Sons.

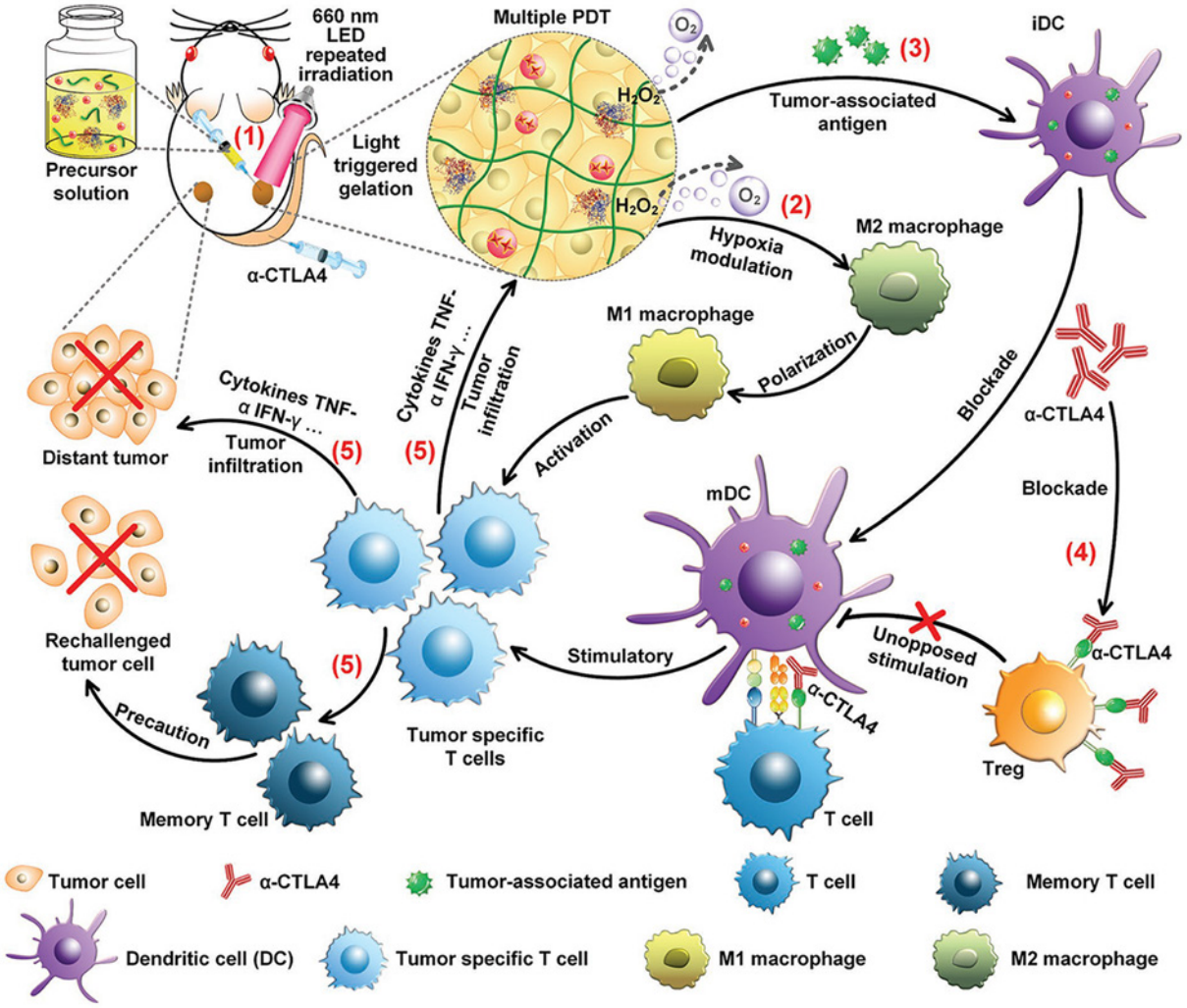


Figure 23. Mechanism of Gel-based PDT-immunotherapy to achieve systemic therapeutic responses by repeated local PDT treatments: 1) Light-triggered *in situ* gelation to enable long-term retention of injected components. 2) Persistent tumor hypoxia relief by tumor-retained CAT can enhance both PDT and immunotherapy. 3) Multiple waves of tumor debris together with nanoadjuvant RPNPs would trigger strong tumor-specific immune responses. 4) Checkpoint blockade by manipulating the immune balance would further enhance antitumor immunities. 5) As the results of those synergistic mechanisms, local tumors, abscopal tumors, and rechallenged tumors could all be effectively eliminated by the Gel-based PDT-immunotherapy. Reproduced with permission from Liu and coworkers.[114] Copyright 2019, John Wiley and Sons.

light exposures is complex, and patient compliance is limited. In addition, the degree to which the *in vivo* degradation cycle of the hydrogel matches the drug release rhythm still needs to be optimized.

Wu *et al.*[120] recently reported a stimuli-responsive photocatalyst strategy that allows biomarker- and light-gated radical polymerization to proceed directly within living cells. As displayed in Fig. 24*a*, the design is based on engineered 3,4,5,6-tetrabromofluorescein (TBF) photocatalysts, which are equipped with protecting groups that respond to endogenous reactive oxygen/sulfur species (ROS/RSS) or specific enzymes. These groups effectively suppress PET-RAFT activity until two conditions are met simultaneously: biomarker activation and light irradiation. This AND-gated logic activation mechanism ensures highly precise spatial and temporal control, restricting polymerization to targeted cellular environments. The employment of a dual-regulatory monomer design, by the authors resulted in the targeted *in situ* polymer formation that selectively disrupts ER integrity, ultimately inducing cell death (Fig. 25*a*–*l*). This advanced platform establishes a versatile chemical methodology for the precise manipulation of organelle function, offering new pathways for therapeutic development and expanding the toolbox of synthetic biology. This work signifies a substantial advancement in the field of bio-orthogonal reaction systems, integrating synthetic chemistry with cellular biology to facilitate precise interventions within intricate biological environments. The response mechanism is complex, and the fluctuation of biomarker concentration in the *in vivo* environment easily affects the activation efficiency. The subcellular localization accuracy of photocatalysts is limited, and there is potential for damage to the normal ER. In addition, the synchronization of multicomponent delivery is difficult to guarantee, which reduces the overall therapeutic efficiency.

3.3.3. Metal-catalyzed prodrug activation

In addition to the extensively studied prodrug activation strategy, metal-catalyzed *in situ* generation of cytotoxic ROS *via* Fenton-type reactions represents a further effective antitumor modality based on intracellular abiotic chemistry. Iron-based metal-organic frameworks (MOFs), featuring tunable porous structures and abundant metal active sites, have been extensively developed

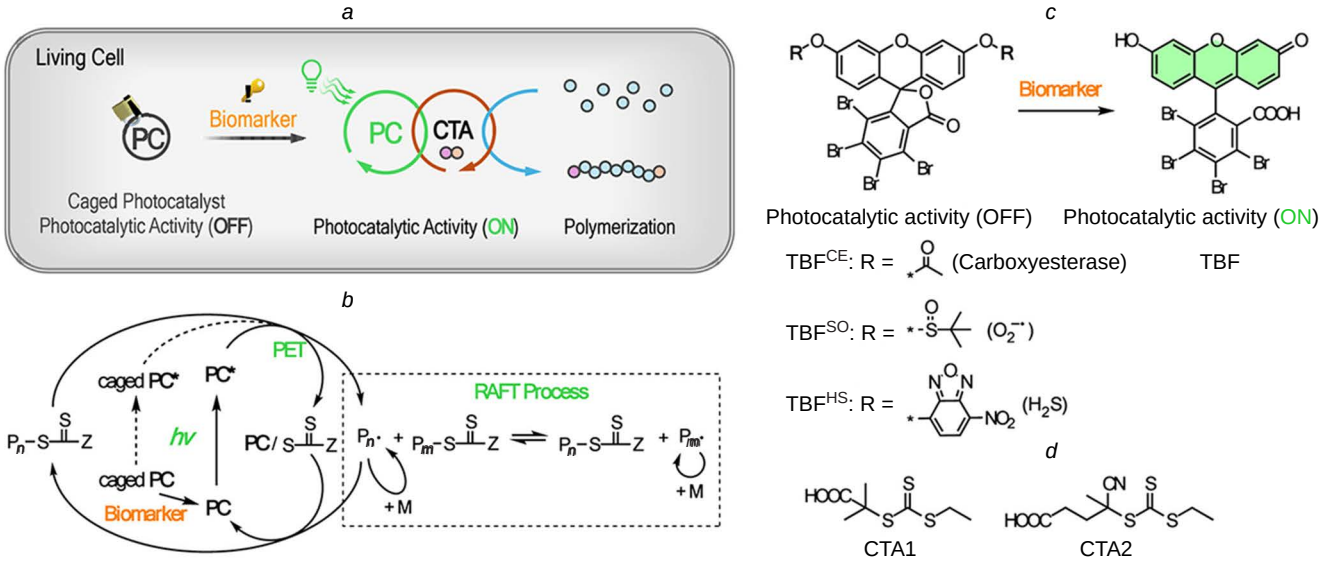


Figure 24. Schematic illustration of intracellular radical polymerization under dual light/biomarker control. Caged photocatalysts, initially inactive, undergo cage motif shedding upon biomarker stimulation, thereby restoring catalytic activity and enabling photoradical-mediated polymerization within cells (*a*). Mechanistic overview of PET-RAFT polymerization and the biomarker-activated caged photocatalyst (*b*). Chemical structures of the designed caged photocatalysts (TBF^{CE}, TBF^{SO}, and TBF^{HS}) and the mechanism of cage release upon biomarker triggering (*c*). Chemical structure of the chain transfer agent employed in PET-RAFT polymerization (*d*). Reprinted with permission from Wu *et al.*[120] Copyright 2025, American Chemical Society.

as tumor-responsive nanocatalysts for chemodynamic therapy. For instance, Du *et al.*[10] constructed a chitosan oligosaccharide-modified etched iron MOF platform (COS@MOF) for synergistic tumor therapy. The thiamine pyrophosphate-etched open cavity structure exposes more catalytic active sites and elevates the Fe(II)/Fe(III) ratio, which can efficiently catalyze endogenous H_2O_2 in tumor cells to generate $^{\bullet}OH$ *in situ via* Fenton reaction. Moreover, the overexpressed endogenous H_2S in colorectal tumors can further accelerate the Fe(II)/Fe(III) redox cycle, thus amplifying ROS production. More importantly, chitosan oligosaccharides as an agonist for autophagy can induce ferritin degradation to break intracellular iron homeostasis, further promoting ferroptosis and synergistically enhancing the nanocatalytic antitumor effect. Zhang and co-workers[116] reported the design of a novel nanocopper-doped cross-linked lipoic acid nanoparticle (Cu@cLANP) that fulfills the stringent criteria required for an ideal nanocatalyst in intracellular biorthogonal chemistry, including biocompatibility, catalytic efficiency, and morphological controllability. This multifaceted platform capitalizes on the dynamic nature of the many interlaced disulfide bonds within the cross-linked lipoic acid matrix. By subjecting these NPs to varying reduction conditions and methodologies, their structural integrity can be restored, thereby facilitating the programmable construction of nanocatalysts with distinct morphologies, such as spherical or rugby-ball-like structures (Fig. 26*a*). Among the synthesized variants, the optimally designed rugby-like Cu@cLANPs I demonstrated significantly superior catalytic efficiency for the intracellular CuAAC reaction compared to their spherical counterparts, Cu@cLANPs II and III (see Fig. 26*b*–*h*). The anisotropic shape of Cu@cLANPs I is believed to facilitate enhanced cellular uptake and provide a more favorable surface geometry for catalytic cycles within the complex intracellular environment. Beyond its immediate application, this cross-linked lipoic acid nanoparticle (cLANP) system is highly generalized. The design principle can be extended to encapsulate other catalytic metals, thereby generating a diverse library of nanocatalysts with tunable morphologies and functions. This adaptability opens significant opportunities for the discovery and optimization of novel biorthogonal reactions directly within living systems, advancing the frontier of intracellular catalysis for biomedical research and therapeutic development. The sustained release of copper ions has the potential to induce systemic toxicity, and long-term accumulation can readily result in liver and kidney function impairment. Nanoparticles exhibit high non-specific uptake by the reticuloendothelial system, and the tumor enrichment efficiency is constrained. Moreover, catalytic efficiency is considerably influenced by the intracellular GSH concentration, leading to marked interindividual variations in efficacy.

Tanaka and co-workers[121] introduced a novel prodrug design strategy centered on a 2′-alkynyl-*N*-methyl-2-biphenylamine framework, enabling the *in situ* synthesis of bioactive compounds *via* transition metal catalysis within a biological context. This approach facilitates the generation of 5-methyl phenanthridinium derivatives through a gold-catalyzed hydroamination cyclization reaction (Fig. 27*a*,*b*). The strategy is particularly powerful as it accomplishes two key objectives: firstly, it generates structural mimics of naturally occurring alkaloids that contain the 5-methyl phenanthridinium pharmacophore, such as sanguinarine; secondly, it provides a route to synthesize quaternary ammonium cations, a class of nitrogenous heteroaromatic compounds prized for their intrinsic reactivity and diverse biological activities. In order to translate this synthetic methodology into a biocompatible therapeutic platform, the researchers employed a gold artificial metalloenzyme (ArM) engineered from human serum albumin as the catalytic trigger for prodrug activation, rather than a small-molecule gold complex (see Fig. 27*c*). This protein-based catalyst has been demonstrated to enhance biocompatibility and *in vivo* stability to a significant degree. The choice of the phenanthridinium product is a deliberate strategy, as this moiety is a recognized scaffold in several DNA-intercalating agents with established antitumor properties, underscoring its

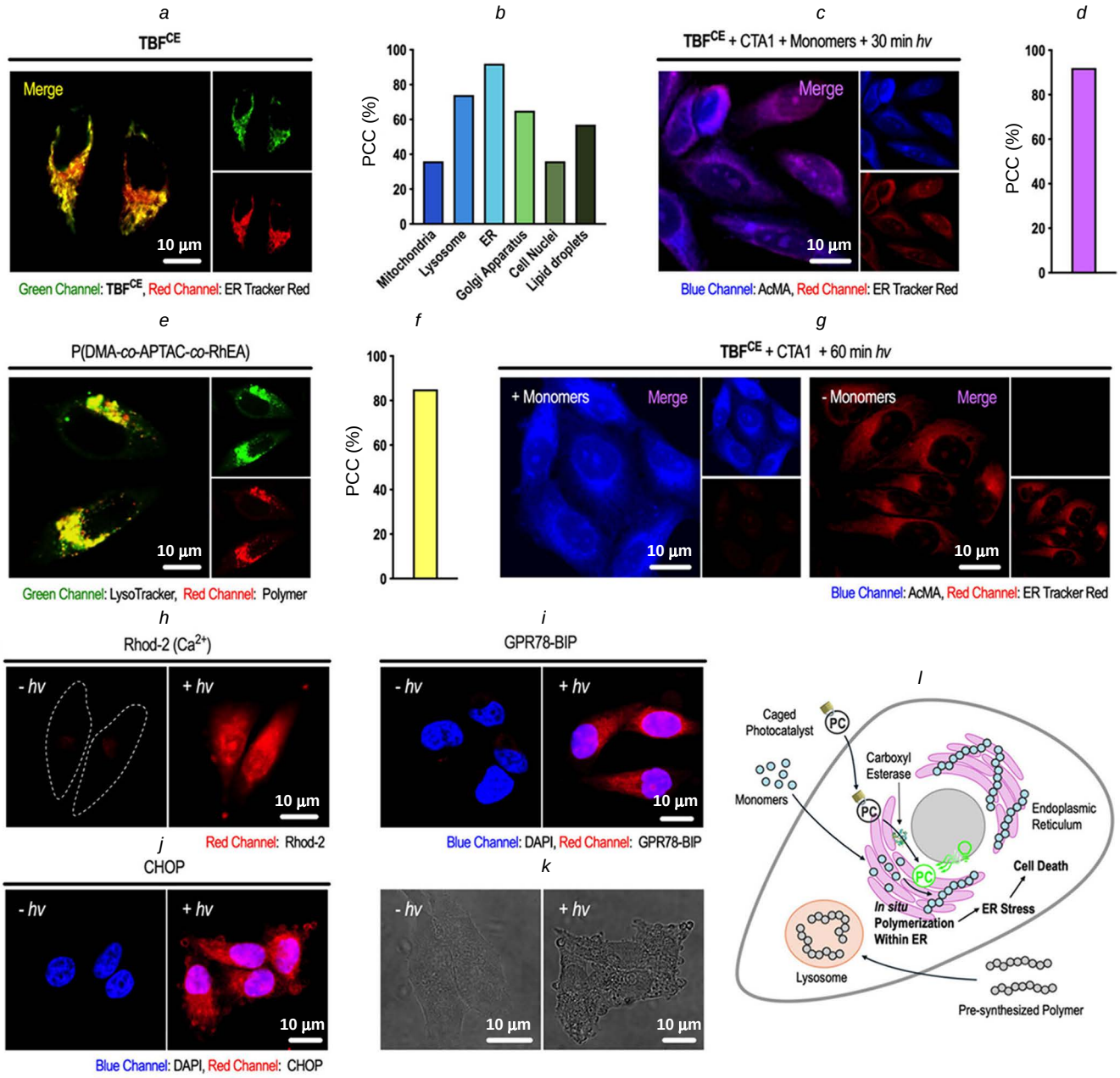


Figure 25. CLSM image of HepG2 cells incubated with TBF^{CE} (2 μM), with ER prelabeled using ER Tracker Red (*a*). Colocalization analysis (Poisson's correlation coefficient, PCC) of TBF^{CE} fluorescence with various organelles in HepG2 cells (*b*). TBF^{CE} (10 μM)/CTA1 (100 μM)-mediated photopolymerization of DMA/APTAC/AcMA (900/100/50 μM) in HepG2 cells: CLSM image after polymerization (3 h incubation +30 min green LED irradiation) (*c*) and PCC of the polymerized product with the ER (postlabeled with ER Tracker Red) (*d*). CLSM analysis of HepG2 cells incubated with presynthesized P(DMA-co-APTAC-co-RhEA): Fluorescence images (*e*) and PCC with lysosomes (labeled using LysoTracker Green) (*f*). Left panel: TBF^{CE}/CTA1-mediated DMA/APTAC/AcMA polymerization (3 h of incubation + 60 min of green LED irradiation). Right panel: CLSM image without monomer (background control). ER-labeled postpolymerization with ER Tracker Red. Imaging of intracellular calcium (by Rhod-2 assay), (*g*), GRP78-BIP/CHOP (by immunoassay) (*h*, *i*), and cell morphology (*j*) in HepG2 cells after photocatalytic polymerization of DMA and APTAC with TBF^{CE}. Schematic diagram illustrating the mechanism of tumor cell death mediated by *in situ* polymerization (*k*). APTAC is 3-acrylamidopropyl)trimethylammonium chloride. PC is photocatalyst. PET is photoinduced electron transfer. RAFT is reversible addition–fragmentation chain transfer, a method of DNA repair that has been discovered by researchers. TBF is tetra bromo fluorescein. DAPI is 4′,6-diamidino-2-phenylindole. Rhod-2 is a rhodamine-based calcium ion fluorescent probe. GPR78-BIP is glucose-regulated protein 78/binding immunoglobulin protein. CHOP is C/EBP homologous protein. CTA1 is chain transfer agent 1. AcMA is 9-amino-6-chloro-2-methoxyacridine. Reprinted with permission from Wu *et al.*[120] Copyright 2025, American Chemical Society.

therapeutic relevance (see Fig. 27 *d*). This study provides substantial evidence to support the hypothesis that a gold-based ArM can function as a precise bio-orthogonal trigger to catalyze the synthesis of a potent phenanthridinium-based drug directly from an inert prodrug precursor *via* hydroamination. The resultant agent exhibits efficacy in cancer therapy models. Consequently, this work highlights the considerable therapeutic potential of albumin-based gold ArMs, positioning them as versatile tools for the conditional and localized activation of novel chemotherapeutic agents, thereby advancing the field of bio-catalyzed prodrug development. Despite the enhancement of stability *in vivo* afforded by albumin carrier, the tumor

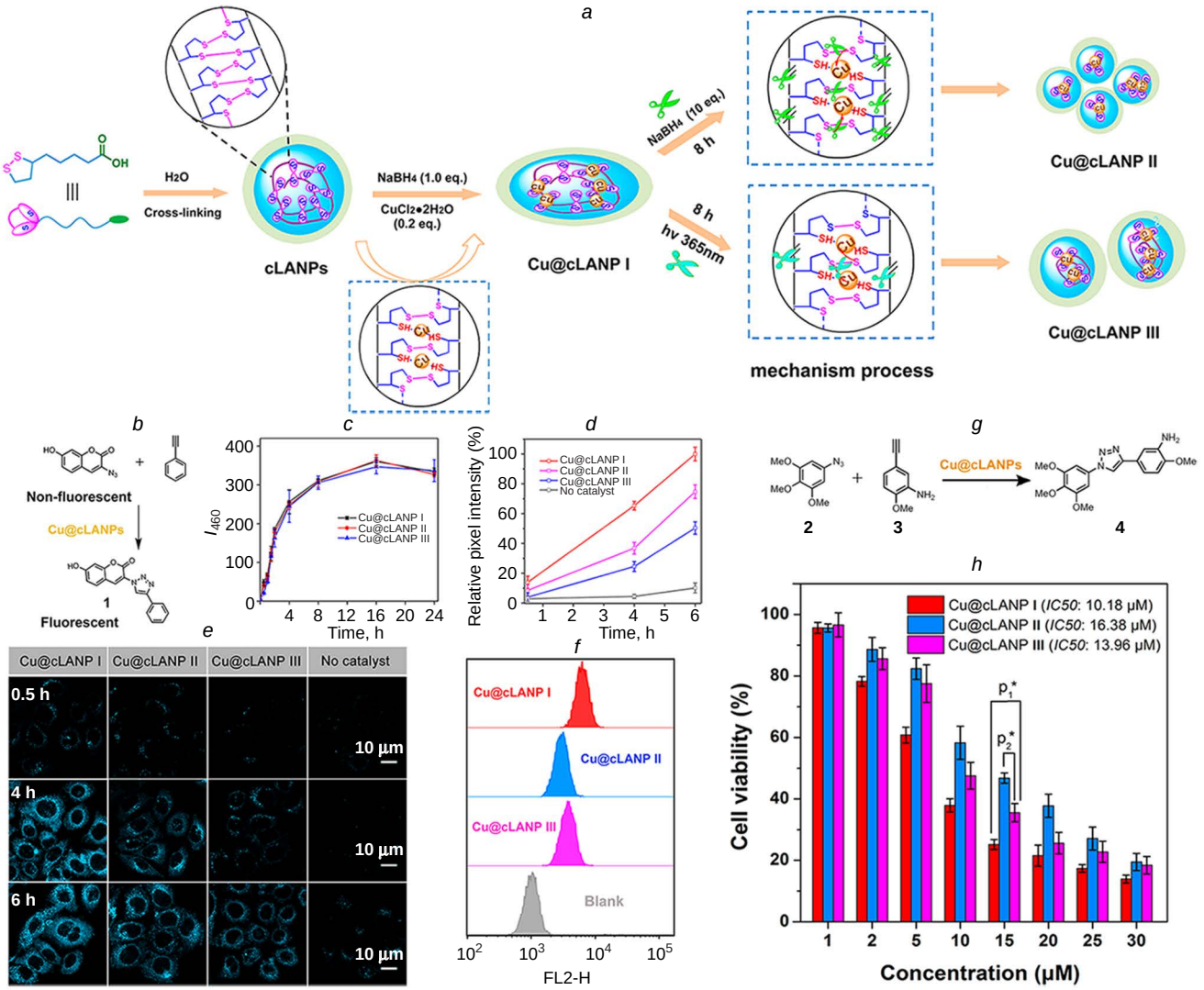


Figure 26. Schematic illustration of the preparation of nanocatalysts Cu@cLANPs I–III (*a*). Investigation of the catalytic activity of Cu@cLANPs I–III in water and in living cells: Cu@cLANPs mediated click reaction between 3-azido-7-coumarin and phenyl acetylene (*b*). The emission intensity at 460 nm (I460) of the reaction system in water, as a function of time (*c*). CLSM images of HeLa cells preincubated with Cu@cLANPs I–III ([Cu] = 15 ppm) and with no catalyst for 2 h, washed with PBS, and subsequently incubated with 1 : 1 (mol/mol) 3-azido-7-coumarin/phenyl acetylene for 48 h at 37°C for 0.5, 4, and 6 h. The scale bars are 10 μm in all images (*d*). Relative pixel intensity of the reaction system in cells as a function of time. The pixel intensity from the 6 h image of cells preincubated with Cu@cLANP I is defined as 1.0 (*e*). Flow cytometry analysis of HeLa cells incubated with the Cu@cLANPs I–III at 37°C for 2 h. The untreated cells were used as a control (*f*). *In situ* synthesis of anticancer bioactive compound 4: the Cu@cLANPs mediated click reaction between 2 and 3 (*g*), cell viability of HeLa cells preincubated with Cu@cLANPs I–III ([Cu] = 15 ppm) for 2 h, washed with PBS, and subsequently incubated with 1 : 1 (mol/mol) 2/3 for 48 h at 37°C with a series of concentrations. HeLa cells incubated without any materials were used as the control. Data are expressed as mean ± standard deviation of three separate experiments (*h*). Reproduced with permission from Zhang and co-workers.[116] Copyright 2018, American Chemical Society.

targeting still relies on the EPR effect, and the enrichment efficiency is limited. The catalytic activity of the gold catalyst is easily quenched by thiol substances, such as GSH, in a complex intracellular environment. Furthermore, the delivery ratio of prodrug and catalyst is difficult to accurately control, which has a detrimental effect on activation efficiency.

Artificial metalloenzymes represent a pioneering approach in biohybrid catalysis, created by the strategic incorporation of a synthetic metal catalyst, often an organometallic complex or coordination compound, within a protein or biomolecular scaffold. This innovative design aims to merge the distinct advantages of natural enzymes, such as high catalytic efficiency, substrate specificity, and the ability to operate under mild aqueous conditions, with the broad reaction scope and tunability of synthetic catalysts, which can mediate transformations not typically accessible in biology.[122,123] By integrating synthetic chemistry and enzymology, ArMs offer a robust platform for expanding the catalytic landscape, facilitating novel reactions that are not found in nature while preserving the programmable and evolvable characteristics of biological macromolecules. This field remains dynamic and evolves rapidly at the intersection of chemistry, biology, and materials science. Building upon nature's evolutionary ingenuity, Bai and co-workers[124] recently developed a biomimetic strategy to integrate whole-cell catalytic platforms into eukaryotic cells *via* an endosymbiotic-inspired approach. This method centers on the creation of artificial metalloenzymes in artificial sanctuaries (ArMAS) through a process known as liquid-liquid phase separation (LLPS). The

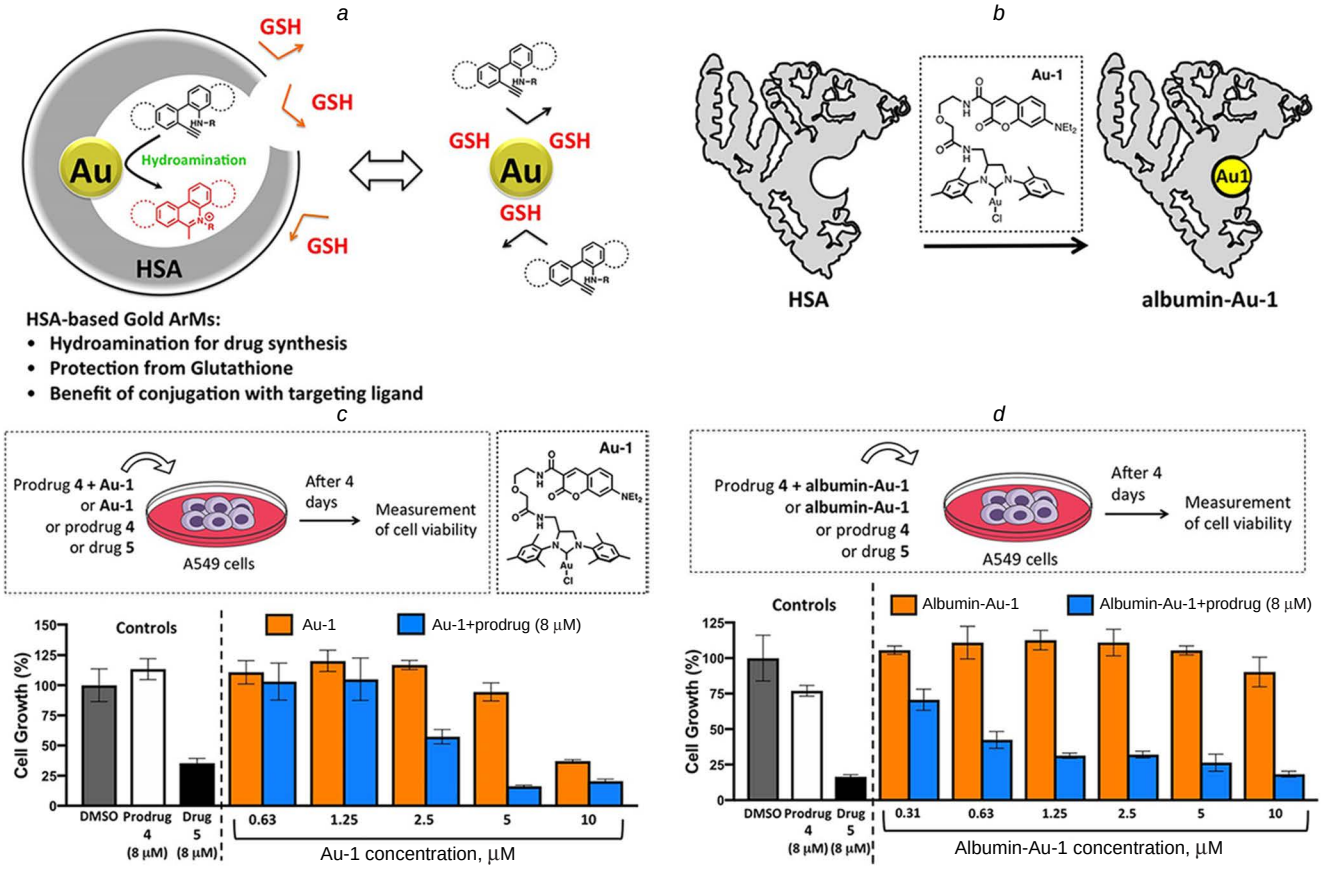


Figure 27. Development of an albumin-based gold ArM for drug synthesis *via* hydroamination to avoid deactivation by GSH (*a*). The albumin-Au complex (albumin-Au-1) was prepared by incubation of the gold catalyst Au-1 with human serum albumin (*b*). Cytotoxicity studies for prodrug activation *via* gold catalysis. A viability assay was carried out using A549 cancer cells. The cells were treated with prodrug 4 (8 mM), followed by immediate addition of Au-1 at the indicated concentrations. In parallel experiments, the cells were only treated with the indicated concentrations of Au-1. In control experiments, cells were treated with DMSO, prodrug 4 (8 mM), or drug 5 (8 mM). To completely dissolve 4, 5, or Au-1 in media, the media used in the viability assay contained 1% DMSO (v/v) (*c*). Cytotoxicity studies for prodrug activation by albumin-Au-1 catalysis. A viability assay was carried out using A549 cancer cells. The cells were treated with prodrug 4 (8 mM), followed by the immediate addition of albumin-Au-1 at the indicated concentrations. In parallel experiments, the cells were only treated with the indicated concentrations of albumin-Au-1. In control experiments, cells were treated with DMSO, prodrug 4 (8 mM), or drug 5 (8 mM). To completely dissolve 4 or 5, the media used in the viability assay contained 1% DMSO (v/v) (*d*). Reproduced with permission from Tanaka and co-workers.[121] Copyright 2021, John Wiley and Sons.

ArMAS-LLPS platform is predicated on a designed phase-separating scaffold, namely a HaloTag-SNAPTag (HS) fusion protein.

When expressed in *E. coli*, this scaffold undergoes LLPS to form distinct, membrane-less catalytic compartments within the bacterial cytoplasm (Fig. 28*a*). Within these condensed liquid droplets, the HS scaffold can be readily equipped with abiotic metal cofactors, specifically those functionalized with alkyl chlorides, that dock into its binding pocket. This generates well-defined ArMs whose catalytic activity can be finely tuned and enhanced through directed evolution. It is noteworthy that these *E. coli* cells, now harboring compartmentalized ArMs, function as self-stabilized and versatile whole-cell catalysts. Subsequent to are subsequently prepared for integration into eukaryotic hosts *via* a straightforward membrane decoration process. Following sterilization and engulfment by eukaryotic cells, these engineered bacterial 'endosymbionts' demonstrate robust catalytic performance across various cell lines. These enzymes have been shown to facilitate the mediation of both unimolecular and bimolecular reactions, utilizing a variety of transition metal cofactors in the process. It is important to note that the utility of this platform extends beyond the domain of cell culture to encompass live animal applications. As illustrated in Fig. 28*b–e*, it offers promising therapeutic strategies, such as the intracellular eradication of bacterial pathogens and the augmentation of cancer therapy. In the latter case, the internalized catalytic *E. coli* can perform on-site activation of inert prodrugs directly within the tumor microenvironment. Given the established power and selectivity of ArM platforms, their deployment as straightforward, exogenous abiotic catalysts within living systems marks a significant advance. This endosymbiosis-mimicking strategy is poised to invigorate chemical biology and biomedical research, providing a novel and versatile toolkit for precision catalysis in complex biological settings. The utilization of engineered bacteria carries with it a high degree of *in vivo* safety risk, with the potential to induce infection and immune rejection. The tumor targeting and colonization efficiency of bacteria exhibits significant inter-individual variability, whilst the therapeutic stability is deemed inadequate. Moreover, the quality control and large-scale production of whole-cell systems are challenging, resulting in non-compliance with clinical preparation specifications.

Wang and co-workers[125] demonstrated a novel strategy for initiating intracellular radical polymerizations by exploiting the

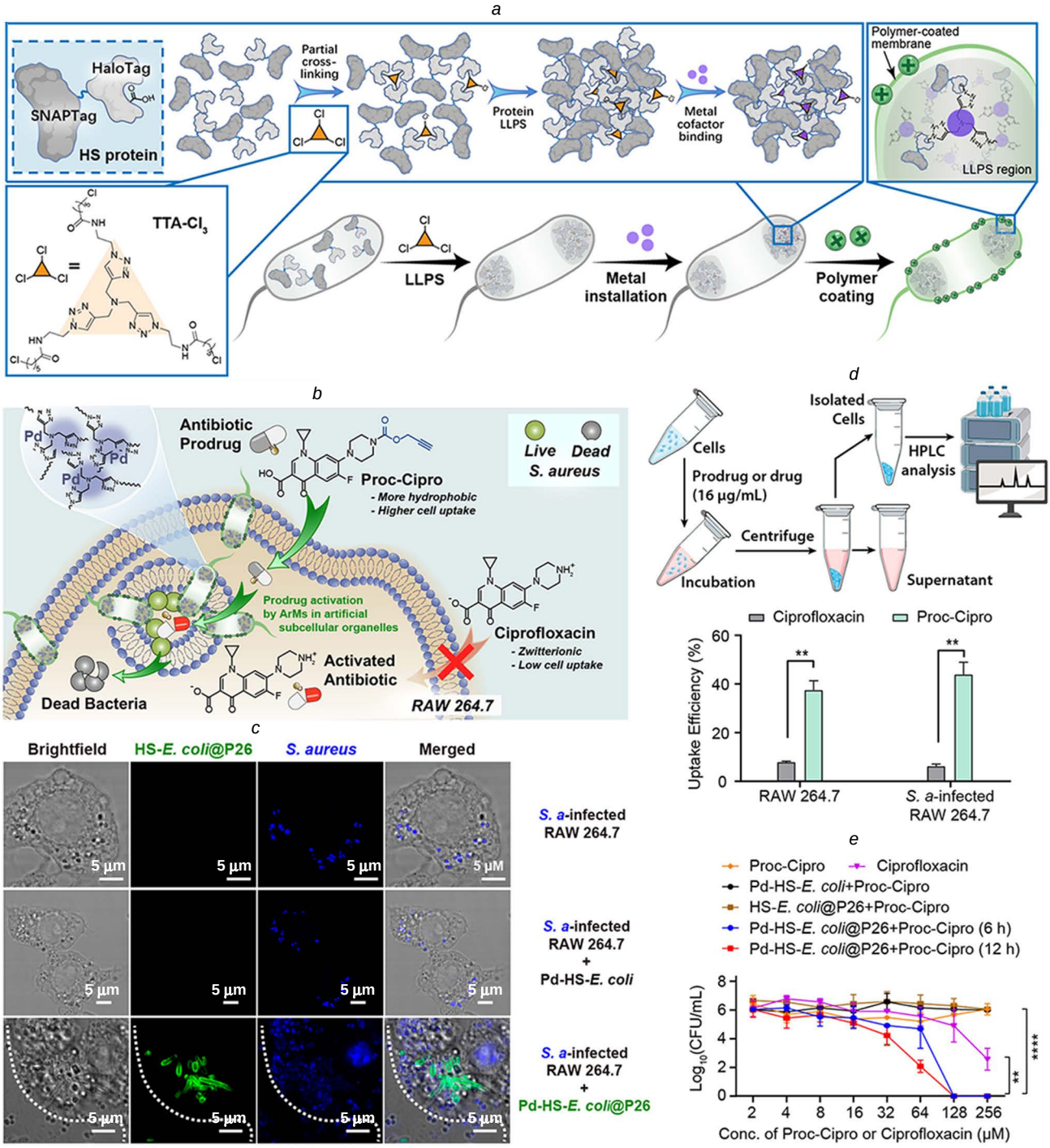


Figure 28. Illustration of the construction of polymer-decorated HS-*E. coli* whole-cell catalytic system with internal compartmentalization for enhanced ArM catalysis (*a*). Cartoon illustration showing polymer-modified whole-cell catalyst Pd-HS-*E. coli*@P26 entering cells to activate prodrugs (Proc-Cipro) to exert antibacterial effects (*b*). Confocal images of *S. aureus*-infected RAW 264.7 cells, and Pd^{II}-HS-*E. coli*@P26 inside them. Polymer modified whole-cell catalysts Pd^{II}-HS-*E. coli*@P26 showed a green color (from fluorescein on P26), and *S. aureus* were blue (from staining with DAPI). DAPI also stained RAW 264.7's nucleus (*c*). Method illustration and results of experiments exploring the cell permeability of ciprofloxacin and its prodrug, Proc-Cipro. The latter had obviously higher cell uptake (*d*). Results showing that Pd^{II}-HS-*E. coli*@P26 mediated Proc-Cipro activation in *S. aureus*-infected RAW 264.7 cells to clear intracellular bacteria (*e*). HS protein is a HaloTag-SNAPtag fusion protein. HPLC is high-performance liquid chromatography. CFU is colony-forming unit. Reproduced with permission from Bai and coworkers.[124] Copyright 2025, American Chemical Society.

redox characteristics of the tumor microenvironment. In this system, a Cu(II)–histidine complex, when exposed to endogenous GSH and externally supplemented NaAsc, undergoes continuous reduction to its active Cu(I) form within living cells. This catalytically active species then initiates the polymerization of monomers such as *N*-hydroxyethyl acrylamide exhibited in Fig. 29. The polymerization process has been demonstrated to exhibit a high degree of responsiveness to the hypoxic and reductive conditions that are characteristic tumor cells. The material demonstrated extensive monomer

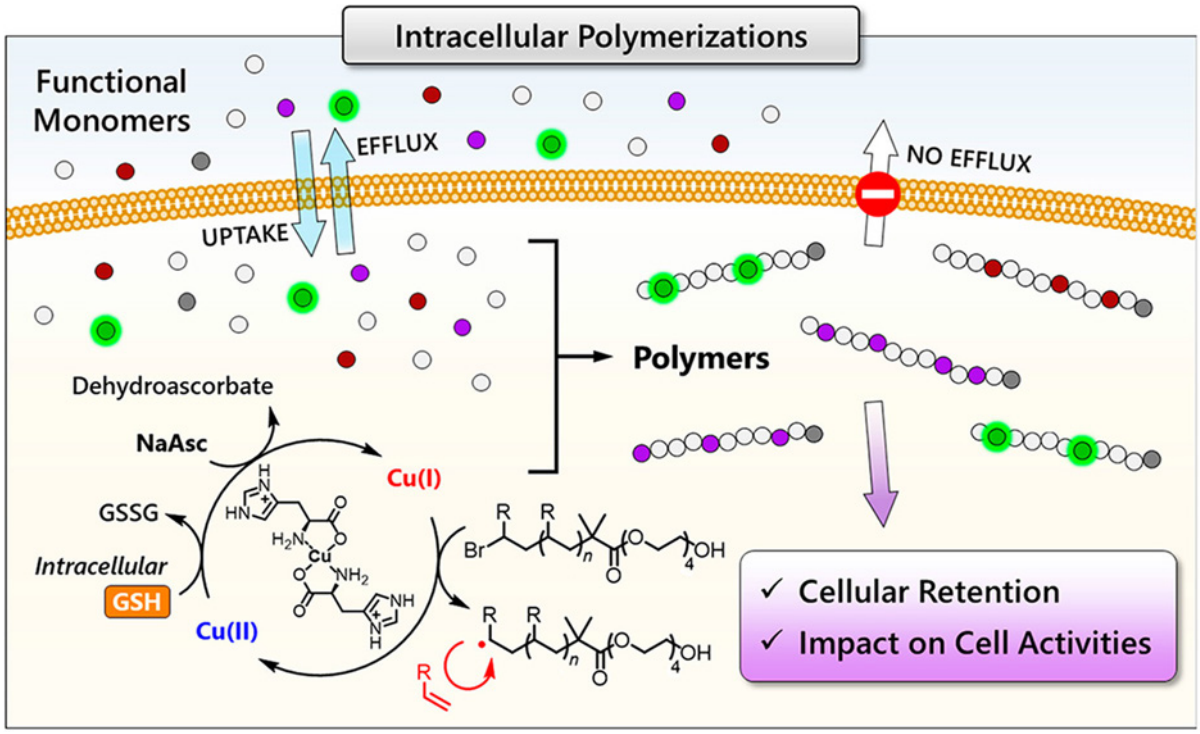


Figure 29. Schematic illustration of the Cu(I)-catalyzed radical polymerization inside living cells. Reproduced with permission from Wang and co-workers.[125] GSSG is glutathione disulfide. Copyright 2021, American Chemical Society.

compatibility, enabling the incorporation of diverse functional monomers. A salient benefit of this methodology is the intracellular retention of the synthesized polymers. Unlike conventional small-molecule drugs, which frequently encounter rapid efflux, the polymerized drugs remained inside HepG2 and HeLa cells, leading to prolonged intracellular circulation and significantly enhanced therapeutic efficacy (Fig. 30 *a–f*). This work establishes intracellular catalytic polymerization as a promising platform for biomedical innovation. This approach has the potential to unlock novel pathways for the development of cellular biosynthetic factories and to inform intelligent therapeutic strategies for the targeted treatment of diseases such as cancer. By enabling radical polymerization of acrylamide derivatives inside cells with high spatiotemporal control, this methodology provides a novel framework to address long-standing challenges in tumor therapy, offering potential for more precise and sustained drug action. The necessity for additional sodium ascorbate supplementation introduces a complexity to the administration regimen. The systemic toxicity of copper ions is a key factor in determining the maximum administered dose. Furthermore, the mechanism of action of polymerized drugs is singular, and it is simple to produce drug resistance.

3.3.4. Bioorthogonal polymerization therapy

Convergence of polymerization chemistry and cellular bioengineering has recently led to the development of an innovative 'lab-in-cell' system by Tang and co-workers.[126] This system utilizes intracellular amino-yne click polymerization for integrated cell imaging and therapy (Fig. 31 *a*). This approach leverages the rapid and bio-orthogonal reaction between a carbonyl-activated terminal diyne monomer and an aggregation-induced emission (AIE)-active diamine containing a tetraphenylethene (TPE) unit. Under physiological conditions, these components spontaneously undergo polymerization within living cells, yielding fluorescent polymers *in situ*. The polymer chains, having been formed, restrict the intramolecular motion of the embedded TPE units. This, in turn, activates the AIE effect and thereby enabling real-time, high-contrast visualization of the polymerization process and its localization. Beyond its imaging applications, this intracellularly generated AIE-active polymer serves a direct therapeutic function. As illustrated in Fig. 31 *b–e*, the polymer exhibits a specific interaction with and disruption of key components of the cytoskeleton, namely tubulin and actin, leading to the collapse of cellular architecture and, consequently, the induction of cell death. This mechanism offers a potential drug-free therapeutic strategy for cancer treatment, where the cytotoxic action is derived from the physical disruption caused by the polymer itself, as opposed to rather than from a conventional small-molecule drug. This dual-function 'lab-in-cell' platform, which performs synthesis, imaging, and therapy within a cellular environment, represents a significant advancement in precision biochemistry. It provides a powerful tool for implementing complex chemical studies directly in a biological context and holds considerable promise for the development of novel theranostic agents that combine diagnostic visibility with inherent therapeutic activity. The synthesis of functional monomers is a complex process involving numerous steps, resulting in low yield and high cost. The specificity of bioorthogonal reactions in complex *in vivo* environments is often compromised by the presence of endogenous biomolecules. Additionally, the long-term intracellular retention of polymerization products carries a risk of chronic inflammation, necessitating long-term biosafety verification.

The clinical translation of strategies for antitumor based on *in situ* chemical reactions is hampered by a series of interrelated challenges spanning chemical synthesis, biological safety, delivery logistics, and operational feasibility:[127–129]

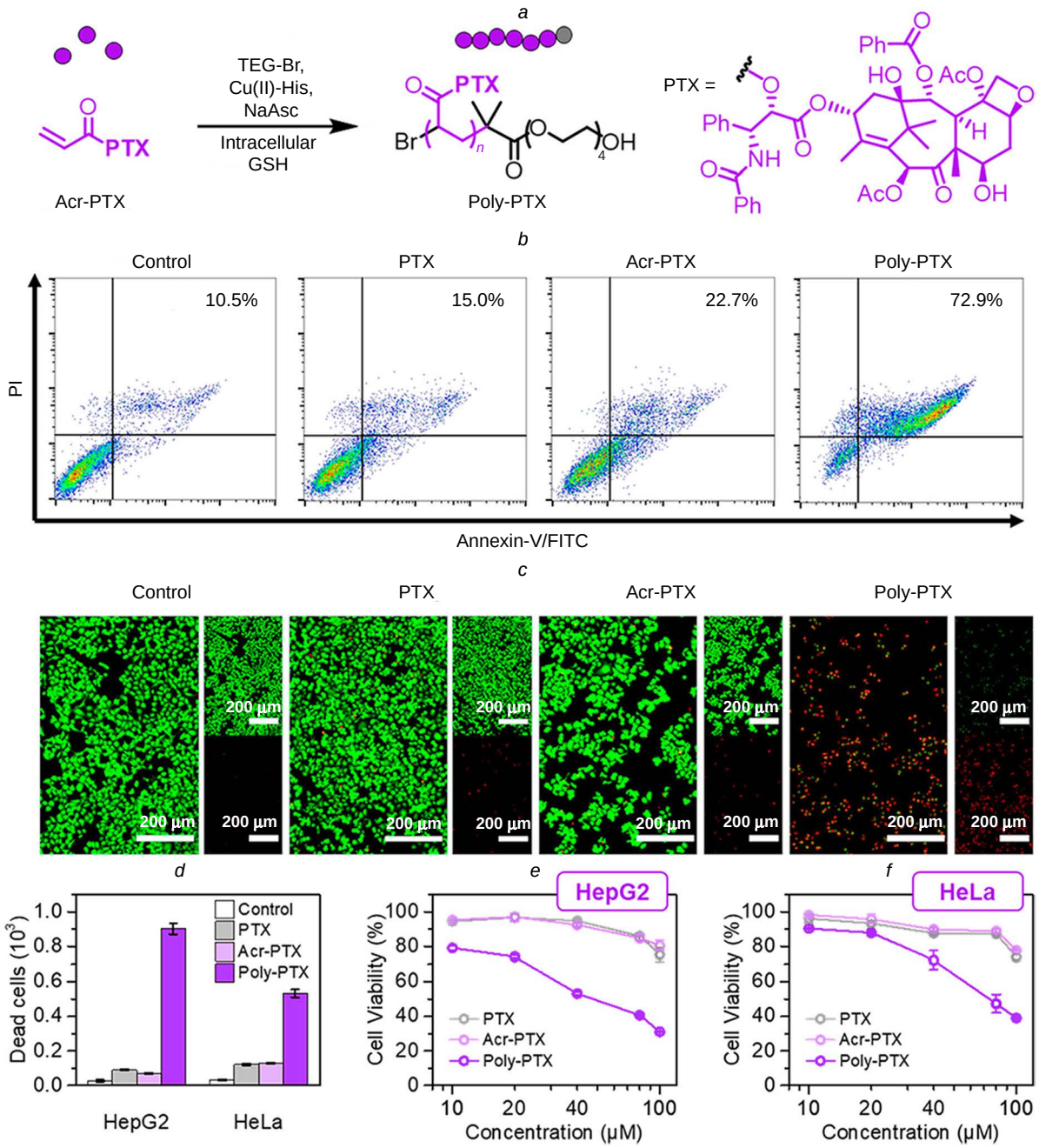


Figure 30. *In situ* polymerization of acryloyl paclitaxel (Acr-PTX) enhanced the apoptosis of HepG2 and HeLa cells: A schematic illustration showing the intracellular polymerization of paclitaxel-containing monomer Acr-PTX (*a*). Flow cytometry analysis of the apoptotic cells under different forms of the PTX agent. The *in situ* polymerized drug (Poly-PTX) proved far more capable of inducing the apoptosis of HepG2 cells than the unmodified PTX and Acr-PTX (*b*). Live/dead staining of HepG2 cells confirmed the greater cytotoxicity of the poly-PTX compared to monomeric forms of PTX. Live and dead cells are displayed by the green and red fluorescence, respectively (*c*). The quantitative analysis of apoptotic cells based on the live/dead staining images (*d*). Cell viability of HepG2 (*e*) and HeLa (*f*) under various concentrations and forms of PTX as obtained by MTT assay. Reproduced with permission from Wang and co-workers.[125] Copyright 2021, American Chemical Society.

(1) From the perspective of scalability and reproducibility, most reaction precursors and catalysts require multistep synthetic routes, which generally suffer from low overall yields and high production costs. This significantly complicates large-scale manufacturing under Good Manufacturing Practice (GMP) standards and restricts the commercial viability of such reagents.

(2) Safety and long-term biocompatibility remain critical concerns. Clinical-grade reagents must undergo rigorous toxicological profiling, yet persistent issues persist regarding the metabolic fate and chronic accumulation of both catalysts and reaction byproducts, raising potential risks of delayed toxicity that are not fully addressed by standard preclinical assessments.

(3) The efficient and synchronous delivery of multiple reaction components (such as monomers, initiators, or catalysts) to the tumor site at appropriate molar ratios constitutes a major pharmacokinetic bottleneck. For light-triggered systems, the inherent attenuation of excitation light in deep-seated tissues further narrows the applicable indications. Additionally, nonspecific sequestration by the mononuclear phagocyte system in the liver and spleen, combined with limited penetration into tumor parenchyma, substantially undermines the effective

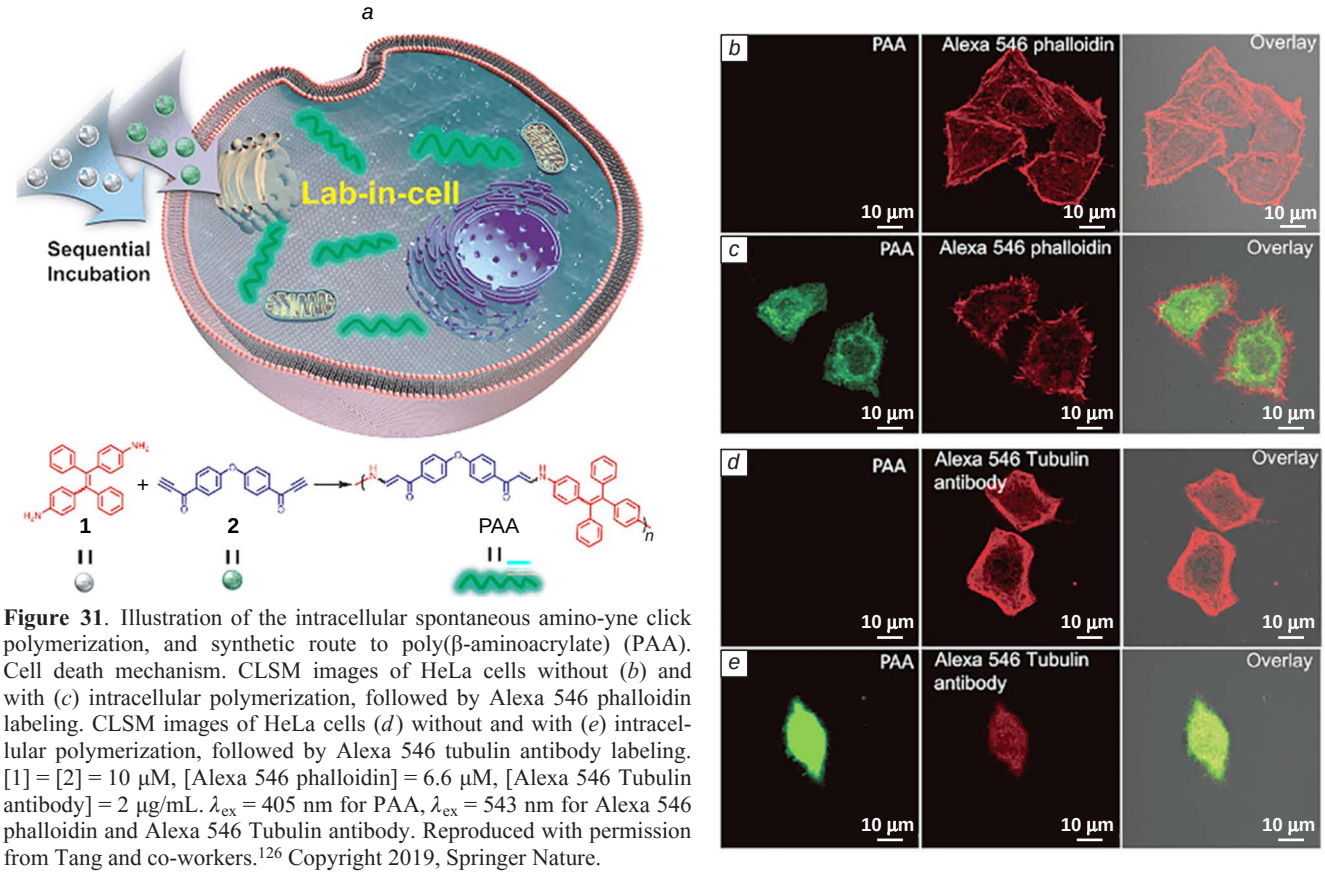


Figure 31. Illustration of the intracellular spontaneous amino-yne click polymerization, and synthetic route to poly(β-aminoacrylate) (PAA). Cell death mechanism. CLSM images of HeLa cells without (*b*) and with (*c*) intracellular polymerization, followed by Alexa 546 phalloidin labeling. CLSM images of HeLa cells (*d*) without and with (*e*) intracellular polymerization, followed by Alexa 546 tubulin antibody labeling. [1] = [2] = 10 μM, [Alexa 546 phalloidin] = 6.6 μM, [Alexa 546 Tubulin antibody] = 2 μg/mL. λ_{ex} = 405 nm for PAA, λ_{ex} = 543 nm for Alexa 546 phalloidin and Alexa 546 Tubulin antibody. Reproduced with permission from Tang and co-workers.[126] Copyright 2019, Springer Nature.

concentration of reaction species at the target site. The scarcity of highly specific tumor-targeting ligands exacerbates this issue, as most current vehicles lack the selectivity required for reliable *in vivo* performance.

(4) The overall clinical adaptability is constrained by the high cost and limited customizability of the specialized reagents, which often fail to meet cost-effectiveness criteria in clinical practice. Moreover, the demanding operational protocols impose stringent requirements on clinical workflows, thereby hindering widespread adoption in routine oncological settings. Taken together, these obstacles underscore the considerable gap between experimental promise and therapeutic reality, necessitating concerted efforts in materials design, delivery engineering, and regulatory science to facilitate successful clinical translation.

In situ chemical reaction strategies have demonstrated distinctive advantages in enhancing tumor targeting and minimizing systemic toxicity, thereby establishing themselves as valuable complements to conventional oncological therapies. Nevertheless, several critical knowledge gaps persist that impede further development and clinical adoption:[130]

(1) Heterogeneity in therapeutic efficacy remains a major concern. The intrinsic variability of the tumor microenvironment, both across patients and among different regions within the same tumor, leads to marked differences in reaction efficiency, resulting in poor uniformity of treatment outcomes.

(2) Delivery bottlenecks constitute a fundamental hurdle. The simultaneous and stoichiometrically balanced co-delivery of multiple reaction components (like catalysts, monomers, or initiators) to the target site *in vivo* is technically challenging, and this imprecise spatiotemporal control severely limits the overall therapeutic performance.

(3) The lack of real-time monitoring tools impedes closed-loop precision therapy. There is currently not non-invasive, quantitative method capable of tracking the extent of the *in situ* reaction and the biodistribution of the products in real time, which precludes timely adjustment of treatment parameters.

(4) Uncertainties regarding long-term safety remain unresolved. The chronic accumulation, metabolic pathways, and potential delayed toxicity of most catalysts and synthetic polymeric products have not been systematically evaluated in large-animal models, nor supported by comprehensive long-term toxicological data. At present, the majority of studies remain at the preclinical stage. To facilitate successful clinical translation, concerted efforts are urgently needed to overcome the aforementioned barriers, particularly in improving delivery efficiency, establishing definitive biosafety profiles, and developing scalable manufacturing protocols that comply with regulatory standards.

4. Conclusion

In situ chemical reactions are fundamentally reshaping biomedical applications by seamlessly integrating precision therapy with real-time imaging. This integration directly addresses the limitations of conventional treatments, such as poor spatiotemporal control, off-target toxicity, and insufficient efficacy. This paradigm represents a significant departure from conventional pharmacology, which relies on the passive distribution of pre-synthesized drugs. Instead, it facilitates the on-demand generation of therapeutic agents, imaging probes, or theranostic constructs directly within living systems. The result is a marked increase in treatment specificity and efficacy

alongside minimized systemic side effects, representing a pivotal advance toward personalized medicine, especially in oncology.

Recent advancements in bioorthogonal chemistry, advanced nanomaterials, and stimuli-responsive platforms have expedited the translation of this concept into actionable strategies. Bioorthogonal chemistry provides a set of 'biologically silent' reactions that proceed rapidly and selectively within complex physiological environments, without interfering with native biochemical pathways. In addition, engineered nanocarriers including liposomes,[131] mesoporous silica NPs and polymer micelles,[132,133] have been shown to enhance improve bioavailability and facilitate targeted delivery, overcoming biological barriers such as the blood-brain barrier and the tumor extracellular matrix. Conversely, stimuli-responsive systems enable the precise activation of reactions *via* external triggers (light, ultrasound)[134] or endogenous cues (tumor acidity, overexpressed enzymes, elevated reactive oxygen species), ensuring transformations occur exclusively at the disease site.

The fundamental objective of this approach is to achieve rigorous spatiotemporal control over molecular processes with high specificity, unlocking novel diagnostic, therapeutic, and theranostic capabilities. In the context of tumor therapy, for instance, the local generation of cytotoxic agents has the potential to circumvent systemic toxicity while concurrently serving as imaging probes for real-time treatment monitoring. A pivotal aspect of this field pertains to the advancement of biocompatible chemistry, with bioorthogonal reactions constituting a foundational toolkit. Key examples include Copper-free click chemistry (such as SPAAC), which avoids the cytotoxicity of copper catalysts and is well-suited for *in vivo* use. Tetrazine ligation, prized for its ultra-fast kinetics and high specificity, enabling rapid conjugation *in situ*. Stimuli-triggered bond-cleavage reactions, leverage tumor microenvironment features (low pH, specific enzymes) or external stimuli (*e.g.*, NIR light) for controlled payload release or probe activation.

The efficacy of implementation is contingent upon the implementation of sophisticated delivery and targeting strategies. The utilization of nanoparticle systems in co-deliver of reaction precursors and targeting ligands has emerged as a significant advancement in the field, leveraging effects such as EPR and receptor-mediated endocytosis. Antibody-drug conjugates offer antigen-specific delivery, while genetic encoding of enzymes enables localized catalytic amplification within target cells. Nevertheless, significant translational challenges persist. These include ensuring absolute reaction specificity amid complex biological milieus, overcoming delivery barriers such as rapid clearance and poor tumor penetration, and managing potential immunogenicity of exogenous materials. Addressing these issues necessitates sustained interdisciplinary collaboration across the domains of chemistry, materials science, biology, and medicine.

To gain a more comprehensive understanding of the practical limitations and future directions of this field, we analyze three key dimensions: clinical translation, delivery technologies, and ethical-regulatory considerations. The clinical translation of *in situ* chemical reaction-based strategies require a rigorous, stepwise validation cascade, ranging from *in vitro* cellular assays and small-animal studies to large-animal models and, ultimately, human clinical trials. At present, several major obstacles impede this process:

(1) There is a conspicuous lack of standardized evaluation criteria for assessing *in vivo* reaction efficiency, biosafety, and therapeutic efficacy. This inconsistency across studies severely complicates cross-study comparisons and hampers the identification of optimal therapeutic protocols.

(2) Long-term toxicological and pharmacokinetic data in mammalian systems remain scarce, which constitutes a critical bottleneck for the submission of Investigational New Drug (IND) applications.

(3) The industrial manufacturing processes for functional reagents are still underdeveloped, and quality control standards for clinical-grade products remain inadequate, further delaying clinical adoption. Looking forward, concerted efforts should be directed toward strengthening industry-academia-research partnerships, establishing harmonized evaluation guidelines, and accelerating the clinical validation of relatively mature strategies, particularly those based on localized photopolymerization and endogenous enzyme-triggered reactions. Addressing these challenges will be essential to bridge the gap between preclinical innovation and tangible therapeutic benefit.

Achieving efficient and targeted delivery of reaction precursors and catalysts to the intended site of action is a fundamental prerequisite for the successful implementation of *in situ* chemical reaction–based therapeutic strategies. However, several significant challenges currently impede this process, including rapid clearance of small-molecule reagents by the reticuloendothelial system, poor penetration of nanocarriers through the dense tumor extracellular matrix, difficulties in synchronizing the delivery and maintaining stoichiometric ratios of multicomponent reaction systems, and nonspecific biodistribution to normal tissues, which may give rise to off-target reactions. To address these obstacles, a range of optimization strategies has been proposed. These include the design of stimuli-responsive nanocarriers that enable tumor microenvironment-triggered release of encapsulated reagents, the surface modification of carriers with targeting ligands to enhance tumor accumulation, the integration of prodrug moieties to reduce the number of distinct components requiring simultaneous co-delivery, and the development of cell-mediated delivery platforms to improve penetration into deep tumor regions. Collectively, these approaches hold promises for overcoming the current delivery barriers and advancing the translational potential of *in situ* chemical reaction technologies.

The application of *in situ* chemical reaction technologies in biomedicine raises a distinct set of ethical and regulatory challenges that warrant careful consideration. From an ethical standpoint, the introduction of exogenous chemical reactions and synthetic substances into living organisms may perturb intrinsic cellular biochemical homeostasis. The potential long-term consequences for human physiological functions remain incompletely understood and thus require thorough evaluation. Moreover, clinical trials involving such interventions must rigorously adhere to the principle of informed consent, ensuring that participants are fully apprised of the investigational nature and associated uncertainties of these novel treatments. From a regulatory perspective, therapeutic products based on *in situ* chemical reactions exhibit a hybrid nature, encompassing attributes of both chemical drugs and biological agents. Current drug classification and approval frameworks are not fully equipped to accommodate such innovative modalities. It is therefore imperative to develop dedicated regulatory guidelines that define clear standards for safety and efficacy evaluation, alongside a comprehensive oversight system covering the entire lifecycle, from raw material production to clinical application. In addition, economic accessibility must not be overlooked. While fostering technological innovation, concurrent efforts

should be directed toward reducing reagent manufacturing costs, thereby mitigating the risk of exorbitant healthcare expenditures that may limit patient access to these advanced therapies. In light of the aforementioned practical challenges and developmental bottlenecks, future research in this field should prioritize targeted strategies to facilitate the clinical translation and responsible implementation of *in situ* chemical reaction technologies.

Looking forward, research endeavors will focus on augmenting the repertoire of biocompatible reactions, encompassing reversible and multi-step cascades, as well as on the development of deeper-tissue-penetrating activation triggers such as NIR-II light and ultrasound. The ultimate goal is to create integrated, autonomous theranostic systems that possess the capacity for closed-loop 'detect-and-treat' functionality. In alignment with this vision, our research endeavors are directed towards the advancement of light-mediated *in situ* intracellular synthesis in the field of oncology, with a particular emphasis on pH-sensitive polymer systems. Light provides non-invasive, externally controllable spatiotemporal precision, while pH-sensitive polymers enable selective reagent release in the acidic tumor microenvironment. The present study will explore both the intracellular and extracellular synthesis of bioactive molecules (such as cytotoxic peptides) *via* light activation. The study will systematically evaluate tumor cell-killing efficacy, apoptosis induction, and overall anti-tumor activity. This synergistic approach aims to maximize specificity and minimize off-target effects.

This technology shows great potential for use in both diagnosis and therapy. In the field of diagnostics, this technology facilitates *in situ* assembly of imaging probes (fluorescent polymers, magnetic nanoparticles), enhancing signal-to-noise ratios for long-term monitoring of tumor progression and treatment response. From a therapeutic standpoint, the mechanism by which it exerts its effects may involve several different processes, including the generation of cytotoxic polymers, the establishment of physical barriers to impede angiogenesis, or the facilitation of controlled combination therapy. With the continued development of biocompatible precursors and deep-tissue light sources, light-mediated polymerization is poised to contribute meaningfully to precision oncology.

In situ chemical reaction engineering is undergoing a rapid transition from a conceptual framework to a practical biomedical platform. By enabling precise molecular interventions directly at pathological sites, this paradigm represents a fundamental shift from treating symptoms to correcting disease at its molecular source. As interdisciplinary innovations continue to address existing challenges, these strategies are set to revolutionize the management of cancer, neurodegenerative disorders, and other complex diseases, ultimately improving therapeutic outcomes and patient quality of life.

Acknowledgments

This work was supported by Natural Science Foundation of Anhui Province (2408085QH233); Young and middle-aged teachers Training Action from Anhui province, Young backbone teachers overseas visiting and training project (JWFX2024026); Excellent Sci-tech Innovation Teams of Universities in Anhui Province (2023AH010073), We also thank the support from Macao Young Scholars Program (AM2024024).

Declaration of competing interest

The authors declare that they have no known competing financial interests or personal relationships that could have appeared to influence the work reported in this paper.

Author contributions

Shaojun Shi and Kaiyang Tao: writing–review & editing, writing–original draft, validation, investigation. **Weijie Xu**, **Ziheng Tong and Zhaoran Hu**: visualization, validation, investigation, and formal analysis. **Shuguo Zheng and Chunfei Wang**: writing–review & editing, visualization, validation, supervision, resources, project administration, funding acquisition, conceptualization.

Shaojun Shi and Kaiyang Tao contributed equally to this work.

5. List of abbreviations

ADC — antibody-drug conjugate;
AIE — aggregation-induced emission;
$AmLH_2$ — aminoluciferin;
APC — antigen-presenting cell;
ArM — artificial metalloenzyme;
ArMAS — artificial metalloenzymes in artificial sanctuaries;
ATP — adenosine triphosphate;
BRET — bioluminescence resonance energy transfer;
BSA — bovine serum albumin;
CAT — catalase;
CB[7] — cucurbit[7]uril;
CBT — 6-amino-2-cyanobenzothiazole;
cLANP — cross-linked lipoic acid nanoparticle;
CLSM — confocal laser scanning microscopy;
COF — covalent organic framework;
CuAAC — Cu(I)-catalyzed azide-alkyne click chemistry;
Cu@cLANP — nanocopper-doped cross-linked lipoic acid nanoparticle;
DFY — Asp-Phe-Tyr tripeptide;
DMA — *N*,*N*-dimethylacrylamide;
EPR — enhanced permeability and retention;
GSH — intracellular glutathione;
HCOP — hollow covalent organic polymer;
HPMA — *N*-(2-hydroxypropyl) methacrylamide;
HRP — horseradish peroxidase;
HSA — human serum albumin;
IEDDA — inverse electron-demand Diels-Alder;
LLPS — liquid-liquid phase separation;
MOE — metabolic oligosaccharide engineering;
MOF — metal-organic framework;
NaAsc — sodium ascorbate;
NIR — near-infrared;
NP — nanoparticle;
PA — photoacoustic;
PBS — phosphate-buffered saline;
PCET — proton-coupled electron transfer;
pDFY — poly(DFY);
PDI — perylenediimide derivative;
PDT — photodynamic therapy;
PEGDA — poly(ethylene glycol) diacrylate;
PET-RAFT — photoinduced electron/energy transfers reversible addition−fragmentation chain transfer;
PPE — poly(phenyleneethynylene);
RPNP — polymeric nanoparticle containing an immune adjuvant;
PSPA — polySPA;
PTX — paclitaxel;
RAFT — reversible addition-fragmentation chain-transfer;
ROS — reactive oxygen species;
SPA — *N*-(3-sulfopropyl) 4-aminodiphenylamine;
SPAAC — strain-promoted azide-alkyne cycloaddition;

TCO — *trans*-cyclooctene;
TME — tumor microenvironment;
TNR — Te nanoreservoir;
Tyr — tyrosine.

6. References

1. D.E.Metzler. In *Biochemistry (Two volume set). The chemical reactions of living cells*. (Elsevier, 2003)
2. H.W. van Roekel, B.J.Rosier, L.H.Meijer, P.A.Hilbers, A.J.Markvoort, W.T.Huck, T.F. de Greef. *Chem. Soc. Rev*., **44** (21), 7465 (2015); https://doi.org/10.1039/c5cs00361j
3. T.Gabaldon. *Annu. Rev. Microbiol*., **75**, 631 (2021); https://doi.org/10.1146/annurev-micro-090817-062213
4. R.Buller, S.Lutz, R.J.Kazlauskas, R.Snajdrova, J.C.Moore, U.T.Bornscheuer. *Science*, **382** (6673), eadh8615 (2023); https://doi.org/10.1126/science.adh8615
5. S.L.Scinto, D.A.Bilodeau, R.Hincapie, W.Lee, S.S.Nguyen, M.Xu, C.W. am Ende, M.G.Finn, K.Lang, Q.Lin, J.P.Pezacki, J.A.Prescher, M.S.Robillard, J.M.Fox. *Nat. Rev. Meth. Primers*, **1** (1), 30 (2021); https://doi.org/10.1038/s43586-021-00028-z
6. R.E.Bird, S.A.Lemmel, X.Yu, Q.A.Zhou. *Bioconj. Chem.*, **32** (12), 2457 (2021); https://doi.org/10.1021/acs.bioconjchem.1c00461
7. K.M.Hartung, E.M.Sletten. *Chem*, **9** (8), 2095 (2023); https://doi.org/10.1016/j.chempr.2023.05.016
8. W.Cao, H.-D.Chen, Y.-W.Yu, N.Li, W.-Q.Chen. *Chin. Med. J*., **134** (7), 783 (2021); https://doi.org/10.1097/CM9.0000000000001474
9. F.Bray, M.Laversanne, H.Sung, J.Ferlay, R.L.Siegel, I.Soerjomataram, A.Jemal. *CA: Cancer J. Clin*., **74** (3), 229 (2024); https://doi.org/10.3322/caac.21834
10. J.H.Du, M.T.Zhou, Q.Chen, Y.C.Tao, J.Ren, Y.Zhang, H.L.Qin. *Adv. Funct. Mater.*, **33** (24), 2215244 (2023); https://doi.org/10.1002/adfm.202215244
11. Z.Wang, J.Shan, X.Zhou, J.Wang, G.Yu, W.Dong, F.Huai, Q.Sun, G.Lu, Z.Ma, H.Liu. *J. Gastrointest. Oncol*., **14** (2), 1155 (2023); https://doi.org/10.21037/jgo-23-84
12. A.Zafar, S.Khatoon, M.J.Khan, J.Abu, A.Naeem. *Discov. Oncol*., **16** (1), 607 (2025); https://doi.org/10.1007/s12672-025-02198-8
13. K.D.Miller, L.Nogueira, T.Devasia, A.B.Mariotto, K.R.Yabroff, A.Jemal, J.Kramer, R.L.Siegel. *CA: Cancer J. Clin*., **72** (5), 409 (2022); https://doi.org/10.3322/caac.21731
14. S.J.Feng, Y.Zhang, Y.Y.Wang, Y.F.Gao, Y.J.Song. *Chem.–Eur. J*., **30** (62), e202402485 (2024); https://doi.org/10.1002/chem.202402485
15. A.B.Sun, J.L.Li, J.Wang, S.C.Zhang, X.Zhang, Y.M.Zhang, C.F.Wang, H.Wang, L.Hu. *Spectrochim. Acta A*, **341**, 126430 (2025); https://doi.org/10.1016/j.saa.2025.126430
16. X.Zhang, J.Wang, S.C.Zhang, J.L.Li, A.B.Sun, T.J.Wei, C.F.Wang, L.Hu, L.T.Zhou, H.Wang. *Org. Biomol. Chem*., **23** (10), 2491 (2025); https://doi.org/10.1039/d4ob01955e
17. L.Hu, L.P.Su, Z.Y.Wang, J.Yang, Y.Q.Wang, J.Wang, X.X.Gu, H.Wang. *Spectrochim. Acta A*, **323**, 124918 (2024); https://doi.org/10.1016/j.saa.2024.124918
18. Y.Li, X.Zhang, S.Liu, C.Li, Q.Wang, J.Ye, Y.Lu, J.Xu. *Chin. Chem. Lett*., **36** (2), 110501 (2025); https://doi.org/10.1016/j.cclet.2024.110501
19. J.X.Chen, G.C.Zhao, Y.Wei, D.X.Feng. *Anal. Methods*, **11** (46), 5880 (2019); https://doi.org/10.1039/c9ay01601e
20. X.W.Luan, Y.F.Gao, Y.C.Pan, Z.Huang, F.Zeng, G.Z.He, B.S.He, D.J.Ye, Y.J.Song. *Anal. Chem*., **97** (6), 3395 (2025); https://doi.org/10.1021/acs.analchem.4c05427
21. Y.P.Wang, S.J.Feng, X.Y.Wang, C.G.Tao, Y.T.Liu, Y.Y.Wang, Y.F.Gao, J.S.Zhao, Y.J.Song. *Lab Chip*, **24** (14), 3521 (2024); https://doi.org/10.1039/d4lc00290c
22. M.G.Clark, G.A.Gonzalez, Y.Y.Luo, J.A.Aldana-Mendoza, M.S.Carlsen, G.Eakins, M.J.Dai, C.Zhang. *Nat. Commun*., **13** (1), 4343 (2022); https://doi.org/10.1038/s41467-022-32071-z
23. Y.-P.Fan, Y.-T.Zhang, G.Zhang, L.Ma, Y.Lv, J.Li, Y.Luan, Y.-X.Zhang, Y.-T.Chen, H.-Y.Ren, W.Liu, M.-H.Li, Y.-X.Wu, S.Chen, B.Han, Q.-Y.Tang, L.-H.Chen, A.Wesselius, W.-C.Su, M.P.Zeegers, Y.Gu, Q.-R.Qin, H.Hao, J.Xia, H.Zhang, E.Y.-W.Yu. *Anal. Chem*., **97** (32), 17368 (2025); https://doi.org/10.1021/acs.analchem.5c01320
24. L.Yang, L.Ran, Y.Li, Y.A.Tan, D.Xia, T.Huang, J.Wang, T.T.Jiang, T.Tao, J.M.Xiao, S.H.Liu. *Colloid. Surf. A*, **725**, 137603 (2025); https://doi.org/10.1016/j.colsurfa.2025.137603
25. L.L.Quan, X.P.Luo, L.J.Xue, J.P.Li, Y.D.Ouyang. *J. Inorg. Organomet. Polym. Mater.*, **30** (7), 2744 (2020); https://doi.org/10.1007/s10904-020-01483-z
26. X.Li, L.Sun, X.Liu, P.Wen, Y.Zhang, Y.Mu, M.Tanaka, Y.Cheng, J.Li, W.Zhou. *J. Control. Release*, **389**, 114363 (2026); https://doi.org/10.1016/j.jconrel.2025.114363
27. Y.H.Guo, F.Jiang, X.H.Zhu, W.He, S.J.Song, X.C.Shou, M.N.Wu, T.Wu, T.J.Huang, Z.Ye, X.Y.Wang, Z.T.Chen, Y.He, Y.H.Yao, Z.W.Chen, H.H.Yang. *Nano Res*., **18** (2), 94907134 (2025); https://doi.org/10.26599/Nr.2025.94907134
28. S.Xiao, C.Han, L.Ma, W.Geng, Y.Gao, M.Adeli, L.Xu, L.Ye, L.Qiu, C.Cheng. *Cell Biomater*., **2** (2), (2026); https://doi.org/10.1016/j.celbio.2025.100194
29. O.Bertrand, J.F.Gohy. *Polym. Chem*., **8** (1), 52 (2017); https://doi.org/10.1039/c6py01082b
30. D.Y.Li, Y.F.Ling, Y.P.Cai, H.H.Jiang, H.Liu. *J. Polym. Sci*., **64** (10), 2022 (2026); https://doi.org/10.1002/pol.20250869
31. W.X.Guo, L.F.Hu, Y.H.Feng, B.Z.Chen, X.D.Guo. *Colloid. Surf. B*, **210**, 112202 (2022); https://doi.org/10.1016/j.colsurfb.2021.112202
32. M.X.Hou, S.Y.Liu. *Biomacromolecules*, **25** (9), 5402 (2024); https://doi.org/10.1021/acs.biomac.4c00688
33. Z.Li, Y.Zhu, J.B.Matson. *ACS Appl. Bio Mater*., **5** (10), 4635 (2022); https://doi.org/10.1021/acsabm.2c00188
34. N.K.Devaraj, M.G.Finn. *Chem. Rev*., **121** (12), 6697 (2021); https://doi.org/10.1021/acs.chemrev.1c00469
35. H.C.Kolb, M.Finn, K.B.Sharpless. *Angew. Chem., Int. Ed*., **40** (11), 2004 (2001); https://doi.org/10.1002/1521-3773(20010601)40:11<2004::AID-ANIE2004>3.0.CO;2-5
36. J.A.Codelli, J.M.Baskin, N.J.Agard, C.R.Bertozzi. *J. Am. Chem. Soc*., **130** (34), 11486 (2008); https://doi.org/10.1021/ja803086r
37. P.V.Chang, J.A.Prescher, E.M.Sletten, J.M.Baskin, I.A.Miller, N.J.Agard, A.Lo, C.R.Bertozzi. *Proc. Natl. Acad. Sci*., **107** (5), 1821 (2010); https://doi.org/10.1073/pnas.0911116107
38. H.Y.Yoon, D.Lee, D.-K.Lim, H.Koo, K.Kim. *Adv. Mater*., **34** (10), 2107192 (2022); https://doi.org/10.1002/adma.202107192
39. A.Vázquez, R.Dzijak, M.Dračínský, R.Rampmaier, S.J.Siegl, M.Vrabel. *Angew. Chem., Int. Ed*., **56**, 1334 (2017); https://doi.org/10.1002/anie.201610491
40. F.Liu, Y.Liang, K.N.Houk. *J. Am. Chem. Soc*., **136** (32), 11483 (2014); https://doi.org/10.1021/ja505569a
41. M.L.Blackman, M.Royzen, J.M.Fox. *J. Am. Chem. Soc*., **130** (41), 13518 (2008); https://doi.org/10.1021/ja8053805
42. M.Wang, H.Wang, C.Q.Niu, T.Zhang, Z.Wu, Z.Li. *Bioconjugate Chem*., **31** (7), 1795 (2020); https://doi.org/10.1021/acs.bioconjchem.0c00264
43. E.M.Sletten, C.R.Bertozzi. *Angew. Chem., Int. Ed*., **48** (38), 6974 (2009); https://doi.org/10.1002/anie.200900942
44. R.Tyburski, T.F.Liu, S.D.Glover, L.Hammarström. *J. Am. Chem. Soc*., **143** (2), 560 (2021); https://doi.org/10.1021/jacs.0c09106
45. C.R.Bertozzi. *Acc. Chem. Res*., **44** (9), 651 (2011); https://doi.org/10.1021/ar200193f
46. N.K.Devaraj. *ACS Cent. Sci*., **4** (8), 952 (2018); https://doi.org/10.1021/acscentsci.8b00251
47. J.Li, P.R.Chen. *Nat. Chem. Biol*., **12** (3), 129 (2016); https://doi.org/10.1038/nchembio.2024
48. L.I.Willems, W.A. van der Linden, N.Li, K.-Y.Li, N.Liu, S.Hoogendoorn, G.A.van der Marel, B.I.Florea,

H.S.Overkleeft. *Acc. Chem. Res*., **44** (9), 718 (2011); https://doi.org/10.1021/ar200125k
49. Y.-X.Chen, G.Triola, H.Waldmann. *Acc. Chem. Res*., **44** (9), 762 (2011); https://doi.org/10.1021/ar200046h
50. J.T.George, S.G.Srivatsan. *Chem. Commun*., **56** (82), 12307 (2020); https://doi.org/10.1039/D0CC05228K
51. M.Kufleitner, L.M.Haiber, V.Wittmann. *Chem. Soc. Rev*., **52** (2), 510 (2023); https://doi.org/10.1039/d2cs00764a
52. P.V.Chang, J.A.Prescher, M.J.Hangauer, C.R.Bertozzi. *J. Am. Chem. Soc*., **129** (27), 8400 (2007); https://doi.org/10.1021/ja070238o
53. L.Carroll, H.L.Evans, E.O.Aboagye, A.C.Spivey. *Org. Biomol. Chem*., **11** (35), 5772 (2013); https://doi.org/10.1039/C3OB40897C
54. H.C.Hang, J.P.Wilson, G.Charron. *Acc. Chem. Res*., **44** (9), 699 (2011); https://doi.org/10.1021/ar200063v
55. Q.Fu, S.Shen, P.Sun, Z.Gu, Y.Bai, X.Wang, Z.Liu. *Chem. Soc. Rev*., **52** (22), 7737 (2023); https://doi.org/10.1039/D2CS00889K
56. W.Yi, P.Xiao, X.Liu, Z.Zhao, X.Sun, J. Wang, L.Zhou, G.Wang, H.Cao, D.Wang, Y.Li. *Sign. Transduct. Targ. Ther*., **7** (1), 386 (2022); https://doi.org/10.1038/s41392-022-01250-1
57. K.E.de Roode, R.Rossin, M.S.Robillard. *Top. Curr. Chem*., **383** (2), 12 (2025); https://doi.org/10.1007/s41061-025-00495-y
58. E.G.Tomarchio, R.Turnaturi, E.Saccullo, V.Patamia, G.Floresta, C.Zagni, A.Rescifina. *Bioorg. Chem*., **150**, 107573 (2024); https://doi.org/10.1016/j.bioorg.2024.107573
59. K.Adhikari, M.Vanermen, G.Da Silva, T.Van den Wyngaert, K.Augustyns, F.Elvas. *EJNMMI Radiopharm. Chem*., **9** (1), 47 (2024); https://doi.org/10.1186/s41181-024-00275-x
60. C.G.Williams. *Trans. R. Soc. Edinburgh*, **21** (3), 377 (2013); https://doi.org/10.1017/s0080456800032208
61. A.P.Gorka, R.R.Nani, M.J.Schnermann. *Org. Biomol. Chem*., **13** (28), 7584 (2015); https://doi.org/10.1039/c5ob00788g
62. R.B.Mujumdar, L.A.Ernst, S.R.Mujumdar, C.J.Lewis, A.S.Waggoner. *Bioconj. Chem*., **4** (2), 105 (2002); https://doi.org/10.1021/bc00020a001
63. B.Chon, W.Ghann, J.Uddin, B.Anvari, V.Kundra. *Int. J. Mol. Sci*., **24** (17), 13030 (2023); https://doi.org/10.3390/ijms241713030
64. W.Mytych, D.Bartusik-Aebisher, D.Aebisher. *Molecules*, **30** (4), 888 (2025); https://doi.org/10.3390/molecules30040888
65. C.H.Shi, J.B.Wu, D.F.Pan. *Biomed. Optics*, **21** (5), 50901 (2016); https://doi.org/10.1117/1.Jbo.21.5.050901
66. A.Levitz, F.Marmarchi, M.Henary. *Molecules*, **23** (2), (2018); https://doi.org/10.3390/molecules23020226
67. G.W.Byers, S.Gross, P.M.Henrichs. *Photochem. Photobiol*., **23** (1), 37 (1976); https://doi.org/10.1111/j.1751-1097.1976.tb06768.x
68. R.R.Nani, J.A.Kelley, J.Ivanic, M.J.Schnermann. *Chem. Sci*., **6** (11), 6556 (2015); https://doi.org/10.1039/c5sc02396c
69. A.P.Gorka, M.J.Schnermann. *Curr. Opin. Chem. Biol*., **33** 117 (2016); https://doi.org/10.1016/j.cbpa.2016.05.022
70. R.Strada, D.Dunlop, P.Sebej. *ChemPlusChem*, **90** (12), e202500279 (2025); https://doi.org/10.1002/cplu.202500279
71. Y.Yamada, A.Okamoto, S.Mizuno, T.Udagawa, T.Agou, Y.Kubota, T.Inuzuka, K.Funabiki. *ChemPhotoChem*, **9** (8), e202500006 (2025); https://doi.org/10.1002/cptc.202500006
72. B.Yamada, P.B.Zetterlund. In *Handbook of Radical Polymerization. General Chemistry of Radical Polymerization*. (Wiley-Interscience, 2002). P. 117
73. R.A.Hutchinson, A.Penlidis. In *Polymer Reaction Engineering. Free-Radical Polymerization: Homogeneous Systems*. (Oxford: Blackwell Publishing Ltd., 2007). P. 118
74. J.Geng, W.Li, Y.Zhang, N.Thottappillil, J.Clavadetscher, A.Lilienkampf, M.Bradley. *Nat. Chem*., **11** (6), 578 (2019); https://doi.org/10.1038/s41557-019-0240-y
75. L.L.Zhang, H.Liu, H.B.Xu, M.Wang, H.F.Liu, W.J.Li, C.Q.Zhang, W.Y.Han, J.Chen, Y.C.Zhang. *J. Am. Chem. Soc*., **147** (26), 23339 (2025); https://doi.org/10.1021/jacs.5c08624
76. M.S.Messina, K.M.M.Messina, A.Bhattacharya, H.R.Montgomery, H.D.Maynard. *Prog. Polym. Sci*., **100**, 101186 (2020); https://doi.org/10.1016/j.progpolymsci.2019.101186
77. K.Matyjaszewski, J.Spanswick. *Mater. Today*, **8** (3), 26 (2005); https://doi.org/10.1016/s1369-7021 (05)00745-5
78. C.F.Liu, Y.F.Jin, J.H.Ma, W.Tian, H.P.Xu. *Chin. J. Polym. Sci*., **43** (8), 1293 (2025); https://doi.org/10.1007/s10118-025-3341-7
79. A.Zhang, S.Zhao, J.Tyson, K.Deisseroth, Z.Bao. *Nat. Synth*., **3** (8), 943 (2024); https://doi.org/10.1038/s44160-024-00560-2
80. D.D.Shah, M.R.Chorawala, N.R.Raghani, R.Patel, M.Fareed, V.A.Kashid, B.G.Prajapati. *Med. Oncol*., **42** (4), 117 (2025); https://doi.org/10.1007/s12032-025-02641-4
81. N.M.Anderson, M.C.Simon. *Curr. Biol.*, **30** (16), R921 (2020); https://doi.org/10.1016/j.cub.2020.06.081
82. A.Sarniak, J.Lipinska, K.Tytman, S.Lipinska. *Postepy Hig. Med. Dosw*., **70**, 1150 (2016); https://doi.org/10.5604/17322693.1224259
83. M.D.Jelic, A.D.Mandic, S.M.Maricic, B.U.Srdjenovic. *J. Cancer Res. Ther*., **17** (1), 22 (2021); https://doi.org/10.4103/jcrt.JCRT_862_16
84. J.N.Moloney, T.G.Cotter. *Semin. Cell Dev. Biol*., **80** 50 (2018); https://doi.org/10.1016/j.semcdb.2017.05.023
85. C.L.Lin, Z.S.Fang, C.Y.Hsu, Y.H.Liu, J.C.Lin, B.Y.Yao, F.A.Li, S.B.Yen, Y.C.Chang, C.J.Hu. *Acta Biomater*., **173** 325 (2024); https://doi.org/10.1016/j.actbio.2023.11.026
86. O.Baghdasaryan, S.Khan, J.C.Lin, J.Lee-Kin, C.Y.Hsu, C.J.Hu, C.Tan. *Trends Biotechnol*., **42** (2), 241 (2024); https://doi.org/10.1016/j.tibtech.2023.08.006
87. Y.J.Sun, D.Zhang, Z.Q.Dong, J.Lyu, C.F.Wang, J.Gong, K.H.Wong, C.F.Wu, X.J.Zhang. *Nat. Commun*., **16** (1), 1115 (2025); https://doi.org/10.1038/s41467-025-56253-7
88. H.B.Xu, H.Y.Chen, J.Lv, B.B.Chen, Z.R.Zhou, S.Chang, Y.T.Gao, W.F.Huang, M.J.Ye, Z.J.Cheng, M.E.Hafez, R.C.Qian, D.W.Li. *Angew. Chem., Int. Ed*., **62** (44), e202311002 (2023); https://doi.org/10.1002/anie.202311002
89. Q.Guan, L.-L.Zhou, Z.Q.Yang, Y.-A.Li, L.Y.Wang, R.B.Wang. *Adv. Mater.*, **38** (16), e10663 (2026); https://doi.org/10.1002/adma.202510663
90. C.F.Liu, H.A.Ma, S.Z.Yuan, Y.F.Jin, W.Tian. *ACS Nano*, **19** (2), 2047 (2025); https://doi.org/10.1021/acsnano.4c16669
91. L.O.Atta, Z.Zhou, G.Roelfes. *Angew. Chem., Int. Ed.*, **62** (1), e202214191 (2023); https://doi.org/10.1002/anie.202214191
92. C.Costentin. *Chem. Rev*., **108** (7), 2145 (2008); https://doi.org/10.1021/cr068065t
93. M.H.V.Huynh, T.J.Meyer. *Chem. Rev*., **107** (11), 5004 (2007); https://doi.org/10.1021/cr0500030
94. E.Paleček, V.Ostatná. *Analyst*, **134** (10), 2076 (2009); https://doi.org/10.1039/b912602c
95. M.Chiku, J.Nakamura, A.Fujishima, Y.Einaga. *Anal. Chem*., **80** (15), 5783 (2008); https://doi.org/10.1021/ac800394n
96. M.Zhu, S.L.Wang, Z.H.Li, J.B.Li, Z.J.Xu, X.M.Liu, X.Huang. *Nat. Commun*., **14** (1), 3598 (2023); https://doi.org/10.1038/s41467-023-39286-8
97. M.Zhianmanesh, A.Gilmour, M.M.M.Bilek, B.Akhavan. *Appl. Phys. Rev*., **10** (2), 021301 (2023); https://doi.org/10.1063/5.0130829
98. R.L.Qi, H.Zhao, X.Zhou, J.Liu, N.Dai, Y.Zeng, E.D.Zhang, F.T.Lv, Y.M.Huang, L.B.Liu, Y.L.Wang, S.Wang. *Angew. Chem., Int. Ed.*, **60** (11), 5759 (2021); https://doi.org/10.1002/anie.202015247
99. E.P.Magennis, F.Fernandez-Trillo, C.Sui, S.G.Spain, D.J.Bradshaw, D.Churchley, G. Mantovani, K.Winzer, C.Alexander. *Nat. Mater*., **13** (7), 748 (2014); https://doi.org/10.1038/nmat3949
100. J.Li, L.Chen, L.Du, M.Li. *Chem. Soc. Rev*., **42** (2), 662 (2013); https://doi.org/10.1039/c2cs35249d

101. G.Zhang, H.Dong, D.Wang, L.D.Sun, C.H.Yan. *J. Rare Earth*., **35** (1), 1 (2017); https://doi.org/10.1016/S1002-0721(16)60165-5
102. D.M.Mofford, S.T.Adams, G.S.K.K.Reddy, G.R.Reddy, S.C.Miller. *J. Am. Chem. Soc*., **137** (27), 8684 (2015); https://doi.org/10.1021/jacs.5b04357
103. R.Weinstain, E.N.Savariar, C.N.Felsen, R.Y.Tsien. *J. Am. Chem. Soc*., **136** (3), 874 (2014); https://doi.org/10.1021/ja411547j
104. Z.Zheng, G.Y.Li, C.F.Wu, M.M.Zhang, Y.Zhao, G.L.Liang. *Chem. Commun*., **53** (25), 3567 (2017); https://doi.org/10.1039/C7cc00999b
105. L.Cui, S.Vivona, B.R.Smith, S.-R.Kothapalli, J.Liu, X.Ma, Z.Chen, M.Taylor, P.H.Kierstead, J.M.J.Fréchet, S.S.Gambhir, J.Rao. *J. Am. Chem. Soc*., **142** (36), 15575 (2020); https://doi.org/10.1021/jacs.0c07594
106. C.D'Avino, S.Gutiérrez, M.J.Feldhaus, M.Tomás-Gamasa, J.L.Mascareñas. *J. Am. Chem. Soc*., **146** (5), 2895 (2024); https://doi.org/10.1021/jacs.3c13647
107. C.Vidal, M.Tomás-Gamasa, P.Destito, FLópez, J.L.Mascareñas. *Nat. Commun*., **9** (1), 1913 (2018); https://doi.org/10.1038/s41467-018-04314-5
108. S.Bose, A.H.Ngo, L.H.Do. *J. Am. Chem. Soc*., **139** (26), 8792 (2017); https://doi.org/10.1021/jacs.7b03872
109. Y.Liu, Q.Guo, Y.Shi, M.Cui, F.Jing. *Front. Oncol*., **14**, 1507958 (2024); https://doi.org/10.3389/fonc.2024.1507958
110. A.H.Wang, H.Y.Li, H.Feng, H.M.Qiu, R.M.Huang, Y.Q.Wang, S.C.Ji, H.Liang, X.C.Shen, B.P.Jiang. *ACS Appl. Mater. Interfaces*, **15** (4), 5870 (2023); https://doi.org/10.1021/acsami.2c19927
111. Y.H.Dai, T.Y.Li, Z.H.Zhang, Y.Z.Tan, S.J.Pan, L.Zhang, H.P.Xu. *J. Am. Chem. Soc*., **143** (28), 10709 (2021); https://doi.org/10.1021/jacs.1c04821
112. Y.Zhang, Q.Gao, W.Li, R.He, L.Zhu, Q.Lian, L.Wang, Y.Li, M.Bradley, J Geng. *JACS Au*, **2** (3), 579 (2022); https://doi.org/10.1021/jacsau.1c00373
113. M.Tang, Z.Q.Yang, X.C.Tang, H.Ma, B.B.Xie, J.F.Xu, C.Gao, D.Bardelang, R.B.Wang. *J. Am. Chem. Soc*., **147** (4), 3488 (2025); https://doi.org/10.1021/jacs.4c14847
114. Z.Q.Meng, X.F.Zhou, J.Xu, X.Han, Z.L.Dong, H.R.Wang, Y.J.Zhang, J.L.She, L.G.Xu, C.Wang, Z.Liu. *Adv. Mater*., **31** (24), 1900927 (2019); https://doi.org/10.1002/adma.201900927
115. Q.L.Zhang, D.W.Zheng, X.Dong, P.Pan, S.M.Zeng, F.Gao, S.X.Cheng, X.Z.Zhang. *J. Am. Chem. Soc*., **143** (13), 5127 (2021); https://doi.org/10.1021/jacs.1c00945
116. J.S.Huang, L.Wang, P.X.Zhao, F.Q.Xiang, J.Liu, S.Y.Zhang. *ACS Catal.*, **8** (7), 5941 (2018); https://doi.org/10.1021/acscatal.8b01337
117. Y.Chen, M.X.Zuo, Y.Chen, P.Y.Yu, X.K.Chen, X.D.Zhang, W.Yuan, Y.L.Wu, W.Zhu, Y.L.Zhao. *Nat. Commun*., **14** (1), 5229 (2023); https://doi.org/10.1038/s41467-023-40935-1
118. S.Y.Dai, Z.Xiao, F.F.Shen, I.Lim, J.H.Rao. *J. Am. Chem. Soc*., **147** (2), 2037 (2025); https://doi.org/10.1021/jacs.4c15644
119. G.Hong, J.E.Chang. *Pharmaceutics*, **16** (11), 1420 (2024); https://doi.org/10.3390/pharmaceutics16111420
120. C.X.Wu, Z.Wei, C.F.Li, S.Yang, G.H.Liu, R.H.Yang. *J. Am. Chem. Soc*., **147** (39), 35604 (2025); https://doi.org/10.1021/jacs.5c10871
121. T.C.Chang, K.Vong, T.Yamamoto, K.Tanaka. *Angew. Chem., Int. Ed*., **60** (22), 12446 (2021); https://doi.org/10.1002/anie.202100369
122. T.Wu, X.H.Chen, Y.T.Fei, G.P.Huang, Y.J.Deng, Y.J.Wang, A.M.Yang, Z.Y.Chen, N.G.Lemcoff, X.X.Feng, Y.G.Bai. *Nat. Chem. Biol*., **21** (5), 779 (2025); https://doi.org/10.1038/s41589-024-01819-7
123. S.Fischer, T.R.Ward, A.D.Liang. *ACS Catal.*, **11** (10), 6343 (2021); https://doi.org/10.1021/acscatal.1c01470
124. T.Wu, Y.T.Fei, Y.J.Deng, X.H.Chen, Y.L.Duan, Y.Liu, Y.G.Bai. *J. Am. Chem. Soc*., **147** (18), 15229 (2025); https://doi.org/10.1021/jacs.5c00473
125. Q.Shen, Y.M.Huang, Y.Zeng, E.D.Zhang, F.T.Lv, L.B.Liu, S.Wang. *ACS Mater. Lett*., **3** (9), 1307 (2021); https://doi.org/10.1021/acsmaterialslett.1c00357
126. R.Hu, X.Chen, T.T.Zhou, H.Si, B.Z.He, R.T.K.Kwok, A.J.Qin, B.Z.Tang. *Sci. China Chem.*, **62** (9), 1198 (2019); https://doi.org/10.1007/s11426-019-9517-9
127. Y.Liu, Y.Zhang, H.Li, T.Y.Hu. *Acta Pharm. Sin. B*, **15** (1), 97 (2025); https://doi.org/10.1016/j.apsb.2024.12.007
128. Z.Zhang, S.Yao, Y.Wang, K.Luo, M.Amiji, K.C.Anderson. *Biomaterials*, **325**, 123615 (2026); https://doi.org/10.1016/j.biomaterials.2025.123615
129. R.Song, X.Li, J.Zhu, J.He, J.Na. *Vaccines*, **13** (5), 469 (2025); https://doi.org/10.3390/vaccines13050469
130. H.Wang, W.He, J.Liao, S.Wang, X.Dai, M.Yu, Y.Xie, Y.Chen. *Adv. Mater*., **37** (1), e2411967 (2025); https://doi.org/10.1002/adma.202411967
131. D.T.Zhou, Z.B.Zhang, L.Q.Pan, Y.Y.Wang, J.J.Yang, Y.F.Gao, Y.J.Song. *Angew. Chem., Int. Ed*., **63** (28), e202404493 (2024); https://doi.org/10.1002/anie.202404493
132. D.M.Wang, G.X.Yao, J.Y.Sun, J.J.Liang, H.Zhou. *Anal. Chim. Acta*, **1346**, 343790 (2025); https://doi.org/10.1016/j.aca.2025.343790
133. S.Miao, J.Sun, Y.Li, Q.Zhang, H.Chen, F.Gao. *Spectrochim. Acta A*, **329**, 125598 (2025); https://doi.org/10.1016/j.saa.2024.125598
134. L.P.Su, X.M.Zhu, H.T.Ding, L.Hu, J.Y.Chen, S.Q.Qi, K.Luo, W.W.Ling, X.H.Tian. *Sens. Actuat. B: Chem*., **412**, 135792 (2024); https://doi.org/10.1016/j.snb.2024.135792